2016

Learning Related Regulation of a Voltage-Gated Ion Channel in the Cerebellum

Jason R. Fuchs
University of Vermont

LEARNING RELATED REGULATION OF A VOLTAGE-GATED ION CHANNEL IN THE CEREBELLUM

A Dissertation Presented

by

Jason R. Fuchs

to

The Faculty of the Graduate College

of

The University of Vermont

In Partial Fulfillment of the Requirements
for the degree of Doctor of Philosophy
Specializing in Psychology

January, 2016

Defense Date: September 17, 2015
Dissertation Examination Committee:

John T. Green, Ph.D, Advisor
Marilyn J. Cipolla, Ph.D, Chairperson
William A. Falls, Ph.D.
Sayamwong E. Hammack, Ph.D.
Anthony D. Morielli, Ph.D.
Cynthia J. Forehand, Ph.D., Dean of the Graduate College

ABSTRACT

The neural mechanisms that support learning and memory are still poorly understood. Much work has focused on changes in neurotransmitter receptor expression, while changes in voltage-gated ion channel expression have been largely unexplored, despite the fact that voltage-gated ion channels govern neuronal excitability. Here we used eyeblink conditioning (EBC) in rats, a model of learning and memory with a well-understood neural circuit, to examine regulation of voltage-gated ion channels as a consequence of learning. EBC is a form of classical conditioning that involves pairings of a behaviorally neutral conditioned stimulus (CS) and an eyeblink eliciting unconditioned stimulus (US) over many trials to produce an eyeblink conditioned response (CR) to the CS in anticipation of the US. The acquisition and generation of the eyeblink CR is governed by plasticity at various sites in the cerebellum, both in the cerebellar cortex and the interpositus nucleus (IPN). Purkinje cells (PCs) are the primary neuron in the cerebellar cortex and these cells represent the sole output of the cerebellar cortex. PCs tonically inhibit the neurons of the IPN; the IPN is the start of the eyeblink pathway. In order for a CR to be generated, the inhibition of the IPN by PCs must be lifted. Basket cells (BCs) are small inhibitory interneurons that form synapses near the PC soma. These neurons are strategically located to strongly regulate PC output through inhibitory input near the axon hillock. BC axon terminals have the highest expression of Kv1.2, an alpha subunit of the Kv1 (*Shaker*) family of voltage-gated potassium channels, in the cerebellum. In addition, significant Kv1.2 expression is found on PC dendrites. Blocking Kv1.2 leads to increased GABAergic input to PCs and facilitates EBC. In the current work, we addressed the question of whether EBC itself regulates surface expression of Kv1.2 in cerebellar cortex. Rats received three days of either EBC, explicitly unpaired stimulus presentations, or no stimuli, and cerebellar tissue was harvested and analyzed via biotinylation/western blot (WB) and multiphoton microscopy (MP) techniques. In the first experiment, the Unpaired group showed significantly reduced surface Kv1.2 expression at BC axon terminals as measured by MP, but no changes observed with the WB measure, which measures expression at both BC axon terminals and PC dendrites. The second experiment used the same procedures but examined cerebellar tissue following a shorter training procedure. We hypothesized that the Paired and Unpaired groups would show similar Kv1.2 surface expression earlier in training. The Unpaired group showed increased surface Kv1.2 compared to the other two groups in the WB measures, but no differences were observed in the MP measure. Paired group rats that did not exhibit CRs showed the same pattern as the Unpaired group. Overall, we observed training and location specific changes in surface Kv1.2 expression, suggesting that learning does appear to regulate voltage-gated ion channel expression in the mammalian brain. Increased surface Kv1.2 early in training before CR expression emerges may set the stage for other mechanisms to govern the expression of the learned response. Prolonged stimulus input that is unmodulated by expression of a learned response, such as in the Unpaired group in the first experiment, leads to long-term changes in surface Kv1.2 expression exclusively at BC axon terminals.

TABLE OF CONTENTS

LIST OF TABLES v

LIST OF FIGURES vii

LIST OF ABBREVIATIONS xi

CHAPTER1: COMPREHENSIVE LITERATURE REVIEW 1
- Section 1.1: What is Eyeblink Conditioning? 1
- Section 1.2: Cerebellar Anatomy 2
- Section 1.3: Eyeblink Response Pathways 3
- Section 1.4: Eyeblink Conditioning Stimulus Pathways 5
- Section 1.5: Acquisition of Eyeblink Conditioned Response 7
  - Section 1.5.1: Mossy Fiber to Interpositus Nucleus 8
  - Section 1.5.2: Parallel Fiber to Purkinje Cell Synapse 12
- Section 1.6: Basket Cells in the Cerebellar Cortex 17
- Section 1.7: Kv1.2 and Its Regulation 18
- Section 1.8: Kv1.2 Regulation by Secretin in the Cerebellar Cortex 20
- Section 1.9: Kv1.2 in Eyeblink Conditioning 23
  - Section 1.9.1: Blockade of Kv1.2 in Eyeblink Conditioning 24
  - Section 1.9.2: Secretin in Eyeblink Conditioning 25
- Section 1.10. The Model 26
- Section 1.11: Next Step 28

CHAPTER 2: MEASURING CHANGES IN Kv1.2 EXPRESSION FOLLOWING EYEBLINK CONDITIONING 29
- Introduction 29
- Materials and Methods 31
  - Eyeblink Conditioning 31
    - Subjects 31
    - Surgery 32
    - Apparatus 33
    - Training Procedure 34
    - Behavior Analysis 35
  - Biotinylation and Western Blot 36
    - Generation of Parasagittal Cerebellar Sections 36
    - Biotinylation 37
    - Gel Preparation 38
    - Imaging Western Blots 39
  - Multiphoton Microscopy 40
    - TsTX-ATTO-594 Stain 40
    - Multiphoton microscopy 41
    - Image Analysis 42
  - Kv1.2 Surface Expression Data Analysis 43

Results....44
Eyeblink conditioning Behavioral Analysis....44
Outlier Analysis for Both Measures....47
Multiphoton Microscopy – Kv1.2 Surface Expression at Basket Cell axon terminals....48
Biotinylation and Western Blot Analysis – Surface Kv1.2 at Basket Cell Terminals and Purkinje Cell Dendrites....51
Discussion....54
References....58

CHAPTER 3: MEASURING CHANGES IN Kv1.2 EXPRESSION AFTER BRIEF TRAINING IN EYEBLINK CONDITIONING....61
Introduction....61
Materials and Methods....63
Eyeblink Conditioning....63
Subjects....63
Surgery and Apparatus....63
Training Procedure....63
Behavior Analysis....64
Western Blot and Multiphoton Microscopy....65
Kv1.2 Surface Expression Data Analysis....65
Results....65
Eyeblink Conditioning Behavioral Analysis....65
Outlier Analysis for both measures....67
Multiphoton Microscopy Analysis of Kv1.2 Surface Expression On Basket Cell Axon Terminals....69
Biotinylation and Western Blot Analysis of surface Kv12 at Basket Cell Axon Terminals and Purkinje Cell Dendrites....71
Discussion....74
References....78

CHAPTER 4: GENERAL DISCUSSION....80
Model Revisited....87
Significance....94
Limitations and Future Directions....94
References....100

APPENDIX I: Validation of Experimental Methods....119
Section 1: Biotinylation of Kv1.2 in Fixed and Non-Fixed Tissue....119
Introduction....119
Materials and Methods....119
Tissue Harvest and Biotinylation....119
Gel Preparation and Imaging....121
Results and Discussion....122
Section 2: Testing the Concentration of Sodium Meta-Periodate....124

Introduction....124
Materials and Methods....125
Subjects, Perfusion, and Sectioning....125
Biotinylation, Gel Preparation, and Imaging....125
Results and Discussion....126
Section 3: Testing the Laser Scanning Microscope (LSM7) Multiphoton Microscope system to Detect Changes in Kv1.2 Surface Expression....128
Introduction....128
Materials and Methods....129
Subject, Perfusion, and Sectioning....129
Drug Treatment and Tissue Preparation....130
Imaging....130
Image Processing and Analysis....130
Results and Discussion....131

APPENDIX II: OUTLIER ANALYSIS FOR EXPERIMENT 1 (CHAPTER 2)....134

APPENDIX III: CR ONSET LATENCY AND ONSET LATENCY STANDARD DEVIATION – EXPERIMENT 1 (CHAPTER 2)....137

APPENDIX IV: OUTLIER ANALYSIS FOR EXPERIMENT 2 (CHAPTER 3)....138

APPENDIX V: EXPERIMENT 2 (CHAPTER 3) PAIRED GROUP PERFORMANCE SPLIT OUTLIER ANALYSIS....142

APPENDIX VI: EXPERIMENT 2 (CHAPTER 3): BIOTINYLATION AND BLOT DATA FOLLOWING OUTLIER ANALYSIS ON PAIRED HIGH AND PAIRED LOW GROUPS....146

APPENDIX VII: MAPPING THE SPREAD OF TITYUSTOXIN INFUSIONS IN THE CEREBELLAR CORTEX MAPPING THE SPREAD....147

LIST OF TABLES

Table 1. Kv1.2 Expression ratios (to GAPDH) for sodium meta-periodate (SMP) experiment. Beads represent the surface expression of Kv1.2 for the non-permeabilized samples. In the permeabilized conditions, Beads represent all Kv1.2 that was tagged with Biotin and pulled onto the Neutravidin beads, not limited to just surface. Total represents all proteins and Post represents the samples taken after incubation with the Beads. Results show greater surface Kv1.2 expression with lower SMP concentrations. Overall, increasing SMP concentration limits Kv1.2 expression on blots, especially in permeabilized samples. 121

Table 2. Outlier Labeling Rule (OLR) Analysis for Western Blot data in Experiment 1. The Lower and Upper limits for outlier threshold are based on the first (Q1) and third (Q3) quartile percentages based on the distribution of the data in each group. Subjects whose score fall outside of the lower or upper range were considered outliers. No outlier identified in any of the groups in the WB measure in experiment 1.....129

Table 3. Outlier Labeling Rule (OLR) Analysis for Multiphoton Microscopy data in Experiment 1. The Lower and Upper limits for outlier threshold are based on the first (Q1) and third (Q3) quartile percentages based on the distribution of the data in each group. Subjects whose score fall outside of the lower or upper range were considered outliers.....130

Table 4. Outlier Labeling Rule (OLR) Analysis for Western Blot data for Experiment 2. The Lower and Upper limits for outlier threshold are based on the first (Q1) and third (Q3) quartile percentages based on the distribution of the data in each group. Subjects whose score fall outside of the lower or upper range were considered outliers. Subject 15-188 was identified as an outlier in this analysis in the No stimulus group. This subject was the same as was identified in the boxplot analysis (Fig. 14) and was subsequently removed from analyses. 133

Table 5. Outlier Labeling Rule (OLR) Analysis for Multiphoton Microscopy data in Experiment 2. The Lower and Upper limits for outlier threshold are based on the first (Q1) and third (Q3) quartile percentages based on the distribution of the data in each group. Subjects whose score fall outside of the lower or upper range were considered outliers. No subjects were identified as outliers. 134

Table 6. Outlier Labeling Rule (OLR) for Western Blot data from Experiment 2 for the Paired High and Paired Low groups. The Lower and Upper limits for outlier threshold are based on the first (Q1) and third (Q3) quartile percentages based on the distribution of the data in each group. Subjects whose score fall outside of the lower or upper range were considered outliers. Subject 15-103 in the Paired Low group identified as an outlier, the same subject identified in the boxplot analysis (Fig. 17).....136

Table 7. Outlier Labeling Rule (OLR) for Multiphoton Microscopy data between the Paired split. The Lower and Upper limits for outlier threshold are based on the first (Q1) and third (Q3) quartile percentages based on the distribution of the data in each group. Subjects whose score fall outside of the lower or upper range were considered outliers. No Subjects were identified at an outlier. 138

LIST OF FIGURES

Figure 1. Brainstem and cerebellar neural pathways involved acquisition of eyeblink classical conditioning. (A) Briefly, Purkinje cells represent the sole, inhibitory output of the cerebellar cortex. IN doing so, they tonically inhibit the neurons of the interpositus nucleus (IPN). The stimulus information is projected through modality-specific brainstem nuclei and then to the cerebellar cortex. Axon collaterals are also projected to the neurons of the IPN. In order for an eyeblink conditioned response to be initiated by the neurons of the IPN, the tonic inhibition of PCs must be listed. The response is projected through various brainstem nuclei that control closure of the eyelid muscle. (B) Example of a well-time eyeblink conditioned response. Responses are scored as CRs if the magnitude of the response exceeds the response threshold. CRs can be distinguished from unconditioned responses based on the timing and amplitude; eyeblink responses should occur temporally close to US onset but will precede that stimulation and the amplitude greater than the activity in between trials. 11

Figure 2. Black and white image of maximum projection of cerebellar section taken on multiphoton microscope system. Brighter punctate staining throughout cortex represents surface Kv1.2 tagged with ATTO-TsTX-594 on basket cell axon terminals. Image created by taking a maximum projection of a Z-stack, compressing the pixels by the maximum value. The maximum projections used to create a mask to identify pinceaus from a sum projection of the same Z-projection. 42

Figure 3. Acquisition data plotted by session for Paired group (green circles), Unpaired group (blue squares), and No Stimulus group (red triangles). Each session consisted of 100 CS-US trials (Paired group), 100 CS-alone and 100 US-alone trials, intermixed (Unpaired group), or 100 "trials" without any stimuli (No Stimulus group). The Paired group showed a significantly greater percentage of trials with a CR than either of the other two groups ($p < 0.001$). Inset: Sessions 1 and 2 displayed as 25-trial blocks for the Paired group. 45

Figure 4. Region-specific analysis of Kv1.2 surface expression on BC axon terminals in the cerebellar cortex near the base of the primary fissure ipsilateral to the conditioning (Paired group), stimulated (Unpaired), or simply electrode-implanted (No Stimulus) eyelid. Raw microscopy data (A) and Mean ±SEM (B). Each subject represented by one number (A) comprised of the fluorescent intensity of PCXs in both cerebellar sections. Significant differences observed between the Unpaired and Paired groups ($p = 0.04$) and Unpaired and No Stimulus groups ($p = 0.006$). No differences observed between Paired and No Stimulus groups ($p = 0.34$). (* denotes $p < 0.05$; ** denotes $p < 0.01$) 47

Figure 5. Kv1.2 surface expression measured at both PC dendrites and BC axon terminals. (A) Data displayed as raw Kv1.2 surface expression for Paired group (green circles), Unpaired group (blue squares), and No Stimulus group (red triangles).

Each data point represents an individual subject. (B) Mean ± SEM normalized to the No Stimulus group. The numbers shown above the group assignments represent the number of subjects in each group. No significant differences were observed between the groups. 50

Figure 6. Percentage of conditioned responses for the Paired (green circles), Unpaired (blue squares), and No Stimulus (red triangles) groups during the one-quarter length training blocks. Data points presented with mean ± SEM. All the groups start at the same point during the first session, but the Paired group exhibited significantly more CRs during the second session compared to the other two groups ($p = 0.016$). Overall, the number of CRs in the Paired group this early in training is on par with what we have previously observed. Contributing to the variability in the Paired group at the second time point, there were several rats (n = 7) that did not show any CRs in either block of trials. 65

Figure 7. Multiphoton microscopy (MP) data. A) Raw MP data measuring surface Kv1.2 expression on BC axon terminals for each of the groups. Numbers under the plots denote the number of subjects in each group. B) Mean ± SEM for each group. Planned comparisons did not reveal any differences between any of the groups. C) Same data as in Fig. 2B, but the Paired group is split between subjects that did not show any CRs during the two training blocks (Low; light green stripes) and subjects that showed CRs during the two training blocks (High; dark green stripes). Post hoc comparisons did not reveal any differences between the groups. 67

Figure 8. Biotinylation and Western Blot (WB) data showing Kv1.2 surface expression in both BC axon terminals and PC dendrites. Data displayed for the Paired, Unpaired, and No Stimulus groups. A) Raw WB Surface-to-Total ratio for each subject. Numbers under the plots for each group denote the number of subjects in that group. B) WB data normalized to the No Stimulus group (Mean ± SEM). Planned comparisons between each of the groups revealed a significant difference between the Unpaired and No Stimulus groups ($p = 0.04$), but no other significant effects. C) Paired group is split between subjects that did not show any CRs during the two training blocks (Low; light green stripes) and subjects that showed CRs during the two training blocks (High; dark green stripes). Post hoc comparisons revealed a significant difference between Paired Low and No Stimulus groups ($p = 0.012$). The significant difference between Unpaired and No Stimulus groups is depicted again. No difference was observed between Paired High and No Stimulus groups. (* denotes $p < 0.05$) 70

Figure 9. Conceptual depiction of what is happening to Kv1.2 surface expression in the (A) Unpaired groups in both experiments and (B) Paired groups in both experiments. Note that data for PC dendrites (green circles) are an inference from the combined results of WB (which measured PC dendrites and BC axon terminals) and MP (which measured only BC terminals). The Kv1.2 surface expression data are conceptualized as a function of (A) US strength and (B) CR expression. 92

Figure 10. Western blot showing surface Kv1.2 expression following surface probe with alkoxyamine-biotin-PEG4. Conditions marked in white text at bottom of the blot. Orange boxes denotes Surface Kv1.2 Expression in the +Biotin conditions. Green boxes denote evidence of permeabilization. Purple boxes denote slight signal when using a smaller than normal section for analysis. Strong Kv1.2 signal observed in 5 of 6 lanes probed with biotin. 117

Figure 11. Live cerebellar sections were treated with forskolin (100μm) or vehicle prior to fixation and TsTX-ATTO-594 incubation. Data points represent pinceaus extracted from Z-stack images for vehicle (black) and forskolin (red) treated sections. Reduced surface Kv1.2 expression in section treated with Forskolin, detected by multiphoton microscopy. 126

Figure 12. Boxplot outlier analysis for western blot (WB) data for Experiment 1. No outliers identified within The Paired (green), Unpaired (blue), and No Stimulus (Red) groups. 128

Figure 13. Boxplot outlier analysis for multiphoton microscopy (MP) data for Experiment 1. No outliers identified within the Paired (green), Unpaired (blue), or No Stimulus (red) groups. 128

Figure 14. Conditioned response (CR) onset latency for Paired (green circles) and Unpaired (blue squares) subjects (solid lines). The dotted lines represent the standard deviation of the CR onset latencies for each of the groups within each of the sessions. Responses scored as CRs for the Paired group remained consistent across the training sessions, while the timing of the "responses" score for the Unpaired group fluctuate within and across sessions. The dotted lines show the variability within each session. The variability within each session for the Paired group remains consistently low and the Unpaired group shows some variability. 131

Figure 15. Boxplot outlier analysis for Experiment 2 Western Blot (WB) Data. One outlier (*47) identified in this analysis as an outlier in the No Stimulus group. Three other subjects (1/group; circles) fell outside of error bars but not considered statistical outliers..... 132

Figure 16. Boxplot Analysis for Multiphoton Microscopy (MP) data for Experiment 2. No outliers were identified in this analysis. Two subjects show Kv1.2 surface expression on BC axon terminals that falls outside of error bars for Paired (n=1) and No Stimulus (n=1) groups. These subjects were not considered statistical outliers. 132

Figure 17. Boxplot outlier analysis for the Western Blot data from Experiment 2. Follow up analysis to determine if there were any other outliers after the subject in the No Stimulus group was removed. No other subjects identified as a statistical outlier. 135

Figure 18. Boxplot outlier analysis for Paired split data from Experiment 2. Subjects that did not show any CRs during the training blocks were split into the Paired Low group and subjects that showed any CRs during the two training blocks split into the Paired High group. One outlier (*13) identified in the Paired Low group 136

Figure 19. Boxplot outlier analysis for Paired Split groups for Multiphoton Microscopy data from Experiment 2. No subjects were identified as statistical outliers. Two subject in the Paired High group fall outside of the error bars but were not considered outliers. 137

Figure 20. Boxplot outlier re-analysis for Paired High and Paired Low groups on Western Blot data following removal of one outlier. No other subjects identified as outliers..... 139

Figure 21. Biotinylation and Western Blot (WB) data showing Kv1.2 surface expression in both BC axon terminals and PC dendrites. Data displayed as mean ± SEM for the Paired Low (No CRs during training blocks; light green stripes), Paired High (Any CRs during training blocks; dark green stripes), Unpaired (blue), and No Stimulus groups (red). Data normalized to the No Stimulus group. These data exclude one subject from Paired Low group that was identified as an outlier. Planned comparisons between each of the groups revealed a significant difference between the Unpaired and No Stimulus groups (p = 0.04), but no other significant effects. Post hoc comparisons between the four groups in Fig. 21 revealed a marginally significant difference between Paired Low and No Stimulus groups (p = 0.07). No Differences observed between Paired High and Paired Low, and Paired High and No Stimulus. (* denotes p <0.05; □ denotes p = 0.07). 140

Figure 22. Photo of a parasagittal section of cerebellum following an infusion of ATTO-TsTX-594 into the lobulus simplex of the cerebellar cortex above the base of the primary fissure. The infusions (red) is limited to regions of the anterior lobe, lobulus simples, and remains above the deep cerebellar nuclei region. 142

LIST OF ABBREVIATIONS

Alphabetically
AC – adenylyl cyclase
Acq – acquisition
AMPA – α-Amino-3-hydroxy-5-methyl—4-isoxazoleproprionic
ANOVA – analysis of variance
BC – basket cell
cAMP – cyclic adenosine monophosphate
CF – climbing fiber
cGKI – cyclic guanosine protein kinase I
cGMP – cyclic guanosine monophosphate
CI – conditioned inhibition
CNQX –6-cyano-7-nitroquinoxaline-2,3-dione
CR – conditioned response
CS – conditioned stimulus
DAO – dorsal accessory olive
DCN – deep cerebellar nuclei
DSI – depolarization-induced suppression of inhibition
EBC – eyeblink conditioning
EMG – electromyogram
EPSC – excitatory postsynaptic current
EPSP - excitatory postsynaptic potential
GC – granule cell
IO – inferior olive
IPN – interpositus nucleus
IPSC – inhibitory postsynaptic current
IP_3 –inositol 1,4,5-triphosphate
ISI – interstimulus interval
LTD – long-term depression
MF – mossy fiber
mGluR – metabotropic glutamate receptors
MP – multiphoton microscopy
m1 mAchR – muscarinic-type acetylcholine receptor 1
NMDA – N-methyl-D-aspartic acid
NO – nitric oxide
OLR – outlier labeling rule
PC – Purkinje cell
PCX – pinceaux
PF – parallel fiber
PKA – protein kinase A
PKC – protein kinase C
PLC – phospholipase C
ROI – region of interest
SK – small conductance calcium-active potassium

TRPC – transient receptor protein canonical
TsTX – tityustoxin-Kα
US – unconditioned stimulus
VGCC – voltage-gated calcium channel
WB – Western blot

CHAPTER 1: COMPREHENSIVE LITERAURE REVIEW

Section 1.1: What is Eyeblink Conditioning?

Eyeblink conditioning (EBC) is a form of classical conditioning that is a powerful model for studying the underlying neural mechanisms of learning and memory. In EBC, an initially neutral conditioned stimulus (CS) is paired with an eyeblink-eliciting unconditioned stimulus (US). The CS is typically a tone or a light, while the US may be a mild periorbital shock or corneal air puff. At the outset of conditioning, the US will elicit a reflexive eyeblink. As training progresses, however, the organism will learn to make an eyeblink conditioned response (CR) to the CS prior to the onset of the US. In delay EBC the CS and US overlap with the CS presentation occurring first and the US being presented at the end of the CS period; the two stimuli terminate at the same time. In extinction of EBC, the procedure is similar, but the US is omitted.

Delay EBC is an effective paradigm for studying the neural mechanisms of learning and memory for several reasons. (1) The stimuli used for conditioning are simple; a tone, light, or tactile stimulus are used for the CS and an eyeblink reflex eliciting stimulus is used for the US such as a periorbital shock or corneal air puff; (2) the eyeblink CR is simple to measure and simple to quantify based on the timing with the CS. (3) Finally, the neural pathways responsible for encoding and expressing the eyeblink CR are very well known (McCormick and Thompson, 1984a, Thompson and Krupa, 1994, Christian and Thompson, 2003, Ramnani, 2006, Thompson and Steinmetz, 2009). Since the neural pathways for EBC have been so well studied and much is known about acquisition of the eyeblink CR, EBC is a suitable paradigm to study the cellular and molecular underpinnings of learning and memory.

Section 1.2: Cerebellar Anatomy

There are several ways to understand the anatomy of the cerebellum. Grossly, there are several main areas: the medial portion is called the vermis, laterally from there are the lateral hemispheres, and ventral and lateral to the hemispheres are the flocculi and paraflocculi (Glickstein et al., 2011). The organization of the cerebellum was based on comparative anatomy research done by several researchers (Glickstein et al., 2011), but a popular system for understanding cortical anatomy was developed by Larsell (1952). This system identifies 10 major cortical divisions (lobules I-X) in the cerebellar cortex (Glickstein et al., 2011). Within the cerebellum, there are two distinct regions: the cerebellar cortex and deep cerebellar nuclei.

The cortical anatomy is distinctive. There are three layers with specific cell types in each that comprise the layers. The outer most layer is the molecular layer. This layer is comprised of Purkinje cell (PC) dendrites, parallel fibers (PFs) from granule cells (GCs), and two types of inhibitory interneurons, stellate cells and basket cells (BCs), that form synapses with PCs. Below that layer is the PC layer comprised of the somas of PCs aligned across the cortical regions. Below that is the granule layer, which is comprised of GCs and PC axons. GCs send axons up towards the molecular layer where their axons bifurcate and form excitatory synapses with PCs. PC axons project down through the granule layer and form inhibitory synapses with the neurons within the deep cerebellar nuclei (DCN) (Thompson and Steinmetz, 2009), with the exception of PCs in the flocculus and paraflocculus that project to the vestibular nucleus. The primary nuclei within the DCN are the dentate (lateral) nucleus, the two interpositus nuclei (anterior and posterior), and fastigial nucleus (medial). Each nucleus receives cortical input from PCs

in specific regions of the cerebellar cortex (Glickstein et al., 2011). Figure 1 represents a simplified version of cerebellar anatomy as it pertains to EBC (also see below).

Section 1.3: Eyeblink Stimulus Pathways

EBC is dependent upon an intact ipsilateral cerebellum (McCormick et al., 1982a). There is an extensive body of literature examining both the CS and US pathways to the cerebellum as well as research examining the role of the cerebellar cortex, DCN and non-cerebellar regions along the EBC pathways (McCormick et al., 1983, McCormick and Thompson, 1984a, b, McCormick et al., 1985, Mauk et al., 1986). For instance, tone evoked neural responses have been measured in several different areas associated with auditory processing including the superior colliculus, pontine nuclei (PN), periaqueductal gray, and other structures that correspond to brainstem regions important for EBC (McCormick et al., 1983). The CS and US are relayed through brainstem nuclei to the cerebellar cortex (McCormick et al., 1985, Mauk et al., 1986). The CS information is gathered in the auditory, visual, and somatosensory subcortical areas depending on the sensory modality and information is then projected to the PN in the brainstem (Glickstein et al., 1980, Brodal and Brodal, 1981, McCormick et al., 1983, Steinmetz et al., 1986, Steinmetz et al., 1987, Knowlton and Thompson, 1988, Freeman et al., 2005). From here, axons called mossy fibers (MFs) project directly to the cerebellar cortex, forming excitatory synapses with GCs in the granule layer (Brodal and Brodal, 1981, Woodruff-Pak et al., 1988). Axon collaterals from the PN also project to the interpositus nucleus (IPN) (Brodal and Brodal, 1981, Voogd and Glickstein, 1998). GCs then project axons up to the molecular layer of the cerebellar cortex, where they bifurcate

and form excitatory synapses with PC dendrites and BCs (Mittmann et al., 2005, Sultan and Glickstein, 2007). The axons projected from the granule layer to the molecular layer of the cerebellar cortex are called PF. It was determined that ~175,000 synapses are formed on a single PC from a network of PFs (Napper and Harvey, 1988). Studies have confirmed that the PN and its projections form the CS pathway in the cerebellum. For example, Steinmetz and colleagues abolished tone-conditioned CRs by making lesions to the PN (Steinmetz et al., 1987). This study showed that the dorsolateral and lateral portions of the PN are both involved. The lesions encompassed both areas and led to the abolition of the learned responses, indicating the necessity of this region for EBC. While this site is necessary, it is not the site where learning occurs. This was demonstrated through stimulation of the PN in replace of the typical auditory tone as the CS (Steinmetz et al., 1986, Freeman et al., 2005). In fact, stimulation of the PN as the CS produces super conditioning, and in a model of abnormal development, stimulation of the PN allows the organism to overcome developmental deficits (Freeman et al., 2005).

The primary nucleus involved in relaying the US information to the cerebellum is the dorsal accessory olive (DAO) of the inferior olivary nucleus, referred to here as the inferior olive (IO). This nucleus receives somatosensory information from cranial nuclei including the motor trigeminal nucleus and relays (through the middle cerebellar peduncle) that information via climbing fibers (CFs) directly to PCs in the cerebellar cortex and collaterals to the IPN (Brodal and Brodal, 1981). It was shown that one CF will create ~26,000 synapses with individual PCs (Nieto-Bona et al., 1997, Ito, 2002). Lesions of the inferior olive prevent learning if made prior to conditioning and facilitate extinction when made after the CR is learned (McCormick et al., 1985). Research has

shown that electrical stimulation to this area can serve as a US (Mauk et al., 1986, Steinmetz et al., 1989).

Section 1.4: Eyeblink Response Pathways

There are two responses in EBC: the conditioned eyeblink response and the unconditioned, or reflexive eyeblink response. While the two responses observed in EBC paradigms share activation of the facial motor nucleus as the final common neural output, they are very different in appearance. The reflexive blink in response to the US is brief and only coincides with the US. The CR on the other hand is an anticipatory or learned response to the tone CS that is sensitive to the inter-stimulus interval (ISI; the interval from CS onset to US onset) (Kreider and Mauk, 2010). When conditioning commences, the CS exerts no control over the eyelid muscles. After repeated pairings of the two stimuli, the output of the cerebellar cortex is modified to make a CR temporally associated with the ISI, where shorter latency CRs will be made to shorter ISIs and longer latency CRs will reflect longer ISIs (Chen and Thompson, 1995, Medina et al., 2000, Svensson et al., 2010).

The IPN of the DCN has been referred to as the start of the eyeblink CR pathway (Chapman et al., 1990). This is substantiated by the findings that stimulation of the IPN in naïve animals produces eyeblinks (Chapman et al., 1988) and lesions of the IPN abolish previously learned eyeblink CRs (McCormick and Thompson, 1984b). From the IPN, the CR information is relayed through the superior cerebellar peduncle to the red nucleus and from there to the abducens, facial nuclei, PN, red nucleus, and the IO (McCormick et al., 1983, Thompson and Steinmetz, 2009). The eyeblink CR and

reflexive eyeblink UR share some of the same brainstem nuclei for governing the responses (Thompson and Steinmetz, 2009). Despite shared reliance on the abducens (eyeball retraction and nictitating membrane response in rabbits) and facial (eyelid movement) nuclei, lesions to the abducens nucleus spare the eyeblink CR in rabbits while the nictitating membrane UR is abolished (Steinmetz et al., 1992). Similarly, lesions to the superior cerebellar peduncle or red nucleus abolish CRs, but URs remain intact (McCormick et al., 1982b).

While the IPN is reported to be the start of the eyeblink CR pathway, modulation of cerebellar cortical output is necessary for the acquisition of the response (McCormick and Thompson, 1984b, Garcia and Mauk, 1998, Garcia et al., 1999). PCs in the cerebellar cortex provide the sole, inhibitory output of the cerebellar cortex and innervate the neurons of the IPN (Teune et al., 1998). The tonic inhibition of the IPN by PCs may be attributed to the recent finding that PCs contain an abundance of low threshold vesicles ready to be released (Kawaguchi and Sakaba, 2015). In another experiment, using infusions of $GABA_A$ receptor antagonist picrotoxin or reversible lesions with $GABA_A$ receptor agonist muscimol, researchers were able to dissect the role of the cerebellar cortex prior to and after acquisition of EBC (Garcia et al., 1999). Rabbits were trained to make a nictitating membrane CR (equivalent to eyeblink CR in rats) to a tone CS. Once learning was established, picrotoxin – a $GABA_A$ antagonist – was infused into the IPN prior to a test session. By infusing picrotoxin, GABA-mediated inhibition of the IPN was blocked and the rabbits continued to show CRs; the CRs however had a shorter latency to onset (Garcia and Mauk, 1998). In the same animals, muscimol – a $GABA_A$ agonist – was infused into the same region and resulted in the abolition of the CR (Garcia and

Mauk, 1998). Furthermore, infusions of muscimol into the IPN prior to acquisition prevented learning (Krupa et al., 1993). Rabbits continued to receive EBC training after the infusions were no longer inhibiting the IPN and appeared naïve to the stimuli, indicating the infusions of muscimol prior to training prevented learning (Krupa et al., 1993). If, however, the infusions are made into the red nucleus – a downstream target of the IPN and an important nucleus in the expression of eyeblink CRs – expression of CRs was blocked but learning still occurred. This was shown by the immediate emergence of the learned CR expressed once the infusions were no longer inhibiting the response pathway (Krupa et al., 1993). Together, these data indicate that the IPN is involved in the acquisition and expression of CRs and that PC inhibition of the IPN is important for precise timing of the response. The necessity of the cerebellar cortex for acquisition of eyeblink CRs was demonstrated by others (Yeo and Hardiman, 1992, Freeman et al., 1995, Gruart and Yeo, 1995, Garcia et al., 1999), showing that lesions to the cerebellar cortex prevents acquisition of eyeblink CRs, lending support for the idea that there are two primary areas of plasticity in the cerebellum and that cortical plasticity is necessary for acquisition of eyeblink CRs (Garcia et al., 1999).

Section 1.5: Acquisition of Eyeblink Conditioned Responses

The acquisition of an eyeblink CR is dependent upon modulation of PC output; in order for a CR to be made, PCs must be briefly inhibited, leading to disinhibition of the IPN (Garcia and Mauk, 1998, Garcia et al., 1999, Attwell et al., 2001). This was demonstrated by infusions of the α-Amino-3-hydroxy-5-methyl—4-isoxazoleproprionic (AMPA) /kainate receptor antagonist, 6-cyano-7-nitroquinoxaline-2,3-dione (CNQX) in

the cerebellar cortex prior to acquisition. Infusions of CNQX prevented learning from taking place such that when the infusion dissipated, the rabbits appeared behavioral naïve to the stimuli (Attwell et al., 2001). Since PCs provide the sole, inhibitory output of the cerebellar cortex through projections to the IPN (Harvey and Napper, 1991), mechanisms must be in place to alter the inhibition of PCs on the IPN. Researchers have postulated that there are two primary sites of plasticity that EBC is dependent upon (Mauk and Donegan, 1997). The first site of plasticity is in the cerebellar cortex, where PF (relaying the CS) and CF (relaying the US) input co-synapse with PC dendrites. The second site is hypothesized to be between MF projections and neurons of the IPN.

Section 1.5.1: Mossy Fiber-to-Interpositus Nucleus Synapse

The connection between MFs and the neurons of the IPN (MF-IPN) was hypothesized to be important for acquisition and expression of CRs (Mauk and Donegan, 1997, Medina and Mauk, 1999). Research cited above points to the IPN as the start of the eyeblink CR pathway (McCormick and Thompson, 1984a, Freeman and Nicholson, 1999). Furthermore, when the cerebellar cortex is disconnected from the IPN, an eyeblink CR can still be exhibited (McCormick and Thompson, 1984a), but it may take the form of a short latency CR to the tone (Ohyama et al., 2006). The MF-IPN connection seems to play an important role in acquisition and expression of CRs. For instance, physical or pharmacological ablation of the IPN prevents acquisition of CRs (Lavond and Steinmetz, 1989, Chapman et al., 1990, Clark et al., 1992, Steinmetz et al., 1992) and can also abolish previously learned CRs (Chapman et al., 1990, Steinmetz et al., 1992). Gould and Steinmetz (1996) showed increased single-unit activity when examining firing rates of

IPN neurons later versus earlier in acquisition. Berthier and Moore (1990) showed increased activity in neurons in the IPN and dentate nucleus on trials in which a CR was exhibited. The responses of neurons in the DCN are not uniform, but the collective firing patterns in these regions seem to be related to the generation and expression of eyeblink CRs (Berthier and Moore, 1990). There is evidence of anatomical changes that correspond with the CR. For instance, rats that received paired (CS-US) training, compared to unpaired or no stimulus training, had more synapses in the IPN than the other two groups (Kleim et al., 2002). Not only does this show that there are anatomical changes that occurred during learning, but it supports the idea of increased synaptic connections through pre-cerebellar areas involved in the eyeblink pathway. A similar result was reported by De Zeeuw and colleagues, showing increased axonal sprouting and more varicosities on mossy fiber axons forming synapses with the neurons of the IPN (Boele et al., 2013). This effect was region specific and depended upon the type of training; no changes were reported in areas not associated with EBC and no increases were observed in untrained mice.

A mechanism that may be accompanying changes at the MF-IPN synapse is intrinsic plasticity changes in the neurons of the IPN. Aizenman and Linden reported increased sensitivity of IPN neurons to MF inputs following strong depolarization (Aizenman and Linden, 2000). Increased calcium influx through N-methyl-D-aspartic acid (NMDA) receptor activation or direct depolarization produced persistent increases in intrinsic excitability (Aizenman and Linden, 2000). Although this experiment was done in the presence of picrotoxin to block $GABA_A$ receptors, the data point to a way MF input to the DCN can modulate the neurons to aid in acquisition of an eyeblink CR. Here,

rather than altering the expression of AMPA receptors, a hallmark of long-term plasticity changes, they reported increased excitability of the neurons as measured by a decrease in spike threshold and increased maximum firing rate (Aizenman and Linden, 2000). These experiments were done with the IPN in isolation from other synaptic input; however, these basic changes to the excitability of neurons may be an important underlying mechanism for EBC.

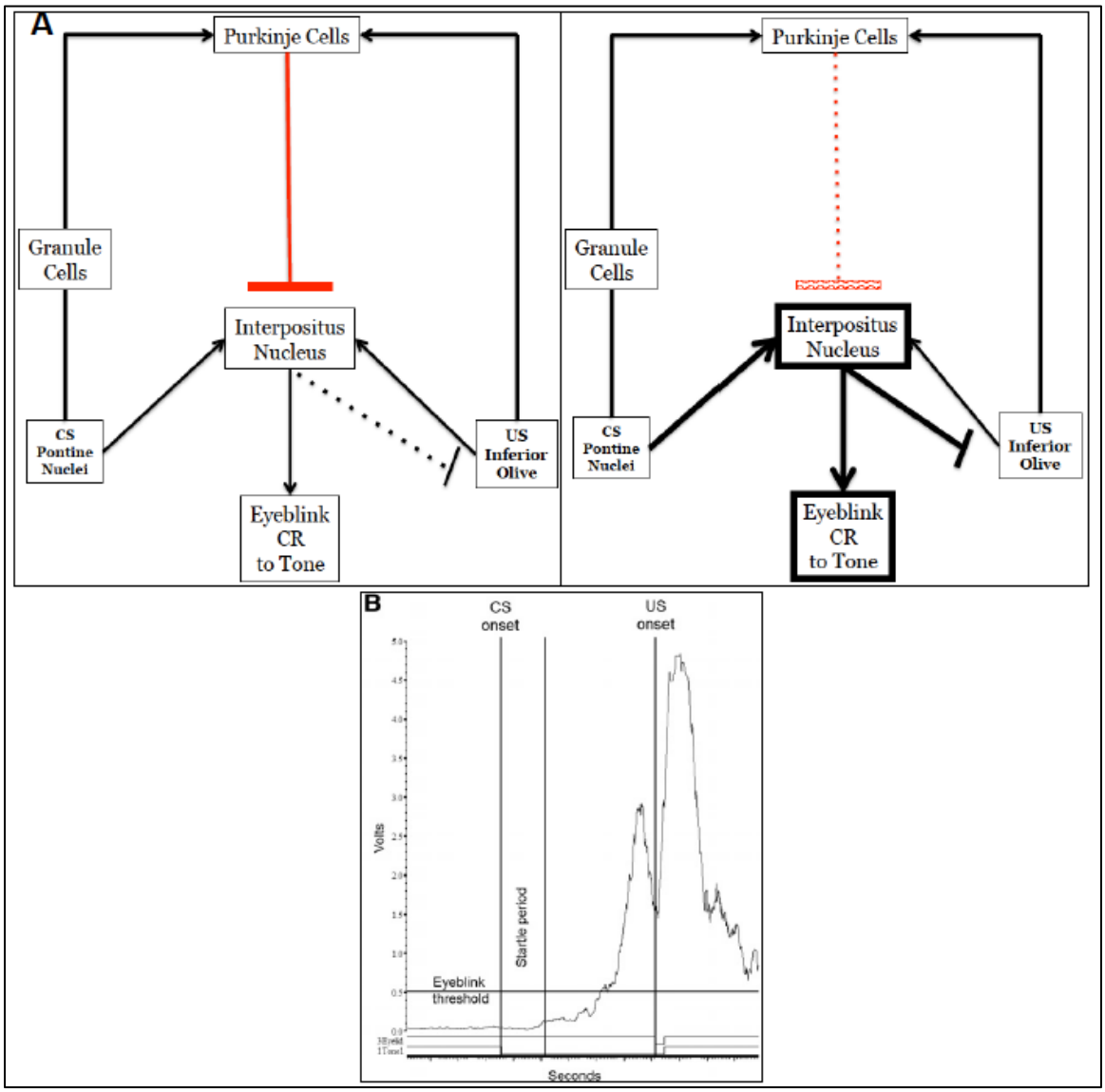

Figure 1. Brainstem and cerebellar neural pathways involved acquisition of eyeblink classical conditioning. (A) Briefly, Purkinje cells represent the sole, inhibitory output of the cerebellar cortex. IN doing so, they tonically inhibit the neurons of the interpositus nucleus (IPN). The stimulus information is projected through modality-specific brainstem nuclei and then to the cerebellar cortex. Axon collaterals are also projected to the neurons of the IPN. In order for an eyeblink conditioned response to be initiated by the neurons of the IPN, the tonic inhibition of PCs must be listed. The response is projected through various brainstem nuclei that control closure of the eyelid muscle. (B) Example of a well-time eyeblink conditioned response. Responses are scored as CRs if the magnitude of the response exceeds the response threshold. CRs can be distinguished from unconditioned responses based on the timing and amplitude; eyeblink responses should occur temporally close to US onset but will precede that stimulation and the amplitude greater than the activity in between trials (from Fuchs et al., 2014).

Section 1.5.2: Parallel Fiber-to-Purkinje Cell Synapse

Postsynaptic long-term depression (LTD) is hypothesized to occur at synapses formed by CS-carrying PFs and PC dendrites (PF-PC). During EBC when the CS is present, PFs increase the excitability of PC dendrites and at the end of the CS period when the US is presented, CF input strongly excites the PC dendrites (Berthier and Moore, 1986). The first demonstration of PF-PC LTD was shown by stimulation of both pathways that led to a decrease in the excitability response in PCs both briefly after the stimulation and for a prolonged period following multiple trials (Ito et al., 1982). Furthermore, they showed that neurons displayed reduced sensitivity to glutamate following similar stimulations, indicating the glutamate may mediate this PC response (Ito et al., 1982). Work from Eccles and colleagues demonstrated the effectiveness of CF activation of PC dendrites. When CFs become active, PCs display a complex spike that is indicative of calcium influx. Climbing fibers were shown to reduce excitatory post-synaptic potentials (EPSPs) in the cerebellum following a tetanus of stimulation (Eccles et al., 1966). In another preparation, LTD was induced via stimulation of PF and CF in the rabbit paraflocculus (Kano and Kato, 1988). When stimulating CF and PF in isolation, there is a little effect on PC excitability; when they stimulated both pathways, an LTD-like effect that persisted for up to one hour was observed (Ito and Kano, 1982). The LTD effect was blocked in the presence of AMPA and NMDA receptor antagonists as well as when the CF pathway was blocked with lidocaine or tetrodotoxin (Kano and Kato, 1988). Other data suggest that an ISI of 250ms (Ekerot and Kano, 1989), similar to the ideal interval between CS onset and US onset for producing EBC, was ideal to produce LTD and that shorter ISIs, simultaneous stimulation, and backward pairings

were unable to achieve LTD, even after an extended number of pairings (Chen and Thompson, 1995). To study this *in vivo*, certain conditions must be mimicked to elucidate the underlying mechanisms. The presence or absence of GABA antagonists plays a large role; when GABA antagonists were present, the LTD-like response at PF-PC synapses was more profound than when GABA antagonists were absent (Alkon et al., 1993). Schreurs and Alkon (1993) showed that co-stimulation of PFs and climbing fibers without the presence of GABA antagonists led to LTD of the PF-PC synapse. When stimulation mimicked *in vivo* conditions where PF activation was paired with depolarization-induced calcium release (Kawaguchi et al., 2011), there was a profound and long-lasting EPSP depression at this synapse.

The hallmark of long-term plasticity is the trafficking of surface-expressed AMPA receptors, and this is especially true in PF-PC synapses (Wang and Linden, 2000). Trafficking of AMPA receptors can be observed on both the pre- and post-synaptic sides of this synapse, and depending on the stimulus parameters, LTP or LTD can be observed (Coesmans et al., 2004, Gao et al., 2012). For the purpose of this review and project, I will focus on LTD on the post-synaptic side. Several researchers identified protein kinase C (PKC) as an effector of LTD induction (Crepel and Krupa, 1988, Linden and Connor, 1991, Linden et al., 1991). LTD in PC dendrites results from a decrease in AMPA-mediated current; AMPA-mediated current was maintained when PKC was inhibited (Crepel and Krupa, 1988, Linden and Connor, 1991), reduced when PKC was activated (Linden and Connor, 1991), and importantly, endocytosis via clathrin-dependent mechanisms was identified as the mediator for this effect (Wang and Linden, 2000). This finding was substantiated by results that showed that clathrin-mediated attenuation of

AMPA currents through activation of the insulin receptor pathway and induction of LTD occluded one another, lending support for clathrin-mediated endocytosis of AMPA receptors as mechanism for LTD in PCs (Wang and Linden, 2000). This research suggests that AMPA receptor endocytosis is necessary for the induction of LTD at PF-to-PC synapses.

The idea of PF-PC LTD being necessary for the acquisition of cerebellar dependent behaviors, such as eyeblink conditioning has been debated. One such paper examined three mechanisms previously implicated in the induction of LTD at this synapse (Schonewille et al., 2011). Here, the researchers employed: a PICK1 knockout mouse that acts as a necessary intermediary between PKC and internalization of AMPA; a GluR2Δ7 knock-in mouse, which interferes with GluR2's interaction with PICK1 and GRIP1/2 through deletion of the last 7 amino acids important for the formation of the AMPAR C-terminal tail; and a GluR2K882A knock-in mouse, which prevents phosphorylation at S880 by PKC and internalization of AMPA receptors while leaving other second messenger pathways intact (Schonewille et al., 2011). Contrary to very specific eliminations targeting AMPA receptor internalization, a presumed integral part of LTD at this synapse, the researchers did not observe any related deficits in learning across three different cerebellar-dependent tasks despite deficits in LTD induction (Xia et al., 2000).

An important signaling molecule for the induction of LTD is calcium (Linden et al., 1991). Intracellular calcium concentrations are increased in PC dendrites through several external mechanisms, including activation of L-type voltage-gated calcium channels (VGCCs) (Liljelund et al., 2000), activation T-type and P/Q-type VGCCs after

dendritic depolarization (Womack et al., 2004, Womack and Khodakhah, 2004), and some permeability through AMPA receptors (Burnashev et al., 1992), as well as internal mechanisms such as inositol 1,4,5-triphosphate (IP_3)-mediated calcium release (Ross et al., 2005) typically activated by Group I glutamatergic activation of metabotropic glutamate receptors (mGluRs) (Finch and Augustine, 1998, Takechi et al., 1998). The training signal that is provided by CFs is recorded as a complex spike (De Zeeuw et al., 2011). Furthermore, CF evoked calcium currents reduce components of the complex spike waveform recorded in PCs (Weber et al., 2003), indicating that the CF input to PCs is important for the induction of LTD. Hansel and Linden (2000) reported that calcium from the CFs provides an important training signal to PC dendrites. Without this input, calcium concentrations within the dendrite may be sub-threshold to induce LTD expression mechanisms, such as AMPA receptor internalization (Coesmans et al., 2004).

There are several other molecules involved in the intracellular cascade that can alter AMPA expression in PC dendrites (Ito, 2002, Hartmann and Konnerth, 2005). For instance, LTD and cerebellar learning were impaired in mice lacking a gene specific for cyclic guanosine monophosphate (cGMP)-dependent protein kinase I (cGKI) (Feil et al., 2003). Cyclic GKI has been shown to be a modulator of LTD within the nitric oxide (NO) pathway of PCs (Feil et al., 2003). NO is released from PFs and has receptors on the post-synaptic side (Ito, 2002). Mice lacking this specific modulator were impaired in the induction of LTD as well as in the adaptation of the vestibular ocular reflex (VOR), another cerebellar-dependent learned behavior (Feil et al., 2003).

Research suggests a role for mGluRs in LTD and acquisition of eyeblink CRs (Linden et al., 1991, Aiba et al., 1994, Miyata et al., 2001, Kishimoto et al., 2002, Ohtani

et al., 2014). Metabotropic GluRs are the post-synaptic glutamate target for both PFs and CFs (Tanaka et al., 2000); thus knocking out this receptor in the mouse model led to widespread deficiencies that were evident in ataxic movements, impaired LTD as measured by a distinct lack of decreased excitatory postsynaptic currents (ESPCs) recorded from PCs, and impaired EBC (Aiba et al., 1994). Furthermore, using an mGluR1 knock-in rescue mouse expressing these receptors in PCs, EBC can be restored (Kishimoto et al., 2002), leading to the conclusion that mGluR1 receptors are necessary for LTD and EBC. Ohtani et al. (2014) explored the role of mGluR1 by examining how the length of the C-terminal tail affects LTD. By both knocking out mGluR1 globally and rescuing the receptor with two different PC-specific knock-in mice, Ohtani et al. (2014) were able to further dissect the pathway involved in the induction of LTD through activation of mGluRs. The knock-in mice included a short or long variant of the C-terminal domain, which mimic endogenous splice variants of the channel (e.g. mGluR1a and mGluR1b) (Ohtani et al., 2014). The functional length of the C-terminal corresponds to different signaling cascades within PCs, with the long variant mediating LTD and eyeblink conditioning through IP_3-mediated calcium influx and the shorter domain governing transient receptor protein canonical (TRPC) channels (Ohtani et al., 2014). They showed that the longer variant rescued LTD induction mechanisms and cerebellar dependent eyeblink conditioning better than the short variant. Furthermore, activation of this channel increased calcium entry through IP_3-mediated signaling (Ohtani et al., 2014).

Similar results reported in the mGluR1 papers were shown with mGluR4 receptor knockout mice (Pekhletski et al., 1996), with the exception that this receptor is primarily targeted by only PFs. One target of mGluR activation is the phospholipase C system

(PLC) (Sugiyama et al., 1999, Hashimoto et al., 2001, Miyata et al., 2001). PLC activates IP_3 (Ito, 2002) which, downstream, increases internal calcium concentration (Sarkisov and Wang, 2008, Finch et al., 2012). IP_3 is first produced through activation of mGluRs that activates PLC (Doi et al., 2005). When CFs strongly depolarize PC dendrites, the IP_3 then causes a release of internal calcium stores, which coincides with influx of calcium from VGCCs (Doi et al., 2005). This detect of spike timing is consistent with timing necessary for induction of LTD in cerebellar learning.

Section 1.6: Basket Cells in the Cerebellar Cortex

Direct modulation of PC output by inhibitory interneurons in cerebellar cortex may be an important mechanism for acquisition of EBC and has been an understudied area related to cerebellar learning. BCs are small inhibitory interneurons that reside in the molecular layer of the cerebellar cortex. BCs are innervated by PFs (Mittmann et al., 2005) and BC axons project down to the PC layer and form "basket" like synapses on PCs around the PC soma known as pinceaux (PCX) (McNamara et al., 1993, Laube et al., 1996, McNamara et al., 1996, Voogd and Glickstein, 1998). BC inhibition of PCs is exerted through the β2 $GABA_A$ subunit (He et al., 2015).

BCs are also targets of retrograde transmission for secretin (Yung et al., 2001, Ng et al., 2002, Lee et al., 2005, Yung et al., 2006), glutamate (Glitsch and Marty, 1999, Satake et al., 2000, Duguid and Smart, 2004, Satake et al., 2006), and endocannabinoids (Kreitzer and Regehr, 2001a, b, 2002) released from depolarized PCs. Since BC axon terminals form inhibitory synapses on PCs near the axon hillock, they are strategically located to regulate PC output and thus, the output of the cerebellar cortex.

Section 1.7: Kv1.2 and Its Regulation

Kv1.2, an α-subunit of the *Shaker* (Kv1) family of voltage-gated potassium channels, is a delayed rectifier channel that is selectively permeable to K^+ ions (Stuhmer et al., 1988, Miller, 2000). Six transmembrane segments structurally form Kv1.2: The first four segments are responsible for pore forming and gating and the last two are responsible for the voltage-sensitive properties (Baumann et al., 1988, Pongs et al., 1988, Stuhmer et al., 1988). The electrophysiological properties of Kv1.2 are similar to an I_D-current sensitive to TEA (Brew and Forsythe, 1995). Kv1.2 serves as a delayed-rectifier channel with an outward rectifying A-type current, which opposes membrane excitability of the axon terminals of BCs (Southan and Robertson, 1998b). When this channel is blocked or the surface expression is reduced, a greater number of depolarizing events are observed (Nesti et al., 2004, Ebner-Bennatan et al., 2012).

BC inhibition of PCs is in part regulated by Kv1 channels containing Kv1.2 subunits. Channels containing this subunit are densely expressed on BC axon terminals (McNamara et al., 1993, Wang et al., 1993, Wang et al., 1994, Veh et al., 1995, Bekele-Arcuri et al., 1996, McNamara et al., 1996, Koch et al., 1997, Southan and Robertson, 1998a, b, 2000, Chung et al., 2001) and PC dendrites (Koch et al., 1997). In fact, a quantitative study using autoradiography reported that Kv1.2 on BC axon terminals represents ~50% of cerebellar Kv1.2, with the remaining expressed throughout the molecular layer (Koch et al., 1997). Interestingly, overlapping expression of Kv1.1 and Kv1.2 was shown in BC axon terminals, whereas in the molecular layer, in particular on PC dendrites, Kv1.1, Kv1.2, Kv1.3 and Kv1.6 were expressed (Koch et al., 1997). In an

immunoprecipitation experiment, the most frequent combination of subunit expression was Kv1.1/Kv1.2 heterotetramers, with some of those containing other subunits (Wang et al., 1994, Veh et al., 1995, Koch et al., 1997). The pharmacological inhibition of Kv1.2 on BCs in the cerebellum increases inhibitory postsynaptic currents (IPSCs) recorded from PCs (Southan and Robertson, 1998a, b, 2000). This result was indicative of neurotransmitter release from BCs because the effect was blocked by bicuculline, a competitive antagonist of the $GABA_A$ receptor (Southan and Robertson, 1998b). Furthermore, deletion of β2 $GABA_A$ subunit prevented inhibitory synaptic plasticity between BCs and PCs (He et al., 2015).

The regulation of Kv1.2 is very important for its function (Nesti et al., 2004). Only surface expressed proteins show active current and suppression of surface channel suppresses its ionic current (Nesti et al., 2004). The regulatory pathways for Kv1.2 have been identified in *in vitro* cell systems and mammalian tissue (Huang et al., 1993, Cachero et al., 1998, Hattan et al., 2002, Nesti et al., 2004, Williams et al., 2007, Connors et al., 2008), and these pathways have been verified in cerebellar tissue (Williams et al., 2012). Surface expression of Kv1.2 has been shown to be regulated by activation of the muscarinic-type acetylcholine receptor 1 (m1 mAchR) (Huang et al., 1993, Tsai et al., 1999); these data identified a possible stimulus-induced mechanism for Kv1.2 expression. Activation of m1 mAchR led to the activation of PLC and direct tyrosine phosphorylation of Kv1.2 (Huang et al., 1993). Morielli and colleagues confirmed these findings and showed that endocytic trafficking of Kv1.2 by tyrosine kinases serve as a primary suppressor of Kv1.2 ionic current (Nesti et al., 2004). In addition to tyrosine phosphorylation regulating the ionic current of Kv1.2, Morielli and colleagues showed

that tyrosine phosphorylation plays a role in the interaction between cortactin, an actin binding molecule, and Kv1.2 (Hattan et al., 2002). Activation of m1 mAchRs reduces the interaction between cortactin and Kv1.2 and resulted in the reduction in the ionic current displayed by Kv1.2 (Hattan et al., 2002, Williams et al., 2007). In addition, Connors and colleagues teased apart the intracellular pathways leading to the regulation of Kv1.2, and found that cyclic adenosine monophosphate (cAMP) maintains homeostatic expression of Kv1.2. Increasing or decreasing cAMP leads to differential effects on Kv1.2 surface expression and ionic current; decreasing levels of cAMP increased surface expression of Kv1.2 through protein kinase A (PKA), while increasing cAMP levels also increased Kv1.2 surface expression, independent of PKA (Connors et al., 2008). The PKA-independent pathway appears to involve adenylyl cyclase (AC); when AC is increased using forskolin, Kv1.2 surface expression was increased (Connors et al., 2008).

Section 1.8: Kv1.2 Regulation by Secretin in the Cerebellar Cortex

The regulation of surface Kv1.2 expression is influenced by secretin in cerebellar tissue (Williams et al., 2012). Secretin, a neuropeptide that is endogenously expressed in PCs in the cerebellar cortex (Yung et al., 2001), was first identified by Bayliss and Starling in the early part of the 20th century (Bayliss and Starling, 1902) as a hormone secreted in pancreas. Recently, it was been studied as a neuropeptide in the cerebellum (Ishihara et al., 1991, Chow, 1995, Yung et al., 2001, Koves et al., 2002, Ng et al., 2002, Nozaki et al., 2002, Chey and Chang, 2003, Koves et al., 2004, Tay et al., 2004, Lee et al., 2005, Siu et al., 2006, Yung et al., 2006, Yuan et al., 2011, Miller et al., 2012, Zhang and Chow, 2014, Zhang et al., 2014). Secretin is hypothesized to function as a retrograde

transmitter that is released from PCs. First, secretin and its receptor are expressed in the cerebellum (Yung et al., 2001). The secretin receptor is expressed on the PCs and interneurons within the lower regions of the molecular layer, such as BCs; secretin mRNA was only found in PCs (Yung et al., 2001, Koves et al., 2002, Koves et al., 2004). As measured by an *in vivo* enzyme immunoassay sampling for changes in secretin release in real-time, the parameters necessary for secretin release were measured (Lee et al., 2005). Secretin release is dependent upon excitation and depolarization of PCs (Lee et al., 2005). Furthermore, secretin release is dependent opening of calcium and sodium channels; blocking calcium channels with cadmium attenuated secretin release, whereas increasing the concentration of potassium increased secretin release (Lee et al., 2005). In the presence of higher potassium concentrations, tetrodotoxin and cadmium both attenuated increased secretin release, suggesting a role for voltage-dependent channels during strong membrane-depolarizing events (Lee et al., 2005). Secretin release from PCs was shown to be dependent upon L-type and P/Q-type VGCCs, as shown by the attenuated secretin release in the presence of nimodipine and Omega-agatoxin IVA, respectively (Lee et al., 2005). The parameters necessary for secretin release as shown in Lee et al. (2005) are similar to events in PCs during climbing fiber input (Ohtsuki et al., 2009, Piochon et al., 2010, Kitamura and Hausser, 2011, Maiz et al., 2012) including calcium entry though VGCCs and NMDA receptors on PCs. Increased calcium entry leads to secretin release from PCs (Lee et al., 2005).

Since the secretin receptor is expressed on both PCs and BCs, secretin can act on either target (Ng et al., 2002). Secretin was shown to have an effect on PC excitability; application of secretin *in vitro* while recording from PCs resulted in an increase of

miniature IPSCs (mIPSCs) (Yung et al., 2001), a current that is indicative of increased GABAergic input to PCs (Yung et al., 2001). It is noteworthy that the application of secretin did not alter glutamatergic input from PFs to PCs (Yung et al., 2001). The modulation of GABAergic input to PCs was shown to be dependent upon proper signaling of the secretin receptor (Yung et al., 2001).

The secretin receptor is a G_s-protein coupled receptor (Siu et al., 2006), where activation leads to increases in AC which leads to increases cAMP concentrations, very similar to the increases in cAMP necessary for trafficking of Kv1.2 (Siu et al., 2006, Connors et al., 2008, Williams et al., 2012). In fact, secretin-mediated increases in mIPSCs in PCs were attenuated by SQ22536, a specific inhibitor of AC (Yung et al., 2001). Additionally, there may be a role for AMPA receptor-mediated enhancement of GABA release from BCs. Blockade of AMPA with CNQX in the presence of secretin reduced mIPSC frequency (Lee et al., 2005). Furthermore, in the presence of AMPA receptor agonists, there was an increase in mIPSC frequency, but not amplitude and this effect was blocked by two different AMPA receptor antagonists (Lee et al., 2005).

The pathways activated by secretin and necessary for secretin's effects on PCs appear similar to the regulatory pathway for Kv1.2 trafficking. If secretin were involved in the regulation of Kv1.2, this could account for some of the findings showing that secretin increases GABAergic input to PCs from BCs (Yung et al., 2001). Thus, the hypothesis linking secretin to Kv1.2 regulation was tested through examination of surface Kv1.2 expression following application of secretin and other activators and inhibitors along the pathway. Cerebellar sections treated with forskolin, an activator of AC, showed reduced Kv1.2 surface expression (Williams et al., 2012), mimicking the effects of

secretin. When sections were treated with secretin and SQ-22636 or KT-5720, inhibitors of AC and PKA respectively, there was no change in surface Kv1.2 expression (Williams et al., 2012). Furthermore, the finding that secretin is released from PCs was also tested by showing that blocking GABA-A receptors with Gabazine reduced surface expression of Kv1.2 (Williams et al., 2012); this may be through increasing membrane depolarization of PCs and increasing secretin release. The effect of decreased surface Kv1.2 expression by endocytosis was attenuated by blocking L-type and P/Q-type VGCCs with Nimopidine and Agatoxin IVA respectively (Lee et al., 2005, Williams et al., 2012). These data point to the idea that secretin is released from PCs (Yung et al., 2001, Lee et al., 2005) and plays a role in the inhibition of PCs, through the regulation of surface Kv1.2 expression (Williams et al., 2012). These data also corroborate the internal signaling pathway highlighted by Connors et al. (2008).

Section 1.9: Kv1.2 in Eyeblink Conditioning

Based on previous research, the mechanisms for Kv1.2 regulation and trafficking are well-understood. Given that Kv1.2 is densely expression at the BC-PC pinceaus (Koch et al., 1997, Chung et al., 2001) and this synapse can exert strong effects on cerebellar cortical output, it was hypothesized that these mechanisms may serve a purpose during EBC. To test this hypothesis we performed intracerebellar cortical infusions designed to alter the function or expression of Kv1.2 and examined acquisition and extinction of EBC.

Section 1.9.1: Blockade of Kv1.2 and Eyeblink Conditioning

In a first look into the role of Kv1.2 *in vivo* in mammalian EBC, we infused a specific blocker of Kv1.2 prior to acquisition of EBC. By blocking Kv1.2 in a localized region of the cerebellar cortex, we were able to extend the *ex vivo* results reported by Southan and Robertson (1998a; 1998b; 2000). Blocking Kv1.2 on BC axon terminals results in increased GABAergic input to PCs (Southan and Robertson, 1998a, b, 2000). Therefore, infusions of tityustoxin (TsTX) – a highly selective blocker of Kv1.2 channels (IC_{50} = 0.550 nM) with little affinity for Kv1.1 (Werkman et al., 1993, Hopkins, 1998) that shares a binding site and function with α-dendrotoxin (Southan and Robertson, 1998a, b, 2000) – were hypothesized to facilitate the inhibition of PCs during EBC and produce faster learning than vehicle infusions. Rats received intracerebellar infusions of either tityustoxin-Kα (TsTX; 1μl; 1μg/μl) or vehicle immediately prior to the first six of seven days of acquisition of EBC. Rats that received TsTX prior to acquisition learned more quickly than the rats that received vehicle infusions over the same time period (Williams et al., 2012). These data suggest that Kv1.2 may play an important role in the acquisition of EBC. The blockade of Kv1.2 results in increased mIPSCs in cerebellar sections (Southan and Robertson, 1998a, b, 2000), an effect that may have been mimicked by infusing TsTX into the cerebellar cortex. By infusing TsTX into a specific region within the cerebellum known to be important for acquisition of EBC, we facilitated EBC, potentially by increasing the inhibition of PCs and disinhibiting the IPN. Disinhibition of the IPN is hypothesized to allow CS-carrying MFs to more strongly activate the neurons within the IPN and allow CRs to be expressed more quickly than in

the vehicle treated group. Important for these data, we determined that infusions of TsTX are limited to regions associated with EBC (Appendix VII).

Section 1.9.2: Secretin and Eyeblink Conditioning

As discussed above, the mechanisms by which secretin exerts its effects on excitability of BCs and inhibitory input to PCs provide a potential mechanism for acquisition of EBC. That is, secretin released during a depolarizing event in PCs that evokes calcium transients leads to increased inhibitory drive in PCs. If CF input during EBC were able to cause the release of secretin as a retrograde transmitter, then manipulating this system may have effects on acquisition of EBC. The role of secretin in EBC was examined in a series of experiments. First, we showed that intracerebellar infusions of secretin (1μg/μl) on the first three of six days of EBC led to a significant increase in the rate of learning; rats that received infusions of secretin learned to make the CR faster than rats the received intracerebellar infusions of vehicle (Williams et al., 2012). The opposite effect was observed when secretin (5-27), an antagonist of the secretin receptor, was infused into the cerebellar cortex prior to the first three of six days of EBC (Fuchs et al., 2014). By blocking the secretin receptor during acquisition, the increased inhibitory drive from BCs to PCs that would occur during EBC would be blocked, leading to slower acquisition rates in the rats that received intracerebellar infusions of secretin (5-27) versus vehicle controls (Fuchs et al., 2014). These behavioral data lend support for the idea that endogenous Kv1.2 regulatory mechanisms such as those involved in secretin modulate EBC.

Section 1.10: The Model

All of the data discussed above lead to a model for acquisition of EBC that may involve the regulation of Kv1.2. Data supporting this model include the finding that Kv1.2 is densely expressed at the BC axon terminals where they form inhibitory synapses with PCs (Koch et al., 1997, Chung et al., 2001) and PC dendrites (Koch et al., 1997). Functional data about the role of Kv1.2 in PC inhibition show that blocking this channel increases inhibition of PCs (Southan and Robertson, 1998a, b, 2000). This inhibitory drive from BCs to PCs is integral for the model because PCs represent the sole, inhibitory output of the cerebellar cortex, and is very important for EBC (Garcia and Mauk, 1998, Garcia et al., 1999). The target of PC output related to EBC is the IPN of the deep cerebellar nuclei (Thompson and Steinmetz, 2009). By modulating PC output, potentially by increasing the inhibition of PCs, we may observe increased learning rates during acquisition of EBC. The regulatory pathways for Kv1.2 overlap with the intracellular cascade initiated by secretin's activation of its receptor (Yung et al., 2001, Lee et al., 2005, Williams et al., 2012). That is, activation of the secretin receptor leads to AC mediated increases in cAMP which in turn increases PKA and results in phosphorylation of membrane proteins (Lee et al., 2005, Siu et al., 2006). This pathway shares important similarities to the regulation of Kv1.2, involving AC and cAMP (Connors et al., 2008). Functional evidence of the connection was shown when secretin applied to cerebellar sections increased mIPSCs in PCs (Yung et al., 2001). Importantly, the pathways worked out by the Chow lab were corroborated when looking at changes in Kv1.2 expression in cerebellar sections (Williams et al., 2012), showing that secretin facilitated Kv1.2 endocytosis and that blocking AC, cAMP, PKA, or clathrin prevented this change.

Finally, the function of Kv1.2 is dependent upon it being expressed on the surface (Nesti et al., 2004).

The data discussed above point to a model in which PCs, strongly depolarized by US projections in the cerebellar cortex during EBC, release secretin. Secretin, released from PCs acts as a retrograde messenger, decreases surface expression of Kv1.2 from BC axon terminals. Meanwhile, CS projections to the cerebellar cortex activate BCs and PCs via PFs. Those BCs with reduced surface Kv1.2 will provide greater inhibitory input to PCs. Thus, BCs with reduced surface expression of Kv1.2 will be in a position to more strongly inhibit the PCs with which they form synapses, PCs that also receive the US via CF input. Increased inhibition of PCs would be expected to disinhibit the IPN and allow acquisition and/or expression of eyeblink CRs. Thus, this mechanism could complement LTD at PF-to-PC synapses as a learning mechanism for EBC, by providing inhibition of PC spontaneous activity that would still be present even after PF-PC LTD (Hesslow et al. 2013).

Based on this model, it is hypothesized that rats that received EBC training will show reduced surface Kv1.2 expression compared to a group that receives explicitly unpaired CS and US presentations and a context control group that does not receive any stimuli during acquisition. It is hypothesized that Kv1.2 surface expression will be reduced using both a region-specific analysis examining the BC-PC synapse and a global measure of Kv1.2 surface expression that uses a validated biotinylation and western blot technique to quantify changes in Kv1.2 surface expression.

Section 1.11: Next Step

Behavioral data presented thus far provide evidence for our model of cerebellar function and EBC. Blocking Kv1.2 via infusions of TsTX prior to acquisition facilitated EBC (Williams et al., 2012). Infusions of secretin in the cerebellar cortex prior to conditioning also facilitated EBC, potentially by stimulating an endogenous pathway involved in regulation of Kv1.2 with an exogenous application of secretin (Williams et al., 2012). When that endogenous pathway was blocked by infusion of secretin (5-27), a specific secretin receptor antagonist, acquisition of EBC was impaired (Fuchs et al., 2014). Given these findings, the next step is to determine if Kv1.2 is regulated during conditioning. In other words, do we observe changes in Kv1.2 surface expression as a result of undergoing EBC?

CHAPTER 2: MEASURING CHANGES IN Kv1.2 EXPRESSION FOLLOWING EYEBLINK CONDITIOING

Introduction

Eyeblink conditioning (EBC) is a useful paradigm for studying the underlying neural mechanisms of learning and memory. In EBC, a behaviorally neutral conditioned stimulus (CS) is repeatedly paired with an eyelid-eliciting unconditioned stimulus (US). Initially, the CS, which is typically an auditory tone or light stimulus, exerts no control over eyeblink responses, but as conditioning progresses the organism will begin to make an eyeblink conditioned response (CR) to the CS. EBC involves a discrete brainstem-cerebellar circuit that is hypothesized to include the inhibition of Purkinje cells (PCs) leading to the disinhibition of the interpositus nucleus (IPN) and initiating an eyeblink CR (McCormick et al., 1982a, McCormick et al., 1983, Mauk et al., 1986). PCs and the neurons in the IPN receive converging CS and US input through their respective brainstem pathways (Thompson and Steinmetz, 2009). There is debate over the types of plasticity that are critical in the circuit (Hesslow et al., 2013), though the importance of PC inhibition is generally accepted.

One cerebellar synapse that is less well-studied in relation to EBC is the basket cell (BC)-to-PC synapse. An important aspect of this synapse for EBC research is that BCs form strong, inhibitory synapses with PCs near the axon hillock, suggesting this synapse plays an important role in the regulation of PC output (Southan and Robertson, 1998a, b, 2000, Williams et al., 2012). We are also interested in this synapse because of the expression of Kv1.2 – an alpha subunit of the *Shaker* family of voltage-gated potassium channels – which is densely expressed on BC axon terminals (Koch et al.,

1997, Chung et al., 2001). Kv1.2 is also, yet less densely, expressed on PC dendrites (Koch et al., 1997). The localized expression and regulation of Kv1.2 is important for its function (Nesti et al., 2004). Kv1.2 serves as a delayed rectifier channel, opposing membrane depolarization and shunting current as it travels down the axon (Cerda and Trimmer, 2010). Blockade of Kv1.2-containing channels resulted in increased GABAergic transmission from BCs to PCs (Southan and Robertson, 1998a, b, 2000), an effect similar to that observed when exogenous secretin is applied to cerebellar sections (Yung et al., 2001, Lee et al., 2005). Surface Kv1.2 expression in the cerebellar cortex is regulated by endogenous secretin (Williams et al., 2012) via an intracellular signaling cascade that includes adenylate cyclase (AC), cyclic adenosine monophosphate (cAMP), and protein kinase A (PKA) (Connors et al., 2008, Williams et al., 2012).

The role of Kv1.2 in EBC has been previously studied by pharmacologically manipulating its function and expression. The first demonstration linking Kv1.2 to EBC was done by infusing a selective and potent inhibitor of Kv1.2, tityustoxin-Kα (TsTX) (Werkman et al., 1993), into the cerebellar cortex prior to EBC. The subjects that received intracerebellar infusions of TsTX prior to EBC showed enhanced conditioning compared to subjects that received vehicle infusions (Williams et al., 2012). By blocking Kv1.2 in a location within the cerebellar cortex previously shown to be important for delay EBC, we showed enhanced learning. By blocking Kv1.2 in the cerebellar cortex, we hypothesize that we increased the inhibition of PCs by BCs to produce faster learning. Additionally, infusions of secretin into the same area of cerebellar cortex prior to acquisition also resulted in enhanced EBC (Williams et al., 2012) and infusions of secretin-(5-27), a selective secretin receptor antagonist, impaired EBC (Fuchs et al.,

2014). While these latter studies did not explicitly measure changes in Kv1.2 expression, the effects observed on learning rates are consistent with changes in Kv1.2 expression (Williams et al., 2012). The current experiment sought to measure changes in Kv1.2 surface expression as a product of EBC. We hypothesized that subjects that received Paired EBC training, compared to Unpaired or No Stimulus training would show reduced surface Kv1.2 expression in the cerebellar cortex. The subjects were assigned to one of three groups: Paired Group, Unpaired Group, or No Stimulus Group, that pertained to their training procedure. The Paired group received EBC training while the Unpaired group was presented with the same stimuli but in an explicitly unpaired fashion. The No Stimulus group served as a context control and did not receive any stimuli during training. Cerebellar sections were analyzed via multiphoton microscopy and biotinylation/western blot methods to measure BC terminal-specific *and* global changes in Kv1.2, respectively.

Material and Methods

Eyeblink Conditioning

Subjects

Male Wistar rats were purchased from Charles River (Quebec, Canada) and housed in pairs upon arrival with access to food and water ad libitum. Rats were single housed after surgery. The colony room was maintained on a 12 hour light-dark cycle (lights on at 7:00 AM and off at 7:00 PM). Rats weighed 200-300g prior to surgery. All behavioral testing took place during the light phase of the cycle and all procedures were

approved by the Institutional Animal Care and Use Committee at the University of Vermont.

Surgery

Surgeries took place 4-6 days after arrival. Surgeries were performed under aseptic conditions. Rats were anesthetized with 3% isoflurane in oxygen. A midline scalp incision was made. Once the wound had been cleaned and the skull was dried, four skull screw holes were drilled and skull screws were placed as anchors for the head stage. The eyeblink portion of the surgeries consisted of implantation of several electrodes. First, a bipolar stimulating electrode (Plastics One, Roanoke, VA) was positioned subdermally immediately dorsocaudal to the left eye. Two electromyogram (EMG) wires for recording activity of the orbicularis oculi muscle were each constructed of a 75-μm Teflon coated stainless steel wire soldered at one end to a gold pin fitted into a plastic threaded pedestal connector (Plastics One). The other end of each wire was passed subdermally to penetrate the skin of the upper eyelid of the left eye and a small amount of insulation was removed so that the bare electrodes made contact with the orbicularis oculi muscle. A ground wire was wrapped around two skull screws at one end and the other end was also soldered to a gold pin fitted into the pedestal connector. Once the ground wire, bipolar and EMG electrodes were implanted, all were cemented to the skull with dental cement. The wound was numbed with a local injection of 0.15 ml bupivacaine, spread out over 3-4 points around the wound. The wound was salved with antibiotic ointment (Povidone). At the end of the surgery, rats received subcutaneous injections of Lactated Ringers (1ml) for hydration and ~0.3ml (5mg/ml) Rimadyl (Carprofen) for post-operative analgesia. A

second injection of the same concentration was given ~24-hours after surgery. Rats were post-operatively checked daily for 4-5 days after surgery. Rats were given 5-6 days to recover prior to eyeblink conditioning.

Apparatus

Eyeblink conditioning took place in one of four identical testing boxes (30.5 x 24.1 x 29.2 cm; Med-Associates, St. Albans, VT), each with a grid floor. The top of each box was altered so that a 25-channel tether/commutator could be mounted to it. Each testing box was kept within a separate electrically-shielded, sound attenuating chamber (45/7 x 91.4 x 50.8 cm; BRS-LVE, Laurel, MD). A fan in each sound-attenuating chamber provided background noise of approximately 60 dB sound pressure level. A speaker was mounted in each corner of the rear wall and a light (off during testing) was mounted in the center of the rear wall of each chamber. The sound-attenuating chambers were housed within a walk-in sound-proof room.

Stimulus delivery was controlled by a computer running Spike2 software (CED, Cambridge, UK). A 2.8 kHz, 80 dB tone, delivered through the left speaker of the sound-attenuating chamber, served as the conditioned stimulus (CS). The CS was 365-ms in duration. A 15-ms, 4.0 mA uniphasic periorbital stimulation, delivered from a constant current stimulator (model A365D; World Precision Instruments, Sarasota, FL), served as the unconditioned stimulus (US) during conditioning. Recording of the eyelid EMG activity was controlled by a computer interfaced with a Power 1401 high-speed data acquisition unit and running Spike2 software (CED, Cambridge, UK). Eyelid EMG signals were amplified (10k) and bandpass filtered (100-1000 Hz) prior to being passed to the Power 1401 and from there to the computer running Spike2. Sampling rate was 2

kHz for EMG activity. The Spike2 software was used to full-wave rectify, smooth (10ms time constant), and time shift (10ms, to compensate for smoothing) the amplified EMG signal to facilitate behavioral data analysis.

Training Procedure

During the first two acquisition training sessions (Days 1 & 2), rats were placed into individual drawers on a rolling cart and transported from the colony room to the sound proof conditioning chambers. Rats were placed into the sound-attenuating conditioning chambers individually. The rats were connected to the tether first by the bipolar stimulating electrode and then by the EMG electrodes. During the final day of training (Day 3), rats were transported to the lab in the same fashion, but were placed into the conditioning boxes once at a time and the next rat was placed in the chambers once the rat before them finished 25% of the trials for that day. On Day 3, the starting times of each of the rats were staggered to allow time for perfusion and tissue harvest. Full sessions took 50-60 minutes and ¼ sessions took ~15 minutes. Throughout the experiment, group assignment and box assignment was counter-balanced so that all groups rotated through all of the boxes.

Once all rats were connected to their electrode tethers, their signals were checked on the oscilloscope and once stable, the programs were started. The Paired training program consisted of 100 CS-US paired trials separated by an average of 30 seconds (range: 20-40 seconds). See the Behavior Analysis section for trial analysis. The Unpaired training program consisted of 100 CS-alone trials and 100-US alone trials. These trials were intermixed throughout the session and were ordered pseudo-randomly, such that the rat could not anticipate which trial type was coming next. On Day 3, the

Unpaired training program was shortened, but the order of the trials remained the same as the previous days. The order of the first 50 trials (25 CS-alone & 25 US-alone) was repeated four times for the full training program. The No Stimulus "training" program consisted of 100 no stimulus trials. During these trials, the same sampling parameters were used during the other two training programs, but no stimuli were delivered. These rats remained in the boxes for an equivalent amount of time as the other groups.

Rats were transported back to their home cages once the program finished on Days 1 and 2. On Day 3, once a subject completed four one-quarter sessions, they were transported via another rolling cart to the room where the perfusion would take place.

Behavior Analysis

For the Paired and Unpaired groups, CS-US or CS-alone trials, respectively, were subdivided into three time periods: (1) a "baseline" period, 280-ms prior to CS onset; (2) a non-associative "startle" period, 0-80ms after CS onset; and (3) a "CR" period, 81-350ms after CS onset. In order for a response to be scored as a CR, eyeblinks had to exceed the mean baseline activity for that trial by 0.5 arbitrary units during the CR period. Eyeblinks that met this threshold during the startle period were scored as startle responses and were analyzed separately. The primary behavioral dependent measure for all experiments was the percentage of trials with an eyeblink response during the "CR period" across all 100 CS-US Paired trials (Paired group), 100 CS-alone trials (Unpaired group; the 100 US-alone trials were not analyzed), or comparable "trial periods" for the No Stimulus group for each session.

The percentage of CRs was the primary dependent measure. These data were analyzed using repeated measures ANOVAs comparing between groups across sessions.

As a confirmation, a one-way ANOVA was run comparing between the groups on the final day of acquisition. The criterion for a significant effect was an α-level of 0.05 or below. The other measures that were examined included CR onset latency, CR amplitude, and CR magnitude. The inclusion criteria for the Paired group was a minimum of 40% CRs during one of the four sessions on the last day.

Western Blot and Multiphoton Microscopy

Generation of Parasagittal Cerebellar Sections

Immediately after the third session of training, rats were deeply anaesthetized using isoflurane. A transcardial perfusion was used to remove the blood and fix the brain. During the perfusion, ~100 ml of 1X PBS (Life Technologies) and ~100ml of 4% paraformaldehyde (Thermo Scientific) were flushed through the circulatory system. Prior to dissecting the cerebellum out, an incision was made bisecting the cerebellum from the cerebrum, another to bisect the cerebellum from the brainstem, and a final one to bisect the hemispheres of the cerebellum through the vermis. Only the left hemisphere (ipsilateral to the eye receiving the US) of the cerebellum was harvested for analysis.

Cerebella were stored in cold PBS in 50ml conical tubes for about 60-90 minutes prior to sectioning. The tubes were kept either in the refrigerator or on ice prior to sectioning. The left hemisphere of the cerebellum was mounted onto the cutting stage of a vibratome using Krazy glue. The glue was allowed to dry for about 1 minute. The cutting stage was filled with ice-cold PBS. In order to section out the region around the base of the primary fissure where the eyeblink microzone is located (Steinmetz and Freeman, 2014), 1,200μm of tissue from the lateral portions of the hemisphere was first

removed. Once down to the appropriate medial-lateral depth, four 400μm sections were kept and placed into individual wells in a 24 well plate that remained in an ice bath.

After the sectioning, half of the sections were used for multiphoton microscopy and the other half were analyzed using biotinylation and western blot methods. The sections were assigned to one of the two experiments in a way that ensured that each slice had an adjacent section in the other experiment. The first and third sections were assigned to the western blot analysis and the second and fourth sections were assigned to the multiphoton analysis. The biotinylation and western blot experiments were performed first while the multiphoton sections were stored at 4°C for about an hour prior to staining.

Biotinylation

Each section assigned to the biotinylation and Western blot (WB) method was transferred into its own well in a new 12-well plate containing 1ml of 1X PBS in each well. The well plate was kept in an ice bath unless otherwise noted. For oxidation, the PBS was replaced with 1ml of 1mM sodium meta-periodate (SMP) for 30 minutes at 4°C. Sections were rinsed with ice-cold PBS and then incubated with 50mM alkoxyamine-biotin-PEG4 (Biotin) for two hours at room temperature. The biotin reaction was quenched with ice-cold 50mM TRIS in PBS. Sections were transferred into individual 1.5ml centrifuge tubes containing RIPA buffer plus 10% HALT protease inhibitor (Life Technologies). Sections were sonicated at 25% amplitude, twice for 2-4 seconds. All centrifuge tubes were spun down at high speed for 20 minutes at 4°C. From the centrifuge tubes, 200μl was transferred to separate tubes marked as “Total” and the remaining ~800μl was transferred to new centrifuge tubes marked “Beads” containing 40μl of rinsed (in RIPA buffer), Neutravidin beads (Beads; Sigma). The biotinylation

sample was incubated with the Beads for one hour at 4°C on a rotating centrifuge tube holder.

After incubation with the Beads, the centrifuge tubes were spun down at 2,000 RPM at 4°C for two minutes. The supernatant was transferred to tubes marked as the "Post" fraction. The Beads were rinsed with RIPA buffer three times for five minutes per rinse. Each rinse consisted of replacing the RIPA, allowing the centrifuge tubes to spin on the rocker, and spin down in centrifuge at the previously mentioned speed and time. Following the last rinse, the Beads were dried and using a vacuum pump with a 27G needle on the end. The beveled tip of the needle was kept on the side of the centrifuge tube and the RIPA buffer was vacuumed out, leaving dry beads on the bottom of the tube. Sample buffer (100mM DTT; 2.5X sample buffer) was added to each sample and centrifuge tubes were mixed. For the Post and Total fractions, 50µl of each was transferred to individual new centrifuge tubes and 50ul of sample buffer (200mM DTT plus 5X sample buffer) was added to each tube, bringing the final concentration to 100mM DTT plus 2.5X sample buffer. All of the samples were incubated for 10 minutes at 55°C. After the incubation, centrifuge tubes were spun down at high speed for ~15 seconds, mixed, and spun down again. All samples were kept at room temperature while gels were being prepped.

Gel Preparation

For this experiment, 10% polyacrylamide, 1mm, 15 lane gels were cast. The "Running Gel" layer consisted of 1.45ml ultra pure water, 1.25 Running gel buffer, 1.65ml Acrylamide (National Diagnostics; Athens, GA), 0.65ml Bis-Acrylamide (National Diagnostics), 25µl of 10% ammonium persulfate (APS; Bio Rad; Hercules,

CA), 10µl TMED (Thermo Fisher), and running layer gels were poured to 4ml. Approximately 1ml of sec-butanol was placed on top of the gel while the gel polymerized for at least 20 minutes. The "Stacking Layer" consisted of 2.73ml ultra pure water, 1.25ml Stacking gel buffer, 0.72ml Acrylamide, 0.29ml Bis-Acrylamide, 25µl of 10% APS, and 10µl TMED. The stacking layer was poured over the Running Layer. A 1mm, 15-lane comb was inserted between the panes of glass holding the gel and air bubbles were replaced with extra Stacking Layer solution. The "Stacking Layer" was allowed to polymerize for at least 45 minutes. Once polymerized, gel lanes were stained with dye and rinsed. The protein ladder marker (4µl; Thermo Scientific) was loaded into one of the outside lanes. For each sample, 15µl of the supernatant was loaded into each lane. Gels were run for 90-95 minutes at 100V. Gels were then transferred to nitrocellulose membrane for one hour at 100V. After the transfer was complete, the blots were placed in 3% bovine serum albumin (BSA; Sigma) for one hour in light-protected boxes. The blots were incubated overnight at 4°C in the following primary antibody concentrations: mouse monoclonal anti-Kv1.2 antibody (1:5000) and rabbit polyclonal anti-calbindin antibody (1:2000). Primary was rinsed off and blots were incubated for one hour in secondary antibodies: Goat anti-mouse-700 (GAM-700) secondary (1:2000) and goat anti-rabbit-800 (GAR-800). Blots were rinsed again prior to imaging.

Imaging Western Blots

All gels were imaged on an Odyssey Infrared Imager (LI-COR, Lincoln, NE, USA). All blots were scanned with a focal distance of 0.0mm and channel intensities remained at 5.0 for both channels across weeks. Images of the blots were analyzed using the same LI-COR software. Rectangular regions of interest (ROI) were drawn around the

Kv1.2 and calbindin expressed in each lane. Numbers were recorded and copied to Microsoft Excel ®. To determine the ratio of surface to total Kv1.2, background was measured outside of the ROI areas on the blot and subtracted from the measured number per lane per condition. For the ratio of surface Kv1.2-to-total Kv1.2, surface values were divided by Total values. The data are presented by using the raw ratios as well as by normalizing the data to the No Stimulus group. A rectangular region of interest (ROI) was drawn around the Kv1.2 band on the surface and total/post blots. Raw ratios consisted of surface expression divided by respective total Kv1.2 lanes. The normalization procedure consisted of dividing the surface-to-total ratios for each subject by the average of the surface-to-total ratios for the No Stimulus group. The baseline or No Stimulus group expression was equal to zero, and the Paired and Unpaired groups either increased or decreased from that value (Fig. 2B). Data are compiled in Graph Pad Prism 6 (Graph Pad Software, La Jolla, CA, USA) and group values are presented using the mean ±SEM.

Multiphoton Microscopy

After the generation of parasagittal cerebellar sections, half of the sections (see assignment above) were analyzed using multiphoton microscopy.

TsTX-ATTO-594 Stain

Slices were kept in individual wells on a 12 well plate in 1X PBS. Sections were incubated in the fluorescently conjugated TsTX, from the scorpion *Tityus serrulatus*, ATTO-TsTX-594 (4nm; Alomone, Israel) overnight at 4°C. TsTX has a high affinity for Kv1.2 containing channels (IC_{50} = 0.550 nM) with little affinity for Kv1.1 (Hopkins,

1998). Sections remained in TsTX-ATTO-594 for 18-20 hours. Sections were then rinsed with ice-cold PBS, post-fixed for one hour at room temperature with 4% paraformaldehyde (Thermo Scientific), rinsed again, and stored at 4°C for ~18 hours prior to imaging.

Multiphoton Microscopy

All images were acquired on an LSM 7 microscope system (Zeiss). Multiphoton excitation was generated by a Coherent Chameleon Vision II Titanium Sapphire pulsed IR laser with dispersion compensation (Coherent Inc.; Santa Clara, CA). The stage was a motorized Prior Z-deck which was fully integrated into the Zeiss Zen software. The objective was a 20X Plan Apo 1.0 NA DIC VIS-IR water immersion lens. The System frame was a Zeiss Axio Examiner specifically optimized for multiphoton microscopy. All images were taken using the same acquisition parameters to allow us to measure changes in Kv1.2 surface expression from slice to slice and to allow us to compare between weeks and conditions. ATTO (Ex: 601 Em: 627) was excited using laser power at 3% tuned to 820nm and the detector gain was maintained at 1000 (Range: 300-1100).

Regions of interested were identified first by illuminating the base of the primary fissure in each section using the light projected through the condenser. The lens was dropped into the PBS and focused until a layer of PCs were visible through the eyepiece. The microscope was then shielded from light and control was converted to the computer. The “Z-stack” and “Tile Scan” functions were used in combination to acquire an image that covered a wide area (~ the bottom half of 1 lobule) while also acquiring three-dimensional images of the pinceaux (PCX) region on the Z-axis. A small region, approximately the size of one of the tiles of the scan was used to set the upper and lower

limits of the Z-stack range. The lower limit was usually when the PCX disappeared from view because the laser power could not penetrate all the way through the tissue. The upper limit of the Z-stack was set by the top of the tissue. The true top of the tissue was not used because the background fluorescence saturated the frame, but just below that level was set as the upper limit. The Tile Scan range was set with the Z-stack function off. To set the Tile Scan range, the center of the Z-stack range was used and single layer scans over a wide area were used to restrict the area to be scanned. Once the area was selected, the zoom was increased to 1.5 and the Tile Scan was increased by one frame on the X- and TsTX-axis. The extra zoom increased the resolution of the images by focusing in on that region. The Z-stack function was turned back on and both features were used to acquire the image. While taking the images, the microscope would cycle from the base to the top of the Z-stack and then move to the next tile. Tiles were acquired from left to right and the microscope cycled back to the left when finished with a row. Only one image was acquired from each section; the image was focused on the base of the primary fissure in the cerebellar cortex. Images were restricted to ~50-100 Z-sections thick and the tile scan range was set so it did not leave the base of the primary fissure area. Images were saved as ".lsm" files and were saved under an anonymous name, indicative of their spot in the 12-well plate.

Image Analysis

Images were opened and analyzed in Image J (NIH). Images were converted to 32-bit images. The background fluorescence was subtracted from each section using a "rolling ball" technique. The rolling ball width was set to 50 pixels and was applied to each Z-section. Next, a Z-projection was used to get the maximum intensity of all of the

sections. Depending on the shape of the lobule being imaged, either all of the Z-sections were included in the maximum projection or a subset of them. When a subset or more were used, it was noted and efforts were made to avoid analyzing certain pinceaus more than once. If subsets of the Z-sections were used, an individual Maximum and Sum projection were used for each range of Z-sections (Fig.2). The threshold was then adjusted so that most of the PCX were visible, but the rest of the tissue was saturated out. The threshold was then set so that only intensities above a certain value (varied between images) were visible. Then, using a mask feature, individual PCX were isolated. This mask was used to pick out objects later in the analysis procedure. Another Z-project was taken using the sum of the Z-sections in the image. A ratio of the summed image to the maximum image referencing the masked image was used to select PCXs from the summed image and data were taken from objects with the range of 50-500 pixels. Of those objects, data were taken on the area, number of pixels, integrated intensity, mean, and standard deviation. Data were compiled in Microsoft Excel ® and graphed in Prism6 (Graph Pad, La Jolla, CA, USA).

Kv1.2 Surface Expression Data Analysis

Data analysis for both the multiphoton microscopy (MP) and biotinylation and western blot (WB) measures of surface Kv1.2 expression used a one-way ANOVA between the groups. Independent samples t-tests were used for planned comparisons between the Paired and Unpaired groups, Unpaired and No Stimulus groups, and the Paired and No Stimulus groups. The criterion for a significant effect was $p < 0.05$.

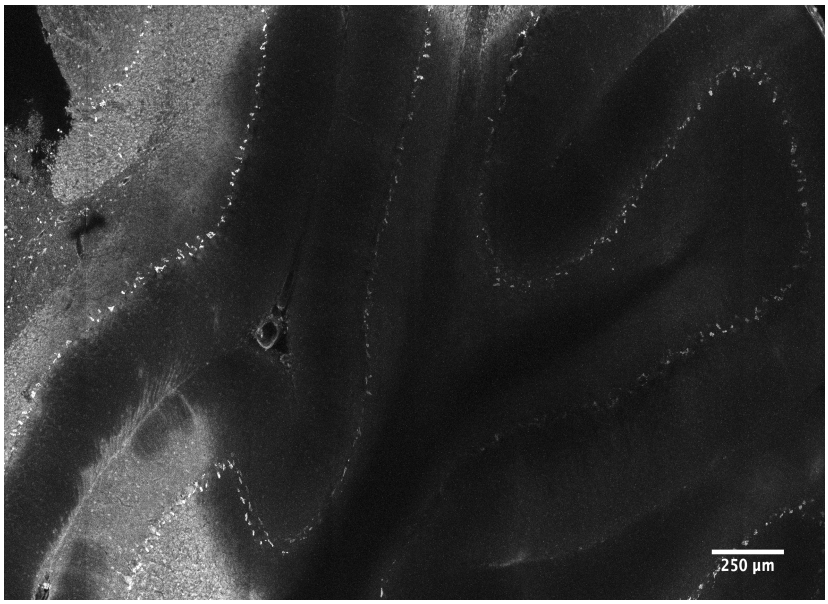

Figure 2. Black and white image of maximum projection of cerebellar section taken on LSM 7 multiphoton microscope system. Brighter punctate staining throughout cortex represents surface Kv1.2 tagged with ATTO-TsTX-594 on basket cell axon terminals. Image created by taking a maximum projection of a Z-stack, compressing the pixels by the maximum value. The maximum projections used to create a mask to identify pinceaus from a sum projection of the same Z-projection.

Results

Eyeblink Conditioning Behavioral Analysis

The goal of this experiment was to determine if we could observe changes in Kv1.2 surface expression following EBC. Kv1.2 surface expression was measured following three days of Paired CS-US training (n = 20), Unpaired CS-alone and US-alone training (n = 20), or no stimulus training (n = 21). The numbers of subjects in each group was determined based on their signals during training. Some of the subjects were removed from one or both of the post-mortem analyses; those subject numbers are noted in their respective sections. Based on previous research we hypothesized that the Paired group would show a reduction in surface Kv1.2 expression at the BC-to-PC synapse measured by multiphoton microscopy (MP) and across the entire section measured by biotinylation and western blot (WB) analysis.

The three-day acquisition (Acq) procedure produced a high level of eyeblink CRs in the Paired group only (Fig. 3). Since the third and final day of acquisition consisted of four blocks of ¼ the length of a normal training session (with short breaks in between blocks), the behavioral data were analyzed several ways. First, a 3(Group: Paired, Unpaired, No Stimulus) by 3(Session: Acq1, Acq2, Acq3) repeated measures analysis of variance (ANOVA) was used to analyze the acquisition data. In this analysis, the mean of the four blocks of trials was used to represent the third day. Additionally, the four blocks of trials were analyzed separately, to determine if the subjects in the Paired group had plateaued in their performance. The first 3(Group: Paired, Unpaired, No Stimulus) by 3(Session: Acq1, Acq2, Acq3) repeated measures ANOVA revealed a significant main effect of session, $F(2,116) = 87.55$, $p < 0.001$, a significant main effect of group, $F(2,58) = 276.86$, $p < 0.001$, and a significant group by session interaction, $F(4,116) = 76.20$, $p < 0.001$, showing that there were significant differences between the groups and only the Paired group showed a significant increase in the percentage of CRs (Fig. 3). A separate 3(Group) by 4(session: Acq3_1, Acq3_2, Acq3_3, & Acq3_4) repeated measures ANOVA was conducted on just the four blocks of trials for the third day of acquisition. This analysis revealed a significant main effect of group, $F(2,58) = 302.73$, $p < 0.001$, but no other significant effects, indicating that the groups were significantly different from one another, but their performances had plateaued (Fig. 3). Overall, Figure 3 shows a robust learning curve for the paired group that is consistent with learning rates observed with a shorter delay interstimulus interval (ISI) procedure from our lab (Fuchs et al., 2014) and others (Steinmetz and Freeman, 2010, 2011). The “responses” made by the Unpaired and No Stimulus groups during the sampling times do not represent CRs for

several reasons: (1) There is no positive contingency between the CS and the US for the Unpaired group and (2) the number of responses recorded remains very low and consistent across all of the training sessions.

Immediately following the last day of acquisition training, rats were anesthetized, perfused with paraformaldehyde, and cerebellum ipsilateral to the eyelid that was stimulated and recorded from was harvested. In general, four 400μm parasagittal sections were taken from each rat and two sections were assigned to each of the analyses. If there was a problem with the sectioning or with another step in the protocol, some rats (MP: Paired = 2, Unpaired =3, No Stimulus = 3; WB: Paired = 1, No Stimulus = 1) only had one section representing them in the data. The missing sections were not systematic, but sporadic; for example, a rat could have two sections for MP and only one for WB. If a subject had two sections, then an average of the two was taken to represent that subject. Examples of reasons why no data were collected from certain sections include poor section quality, an inability to locate the base of the primary fissure, poor fixation, or the section being damaged under the lens of the microscope.

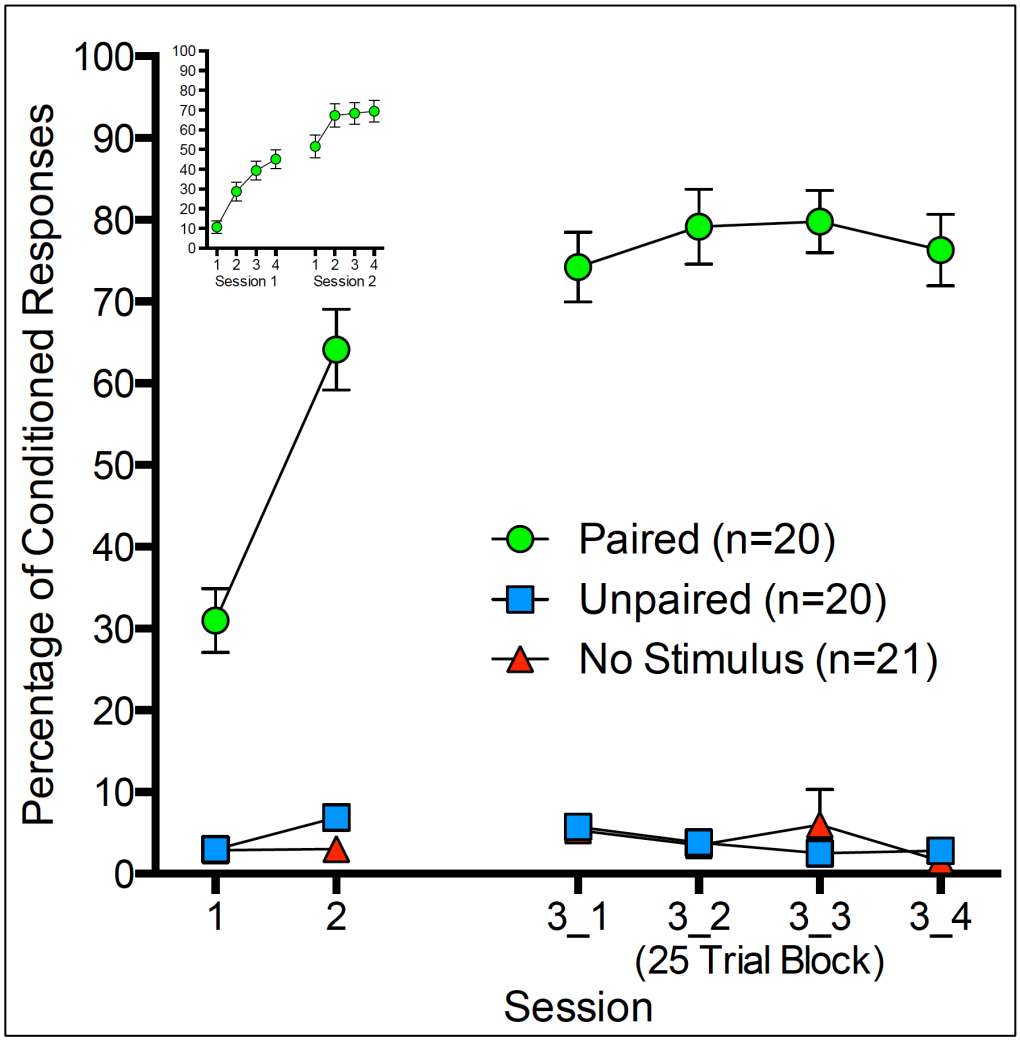

Figure 3. Acquisition data plotted by session for Paired group (green circles), Unpaired group (blue squares), and No Stimulus group (red triangles). Each session consisted of 100 CS-US trials (Paired group), 100 CS-alone and 100 US-alone trials, intermixed (Unpaired group), or 100 "trials" without any stimuli (No Stimulus group). The Paired group showed a significantly greater percentage of trials with a CR than either of the other two groups ($p < 0.001$). Inset: Sessions 1 and 2 displayed as 25-trial blocks for the Paired group.

Outlier Analysis for Both Measures

Prior to data analysis for both the MP and WB measures, the data were tested for outliers within the groups and measures. First, data were plotted on boxplots to determine if a standard deviation analysis would isolate any outliers. This analysis did reveal any outliers within either measure or any of the groups (Appendix II). The second method

was the Outlier Labeling Rule (OLR), developed by Tukey and colleagues (Hoaglin et al., 1986, Hoaglin and Iglewicz, 1987). This outlier analysis method relies on the distributions and quartile percentage limits of the data to mathematically determine if there are outliers. Consistent with the boxplot analysis, the OLR did not reveal any outliers in either of the measures or within the groups. The factor used in this analysis was shown to be conservative by identifying only extreme outliers that fall outside of the normal distribution by several standard deviations (Appendix II).

The two techniques that were used in this experiment provided complementary data about what is happening to Kv1.2 surface expression at the two main expression sites within the cerebellar cortex: BC axon terminals and PC dendrites. It should be mentioned that the WB blot technique not only represents surface Kv1.2 expressed on PC dendrites, but also measures surface Kv1.2 expressed on BC axon terminals. Two between-group comparisons were planned prior to data acquisition: Paired vs. Unpaired and Paired vs. No Stimulus, to be tested by using independent samples t-tests. For consistency with data analytical techniques within this field, both measures were first analyzed by using a one-way ANOVA.

Multiphoton Microscopy - Kv1.2 Surface Expression on Basket Cell Terminals

Kv1.2 is expressed in two distinct sites in the cerebellar cortex, BC axon terminals and PC dendrites (Koch et al., 1997). Kv1.2 is densely expressed on the surface of BC axon terminals where they form inhibitory synapses near the axon initial segment of PCs (Fig. 2). This synapse is strategically located to strongly regulate PC output, inhibition that is important for acquisition of EBC. It was hypothesized that three days of

paired CS-US presentations resulting in robust learning during EBC would produce a reduction in Kv1.2 surface expression on BC axon terminals. This was measured by taking three dimensional images on a multiphoton microscope of cerebellar sections probed with a fluorescently conjugated version of tityustoxin (ATTO-TsTX-594), a highly selective blocker of Kv1.2 (Werkman et al., 1993, Hopkins, 1998), to measure changes in Kv1.2 surface expression between groups of rats that received Paired CS-US training (n = 20), explicitly Unpaired CS-alone and US-alone training (n = 20), or equivalent exposure to only the training context (No Stimulus; n = 21). A one-way ANOVA yielded a significant main effect of group $F(2,58) = 4.15$, $p = 0.021$. Figure 4B shows that the Unpaired group had significantly less surface Kv1.2 expression at BC axon terminals than the Paired group and the No Stimulus group. These effects were corroborated by independent samples t-tests, $t(38) = 2.18$, $p = 0.036$ and $t(39) = -2.94$, $p < 0.006$, respectively. No differences were observed between the Paired and No Stimulus group ($p = 0.34$). These data show us that the Unpaired group showed the reduced Kv1.2 surface expression compared to the other groups.

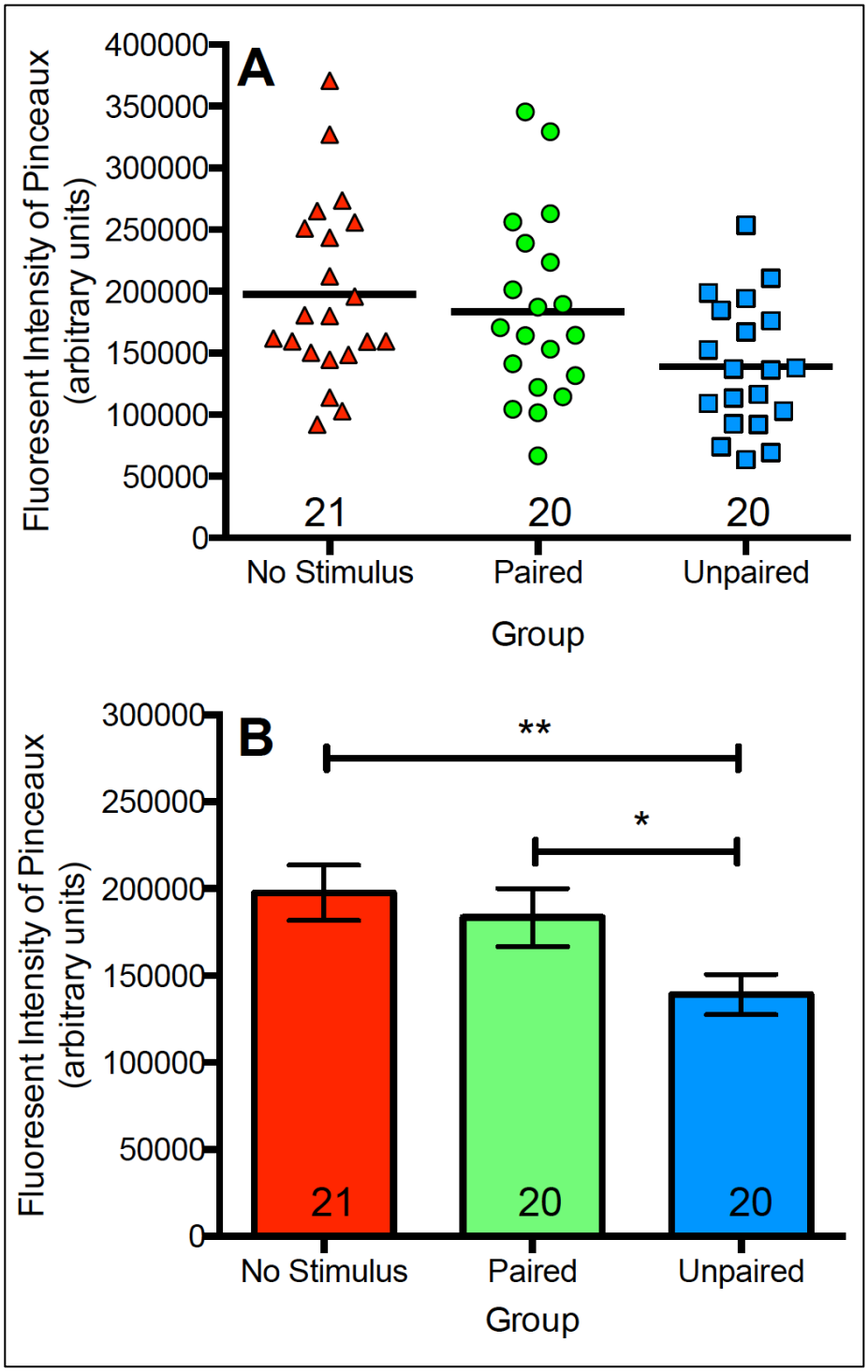

Figure 4. Region-specific analysis of Kv1.2 surface expression on BC axon terminals in the cerebellar cortex near the base of the primary fissure ipsilateral to the conditioning (Paired group), stimulated (Unpaired), or simply electrode-implanted (No Stimulus) eyelid. Raw microscopy data (A) and Mean ±SEM (B). Each subject represented by one number (A) comprised of the fluorescent intensity of PCXs in both cerebellar sections. Significant differences observed between the Unpaired and Paired groups ($p = 0.04$) and Unpaired and No Stimulus groups ($p = 0.006$). No differences observed between Paired and No Stimulus groups ($p = 0.34$). (* denotes $p < 0.05$; ** denotes $p < 0.01$)

Biotinylation and Western Blot Analysis – Surface Kv1.2 at Basket Cell Terminals and Purkinje Cell Dendrites

The other site of Kv1.2 expression in the cerebellar cortex is on PC dendrites in the molecular layer. Here, when Kv1.2 is expressed on the surface, it works to shunt excitation coming down the dendritic arbors thereby reducing PC excitability (Khavandgar et al., 2005). We hypothesized that Kv1.2 expression would be reduced in the Paired group compared to the other two groups. While the MP focused on Kv1.2 expressed at the BC axon terminal, it would not be feasible to perform this analysis for the PC dendrites for several reasons: (1) The resolution that we are able to obtain with the MP technique was suitable for the strong and localized expression of surface Kv1.2 found on BC axon terminals because of their distinct structure and location (Fig. 2). It would be difficult to accurately identify Kv1.2 expressed on PC dendrites and identify individual dendrites for analysis since Kv1.2 is less densely expressed on these structures. (2) If we were able to identify individual dendrites, the resolution would have been too poor given the amount of data in the image. Therefore, a biotinylation and western blot technique was used to complement the MP data by providing a measure of Kv1.2 surface expression that included the expression on PC dendrites in addition to expression on BC axon terminals. To do this with fixed tissue, we modified the procedure used in Williams et al. (2012) to create a new binding site for the biotin to bind to on external proteins (Appendix I).

The WB data were analyzed first by using a one-way ANOVA to compare the raw WB scores for the Paired (n = 20), Unpaired (n = 20), and No Stimulus (n = 19) groups. The raw (Fig. 5A) and normalized data (Fig. 5B) yielded the same statistical

values, therefore the raw data were used for analysis and both sets of data are shown in Figure 5B. This analysis yielded no significant differences between the groups ($p = 0.62$). Even though the ANOVA did not yield a significant effect of group, we used the same planned comparisons as for the MP data by using independent samples t-tests to compare the Paired and Unpaired groups and the Paired and No Stimulus groups. Neither of these t-tests revealed significant differences between these pairs of groups ($p = 0.32$; $p = 0.34$, respectively). These data suggest that were no differences between the groups on this measure of surface Kv1.2 expression in the cerebellar cortex.

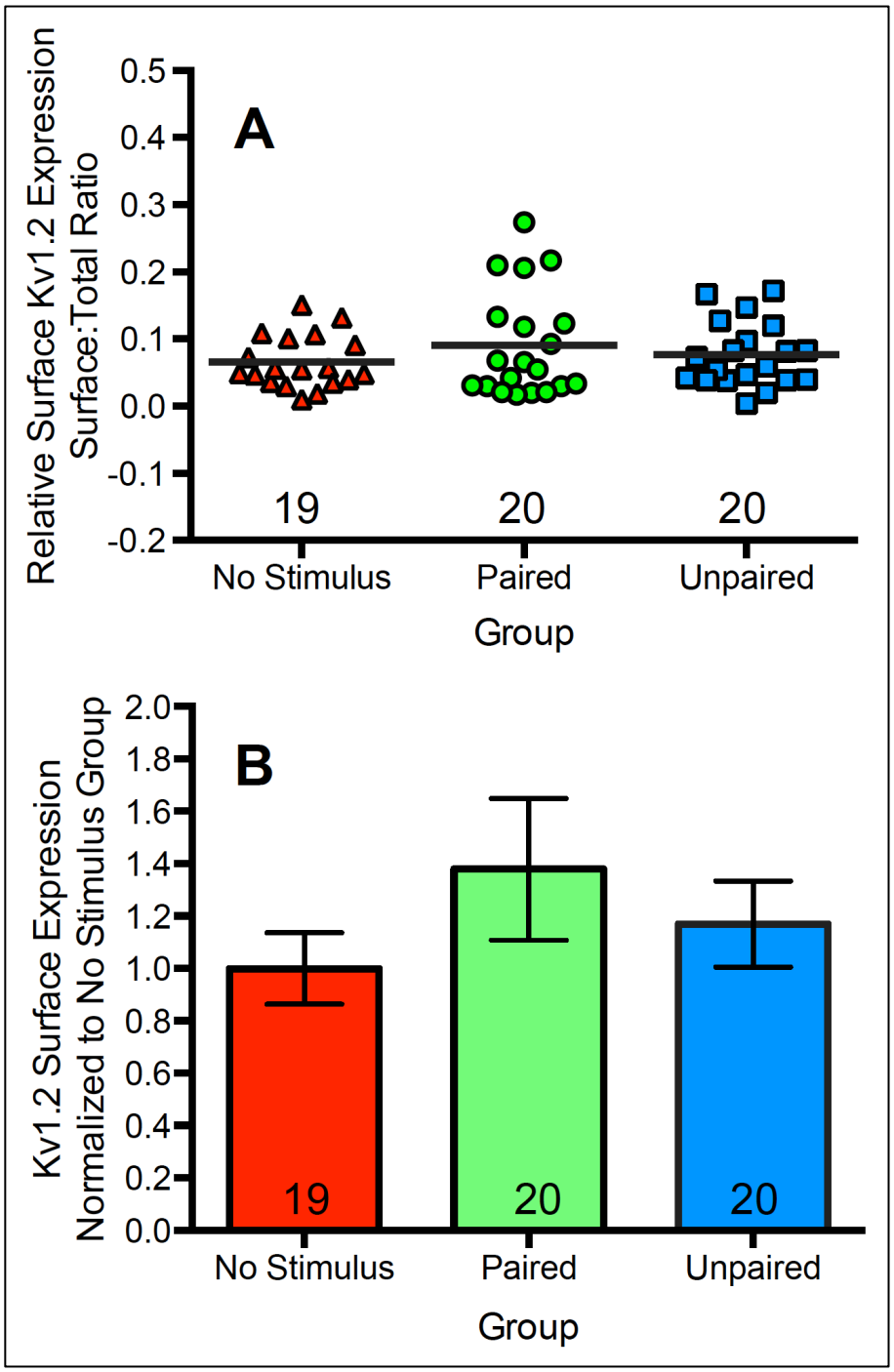

Figure 5. Kv1.2 surface expression measured at both PC dendrites and BC axon terminals. (A) Data displayed as raw Kv1.2 surface expression for Paired group (green circles), Unpaired group (blue squares), and No Stimulus group (red triangles). Each data point represents an individual subject. (B) Mean ± SEM normalized to the No Stimulus group. The numbers shown above the group assignments represent the number of subjects in each group. No significant differences were observed between the groups.

Discussion

When looking at Kv1.2 surface expression on just BC axon terminals, we observed a significant decrease in Kv1.2 surface expression (Fig. 4) in the Unpaired group compared to the other two groups. The lack of effect in the WB measure suggests the possibility of an increase in Kv1.2 surface expression in PC dendrites in the Unpaired group (Fig. 5). These findings were in contrast to what we hypothesized, given what we have previously shown linking Kv1.2 to EBC. First, infusions of tityustoxin (TsTX) facilitated acquisition to EBC when infused into an area close to where we are measuring Kv1.2 in this experiment (Williams et al., 2012), thereby linking Kv1.2 to acquisition of EBC. These were relatively large infusions (1µl), likely hitting more than just the area we sampled surface Kv1.2 here. Furthermore, 1µl infusions of the neuropeptide secretin or a secretin receptor antagonist, 5-27 secretin, facilitated or impaired acquisition, respectively, when infused into a similar cortical location (Williams et al., 2012, Fuchs et al., 2014). Infusions of secretin should facilitate the endocytosis of Kv1.2 in the cerebellar cortex leading to enhanced EBC, while 5-27 secretin should prevent secretin-induced Kv1.2 endocytosis, keeping the channel at the surface and attenuating BC inhibition of PCs (Williams et al., 2012). Based on these findings from the infusion studies, we expected to observe reduced surface Kv1.2 expression in the Paired group, not the Unpaired group, following three days of training. What these data indicate is that there may be a time course for the regulation of Kv1.2 during EBC.

Based on the findings that secretin is endogenous to the cerebellum and released from PCs (Yung et al., 2001, Ng et al., 2002, Lee et al., 2005, Yung et al., 2006), we theorized that US stimulation of PCs via climbing fiber (CF) projections from the inferior olive (IO) is in part responsible for secretin release during EBC. Research has suggested that when a CR is generated by the interpositus nucleus (IPN), projections from the IPN not only lead to an eyeblink CR but also increase GABAergic input to the IO (Sears and Steinmetz, 1991, Hesslow and Ivarsson, 1996, Kim et al., 1998, Medina et al., 2002). Serving as a negative feedback loop, CR generation subsequently inhibits IO activity and limits the activation of PCs by US input as EBC progresses. This mechanism would be active in the Paired group in the current experiment, since they are the only group to exhibit CRs. Thus, it is possible that as the Paired group learned to make CRs, each CR is inhibiting the IO and the climbing fiber (CF) input to PCs from the US is being reduced. Since the Paired group learned to ~75% CRs on Day 3 (Fig. 3), learning is established and the IO would be inhibited during the US by the IPN (Fig. 1). This would mean that this group is receiving less US stimulation later in acquisition and thus, less secretin release from PCs in the cerebellar cortex. The Unpaired group, however, does not learn to make a CR to the CS. Since this group received the exact same stimulation but did not display any CRs, the inhibition of the IO should be minimal and each US that is presented should fully activate the PCs and lead to the release of secretin. If secretin release as a result of US activation of PCs is unaffected in the Unpaired group, this may explain why this group showed reduced surface Kv1.2 expression after three days of training compared to the Paired group.

The finding that the Paired group did not differ from the No Stimulus group is more difficult to explain from these data. We hypothesize that there is a reduction in the Paired group at the beginning of training, which disappears as training continues. At the start of training when very few CRs are exhibited, the inhibition of the IO by the IPN should be minimal, allowing CFs to stimulate the PCs during the US, causing a release of secretin. Secretin stimulates the endocytosis of Kv1.2 from BC axon terminals. Based on these data, we hypothesize that Kv1.2 is returning to the surface in the Paired group once CRs are regularly generated, implicating a reduction in Kv1.2 surface expression in initial learning but not in expression of CRs. In contrast, the Unpaired group remains in an "initial learning state" in terms of Kv1.2 surface expression at BC axon terminals. An experiment to test this hypothesis is to measure Kv1.2 surface expression using the same methods as above, but at an earlier time point of training. We hypothesize that Kv1.2 surface expression would be reduced at BC axon terminals earlier in training in both the Paired and Unpaired groups compared to the No Stimulus group.

The inhibition of the IO hypothesis may explain the finding that Kv1.2 surface expression is reduced at BC axon terminals in the Unpaired group. We must, however, consider the fact that Kv1.2 is also expressed on PC dendrites. The second highest expression of these channels is in the molecular layer of the cerebellar cortex on PC dendrites (Koch et al., 1997). While the majority of surface Kv1.2 is expressed on BC axon terminals near PC somas, the amount of Kv1.2 expressed in the molecular layer, on PC dendrites, is not trivial. Since we observed a trend for an increase in Kv1.2 surface expression in the Unpaired group as measured by WB, this suggests a possibility that EBC produces an increase in surface Kv1.2 expression at PC dendrites, and that this

effect is somewhat larger than the decrease observed in surface Kv1.2 expression at BC axon terminals. Kv1.2 in PC dendrites helps to oppose depolarization by preventing spontaneous calcium spikes from occurring (Khavandgar et al., 2005). Since stimuli in the Unpaired group are being presented in isolation and randomly throughout the sessions, then increasing expression of Kv1.2 in this region may help to maintain PC excitability or prevent hyperexcitability. The divergent effect of Kv1.2 surface expression within these two regions may have prevented us from observing a significant difference in the Unpaired group in the WB analysis.

References

Cerda O, Trimmer JS (2010) Analysis and functional implications of phosphorylation of neuronal voltage-gated potassium channels. Neurosci Lett 486:60-67.

Chung YH, Shin C, Kim MJ, Lee BK, Cha CI (2001) Immunohistochemical study on the distribution of six members of the Kv1 channel subunits in the rat cerebellum. Brain Res 895:173-177.

Connors EC, Ballif BA, Morielli AD (2008) Homeostatic regulation of Kv1.2 potassium channel trafficking by cyclic AMP. J Biol Chem 283:3445-3453.

Fuchs JR, Robinson GM, Dean AM, Schoenberg HE, Williams MR, Morielli AD, Green JT (2014) Cerebellar secretin modulates eyeblink classical conditioning. Learn Mem 21:668-675.

Hesslow G, Ivarsson M (1996) Inhibition of the inferior olive during conditioned responses in the decerebrate ferret. Exp Brain Res 110:36-46.

Hesslow G, Jirenhed DA, Rasmussen A, Johansson F (2013) Classical conditioning of motor responses: what is the learning mechanism? Neural networks : the official journal of the International Neural Network Society 47:81-87.

Hoaglin DC, Iglewicz B (1987) Fine-Tuning Some Resistant Rules for Outlier Labeling. Journal of the American Statistic Association 82:1147-1149.

Hoaglin DC, Iglewicz B, Tukey JW (1986) Performance of some resistnt rules for outlier labeling. Journal of the American Statistic Association 81:991-999.

Hopkins WF (1998) Toxin and subunit specificity of blocking affinity of three peptide toxins for heteromultimeric, voltage-gated potassium channels expressed in Xenopus oocytes. J Pharmacol Exp Ther 285:1051-1060.

Khavandgar S, Walter JT, Sageser K, Khodakhah K (2005) Kv1 channels selectively prevent dendritic hyperexcitability in rat Purkinje cells. J Physiol 569:545-557.

Kim JJ, Krupa DJ, Thompson RF (1998) Inhibitory cerebello-olivary projections and blocking effect in classical conditioning. Science 279:570-573.

Koch RO, Wanner SG, Koschak A, Hanner M, Schwarzer C, Kaczorowski GJ, Slaughter RS, Garcia ML, Knaus HG (1997) Complex subunit assembly of neuronal voltage-gated K+ channels. Basis for high-affinity toxin interactions and pharmacology. J Biol Chem 272:27577-27581.

Lee SM, Chen L, Chow BK, Yung WH (2005) Endogenous release and multiple actions of secretin in the rat cerebellum. Neuroscience 134:377-386.

Mauk MD, Steinmetz JE, Thompson RF (1986) Classical conditioning using stimulation of the inferior olive as the unconditioned stimulus. Proc Natl Acad Sci U S A 83:5349-5353.

McCormick DA, Clark GA, Lavond DG, Thompson RF (1982) Initial localization of the memory trace for a basic form of learning. Proc Natl Acad Sci U S A 79:2731-2735.

McCormick DA, Lavond DG, Thompson RF (1983) Neuronal responses of the rabbit brainstem during performance of the classically conditioned nictitating membrane (NM)/eyelid response. Brain Res 271:73-88.

Medina JF, Nores WL, Mauk MD (2002) Inhibition of climbing fibres is a signal for the extinction of conditioned eyelid responses. Nature 416:330-333.

Nesti E, Everill B, Morielli AD (2004) Endocytosis as a mechanism for tyrosine kinase-dependent suppression of a voltage-gated potassium channel. Mol Biol Cell 15:4073-4088.

Ng SS, Yung WH, Chow BK (2002) Secretin as a neuropeptide. Mol Neurobiol 26:97-107.

Sears LL, Steinmetz JE (1991) Dorsal accessory inferior olive activity diminishes during acquisition of the rabbit classically conditioned eyelid response. Brain Res 545:114-122.

Southan AP, Robertson B (1998a) Modulation of inhibitory post-synaptic currents (IPSCs) in mouse cerebellar Purkinje and basket cells by snake and scorpion toxin K+ channel blockers. Br J Pharmacol 125:1375-1381.

Southan AP, Robertson B (1998b) Patch-clamp recordings from cerebellar basket cell bodies and their presynaptic terminals reveal an asymmetric distribution of voltage-gated potassium channels. J Neurosci 18:948-955.

Southan AP, Robertson B (2000) Electrophysiological characterization of voltage-gated K(+) currents in cerebellar basket and purkinje cells: Kv1 and Kv3 channel subfamilies are present in basket cell nerve terminals. J Neurosci 20:114-122.

Steinmetz AB, Freeman JH (2010) Central cannabinoid receptors modulate acquisition of eyeblink conditioning. Learn Mem 17:571-576.

Steinmetz AB, Freeman JH (2011) Retention and extinction of delay eyeblink conditioning are modulated by central cannabinoids. Learn Mem 18:634-638.

Steinmetz AB, Freeman JH (2014) Localization of the cerebellar cortical zone mediating acquisition of eyeblink conditioning in rats. Neurobiol Learn Mem 114:148-154.

Werkman TR, Gustafson TA, Rogowski RS, Blaustein MP, Rogawski MA (1993) Tityustoxin-K alpha, a structurally novel and highly potent K+ channel peptide toxin, interacts with the alpha-dendrotoxin binding site on the cloned Kv1.2 K+ channel. Mol Pharmacol 44:430-436.

Williams MR, Fuchs JR, Green JT, Morielli AD (2012) Cellular mechanisms and behavioral consequences of Kv1.2 regulation in the rat cerebellum. J Neurosci 32:9228-9237.

Yung WH, Chan YS, Chow BK, Wang JJ (2006) The role of secretin in the cerebellum. Cerebellum 5:43-48.

Yung WH, Leung PS, Ng SS, Zhang J, Chan SC, Chow BK (2001) Secretin facilitates GABA transmission in the cerebellum. J Neurosci 21:7063-7068.

CHAPTER 3: MEASURING CHANGES IN Kv1.2 EXPRESSION AFTER BRIEF TRAINING IN EYEBLINK CONDITIONING

Introduction

The regulation of voltage-gated ion channels has been studied in relation to what role this process plays in maintaining membrane excitability (Khavandgar et al., 2005). Little is known about what role the regulation of voltage-gated ion channels has in other processes such as learning and memory. Recently, we have shown that Kv1.2, a voltage-gated potassium channel densely expressed at key sites in the cerebellar cortex, is regulated during Unpaired eyeblink conditioning (EBC) stimuli presentations (Chapter 2). Compared to a group that received Paired presentations of the stimuli (which produced conditioning) and a No Stimulus control group, the group that received three days of Unpaired training showed significantly less surface Kv1.2 expression on basket cell (BC) axon terminals. Originally, we hypothesized that this effect would be present in the Paired training group, but these long-term changes may be attributed to the fact that the Paired group was exhibiting many CRs at the end of training while the Unpaired group was not.

Kv1.2 is densely expressed on basket cell (BC) axon terminals and Purkinje cell (PC) dendrites in the cerebellar cortex (Koch et al., 1997, Chung et al., 2001). The localized surface expression and regulation of Kv1.2 is important for is function (Nesti et al., 2004). BCs form inhibitory synapses with PCs near the axon initial segment, situating this synapse in a position to strongly regulate PC output. PC output is the sole, inhibitory output of the cerebellar cortex; PCs tonically inhibit the interpositus nucleus (IPN). The IPN has been shown to be the start of the EBC CR pathway: stimulation of the IPN in

naïve animals results in eyeblinks (Chapman et al., 1988), lesions to the IPN prior to EBC prevent learning and lesions made to this region once EBC is established resulted in the abolition of CRs (McCormick and Thompson, 1984b). When a CR is generated by the IPN, the IPN inhibits brainstem nuclei responsible for relaying US information to the cerebellar cortex (McCormick et al., 1985). This projection may contribute to why we did not observe a reduction in surface Kv1.2 expression at BC axon terminals in the paired training group in the previous experiment. If CR generation in the Paired group is limiting the US stimulation during training once CRs have emerged, then secretin release from PCs (Lee et al., 2005) may be limited. Previously, we demonstrated that secretin facilitates the endocytosis of Kv1.2 in the cerebellar cortex and intra-cerebellar infusions of secretin enhances EBC (Williams et al., 2012). If the US is enhancing this release and US stimulation is reduced when CRs are expressed, then we would predict that Kv1.2 is returning to the BC axon terminal surface later in training, but may still be reduced earlier. The current experiment was designed to test the hypothesis that the Paired group and Unpaired group would show similar levels of Kv1.2 surface expression earlier in training, and both groups would differ from the No Stimulus group. Rats were trained in the same three groups as the previous experiment, but instead of the three days of trials, rats underwent 50 CS-US trials (Paired group), 50 CS-alone and 50 US-alone trials (Unpaired group), or 50 no stimulus "trials" (No Stimulus group) in one short training session. The goal was to provide enough stimulus exposure to affect Kv1.2 surface expression in the paired and unpaired groups, but not enough to produce robust CR expression in the paired group.

Material and Methods

Eyeblink Conditioning

Subjects

Male Wistar rats were purchased from Charles River (Quebec, Canada) and housed in pairs upon arrival with access to food and water ad libitum. Rats were single housed after surgery. The colony room was maintained on a 12 hour light-dark cycle (lights on at 7:00 AM and off at 7:00 PM). Rats weighed 200-300g prior to surgery. All behavioral testing took place during the light phase of the cycle and all procedures were approved by the Institutional Animal Care and Use Committee at the University of Vermont.

Surgery and Apparatus

The same surgery and apparatus methods were employed in this experiment as the previous experiment. Refer to the Materials and Methods section of Experiment 1 (Chapter 2) for details.

Training Procedure

All training was completed in a single 30 minute session. Rats were placed into individual drawers on a rolling cart and transported from the colony room to the sound proof conditioning chambers. Rats were placed into the sound-attenuating conditioning boxes individually. The rats were connected to the tether first by the bipolar stimulating electrode and then by the EMG electrodes.

Training was staggered such that each rat began training about 15 after the previous rat and ended training about 15 minutes before the next rat. The training program for the Paired group consisted of 25 CS-US trials with an average of 30 seconds

between trials (range: 20-40 seconds), 25 CS-alone and 25 US-alone for the Unpaired group, and 25 no stimuli trials for the No Stimulus group. These training programs were one quarter the length of a full daily session and lasted ~12-15 minutes each. Once each subject completed two iterations of the training program, they were disconnected from the conditioning chamber and transported in a separate wheeled cart to the room where the perfusion took place.

Behavior Analysis

For the Paired and Unpaired groups, CS-US or CS-alone trials, respectively, were subdivided into three time periods: (1) a "baseline" period, 280-ms prior to CS onset; (2) a non-associative "startle" period, 0-80ms after CS onset; and (3) a "CR" period, 81-350ms after CS onset. In order for a response to be scored as a CR, eyeblinks had to exceed the mean baseline activity for that trial by 0.5 arbitrary units during the CR period. Eyeblinks that met this threshold during the startle period were scored as startle responses and were analyzed separately. The primary behavioral dependent measure for all experiments was the percentage of trials with an eyeblink response during the "CR period" across all CS-US Paired trials (Paired group), CS-alone trials (Unpaired group; the US-alone trials were not analyzed), or comparable "trial periods" for the No Stimulus group for each session. There was no inclusion criterion for this experiment for the Paired group since the goal was to capture Kv1.2 surface expression when CRs were beginning to emerge. Some subject learned and other did not. We did confirm that all of the rats included in the analysis had acceptable signals.

For the percentage of CRs, the data were analyzed using repeated measures ANOVAs comparing the group groups across the two training blocks on Day 1.

Independent samples t-tests were used for planned comparisons between all of the groups for the WB and MP measures. The criterion for a significant effect was an α-level of 0.05 or below.

Western Blot and Multiphoton Microscopy

The same methods for tissue analysis in both the biotinylation and western blot (WB) and multiphoton microscopy (MP) measures were the same as in the previous experiment. Refer to Materials and Methods section in the previous chapter (Experiment 1) for detailed information.

Kv1.2 Surface Expression Data Analysis

Data analysis for both the multiphoton microscopy (MP) and biotinylation and western blot (WB) measures of surface Kv1.2 expression used a one-way ANOVA between the groups. Independent samples t-tests were used for planned comparisons between the Paired and Unpaired groups, Unpaired and No Stimulus groups, and the Paired and No Stimulus groups. The criterion for a significant effect was $p < 0.05$.

Results

Eyeblink Conditioning Behavioral Analysis

In the previous experiment, we showed that presenting EBC stimuli in an Unpaired fashion over three days of training led to a reduction in surface Kv1.2 expression on BC axon terminals, but no differences observed in the WB measure. The finding in the previous experiment was contrary to our original hypothesis stating that

paired training would lead to a reduction in surface Kv1.2 expression. This discrepancy may be attributed to the observation that, when a CR is generated in the IPN, output from the IPN inhibits the inferior olive (IO), the nucleus responsible for relaying US information to the cerebellar cortex (Sears and Steinmetz, 1991, Hesslow and Ivarsson, 1996, Kim et al., 1998, Medina et al., 2002). In the previous experiment, the Paired training group showed robust learning over the three days of training while the Unpaired group did not learn and showed very little eyeblink activity to the tone. If the US input from the IO to the cerebellar cortex was uninhibited in the Unpaired group and inhibited in the Paired group, the amount of US stimulation reaching the cerebellar cortex may hold the key to understanding what is happening to Kv1.2 expression during EBC.

The current experiment was designed to test what happens to Kv1.2 surface expression earlier in training, highlighting what happens before CR expression emerges. We hypothesized that the Paired group (n = 25) and the Unpaired group (n = 25) would show a reduction in Kv1.2 surface expression at BC axon terminals measured by MP. For the WB measure, we only hypothesized that the Paired and Unpaired groups would be different from the No Stimulus group (n = 22); it is difficult to hypothesize a specific direction since this measure samples Kv1.2 at both sites and those sites may be changing in opposite directions. The number of subjects in each of the groups was determined based on the number of subjects in each group that successfully completed EBC training. Reasons for exclusion included poor EMG signal or being unable to connect to the conditioning chambers.

The shorter training procedure that was used in this experiment led to more variability in the number of learned eyeblink responses emitted by the Paired group.

Overall, the Paired group did show some learning and the rate of learning is similar to the previous experiment for the first 50 trials (Fig3, inset). To determine if there were differences between the groups, a 3(Group; Paired, Unpaired, No Stimulus) by 2(Block: Acq1_1, Acq1_2) repeated measures analysis of variance (ANOVA) yielded a not quite significant main effect of session $F(1,69) = 3.56$, $p = 0.063$, a significant main effect of group, $F(2,69) = 29.73$, $p = 0.004$, and a significant group by session interaction, $F(2,69) = 14.51$, $p = 0.001$, indicating that there was a change across the sessions, but this change was dependent upon the training program that was used. The Paired group showed some CRs in the second training block, but there was a lot of variability within this group (Fig. 6). Within this group there were several rats ($n = 7$) that did not show any CR activity during the two training blocks and another subset that did show CRs during the training blocks ($n = 18$). At the second time point, an independent samples t-test revealed a significant performance difference between these two subsets of the Paired group, $t(27) = -2.60$, $p = 0.016$. The observation of little to no CRs this early in training is not uncommon; if the procedure went on longer, it is likely that these rats would have exhibited CRs. Furthermore, inspection of EMG signals in the non-learning group did not indicate that there were technical problems contributing to the lack of eyeblink CRs.

Outlier Analysis for Both Measures

Prior to analyzing the data for both the WB and MP measures, the data were tested to determine if there were any outliers within the groups. Two methods were used and similar to the previous experiment; the outlier analysis was done by looking at the boxplots and using the "Outlier Labeling Rule" (OLR) (Hoaglin et al., 1986, Hoaglin and Iglewicz, 1987). The OLR identifies outliers based on the quartile percentages derived

from the distribution of the data and the boxplot analysis identified outliers by how many standard deviations that data point is from the mean. The boxplots and the OLR analysis can be found in the Appendix IV. For the WB data, one data point was identified by both methods as an outlier. As can be seen in the box plot (Fig. 15; Appendix IV), there is one subject that falls well outside of the error bar in the No Stimulus group. The OLR also identified this subject as an outlier (Table 4; Appendix IV). This data point was removed from the No Stimulus group for the WB analysis, but remained in the behavioral analysis and the MP analysis. Upon re-examination of the WB data using both outlier analyses, no other subjects were identified (Appendix IV). For the MP data, no subjects were identified at outliers within any of the groups (Appendix IV).

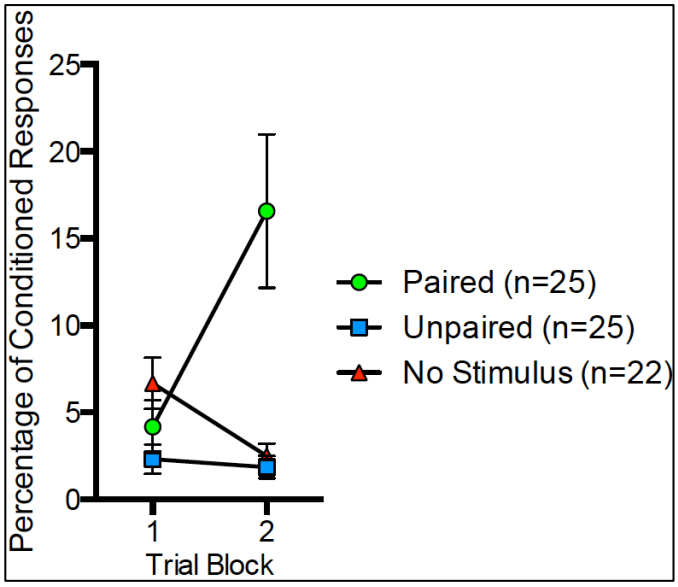

Figure 6. Percentage of conditioned responses for the Paired (green circles), Unpaired (blue squares), and No Stimulus (red triangles) groups during the one-quarter length training blocks. Data points presented with mean ± SEM. All the groups start at the same point during the first session, but the Paired group exhibited significantly more CRs during the second session compared to the other two groups (p = 0.016). Overall, the number of CRs in the Paired group this early in training is on par with what we have previously observed. Contributing to the variability in the Paired group at the second time point, there were several rats (n = 7) that did not show any CRs in either block of trials.

Multiphoton Microscopy Analysis – Kv1.2 Surface Expression on Basket Cell Terminals

Immediately following the last training session, subjects were anesthetized, perfused with paraformaldehyde to preserve what occurred during training thereby taking a snapshot of what is happening to Kv1.2 surface expression following a shorter training procedure, and the tissue was sectioned and assigned to either the MP or WB measure. The tissue that was assigned to the MP measure was stained with ATTO-TsTX-594 overnight and then imaged on a multiphoton microscope. This analysis was used to examine changes in surface Kv1.2 expression exclusively on BC axon terminals. In the previous experiment (Chapter 2), we observed a significant reduction in surface Kv1.2 expression at BC axon terminals in the Unpaired group compared to the other two groups. By looking at Kv1.2 surface expression earlier in training, we may be able to sample Kv1.2 surface expression at BC axon terminals prior to robust CR expression in the Paired group. Based on this, we hypothesized that the Paired (n = 24) and Unpaired (n = 22) groups would show reduced surface Kv1.2 expression earlier in training compared to the No Stimulus group (n = 22). A one-way ANOVA did not yield a significant difference between the groups in the MP analysis (p = 0.31) (Fig. 7B). Planned comparisons between all of the groups were conducted with independent samples t-tests. First, as hypothesized, there were no differences between the Paired and Unpaired groups (p = 0.26). There were also no differences between the Paired and No Stimulus groups (p = 0.78) or between the Unpaired and No Stimulus groups (p = 0.15). Overall, Kv1.2 surface expression on BC axon terminals was similar across all three conditions in this experiment (Fig. 7B).

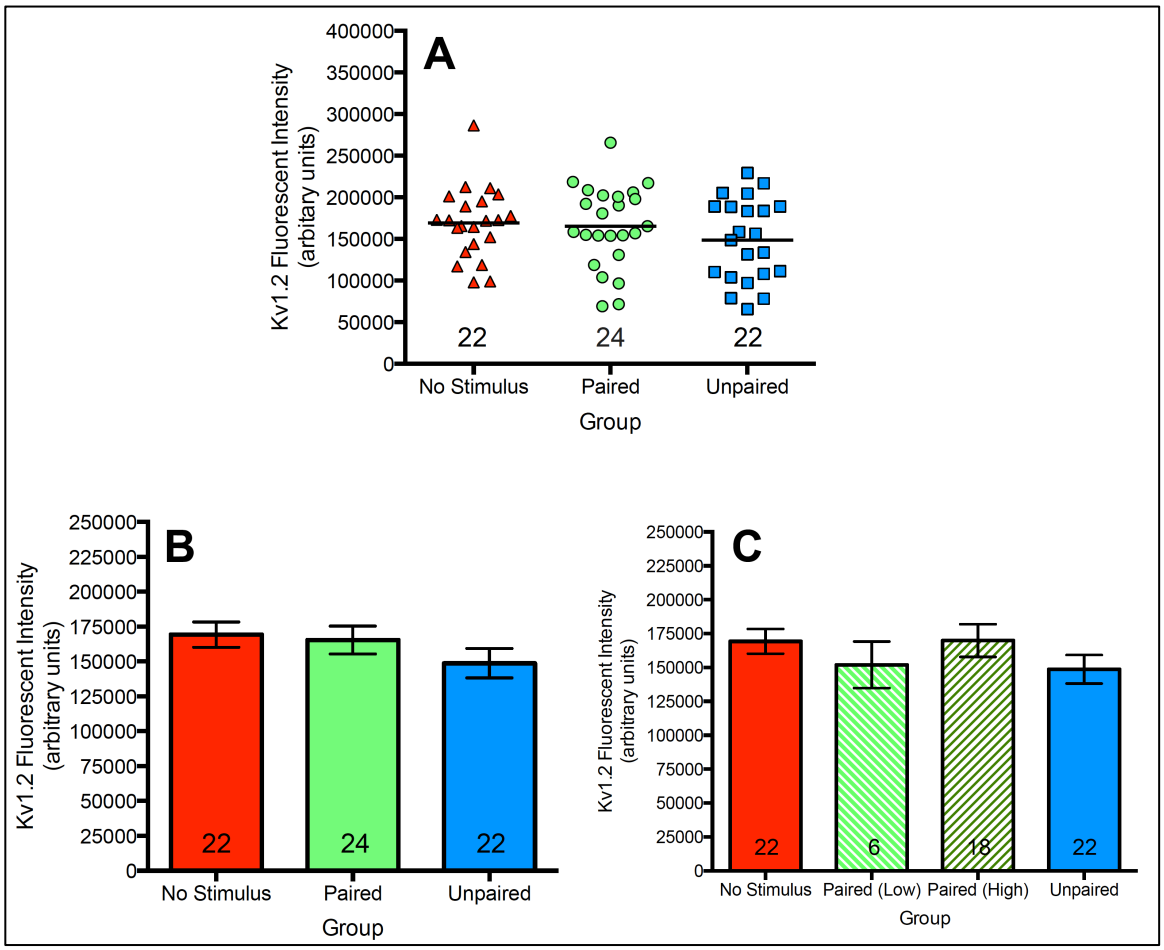

Figure 7. Multiphoton microscopy (MP) data. A) Raw MP data measuring surface Kv1.2 expression on BC axon terminals for each of the groups. Numbers under the plots denote the number of subjects in each group. B) Mean ± SEM for each group. Planned comparisons did not reveal any differences between any of the groups. C) Same data as in Fig. 2B, but the Paired group is split between subjects that did not show any CRs during the two training blocks (Low; light green stripes) and subjects that showed CRs during the two training blocks (High; dark green stripes). Post hoc comparisons did not reveal any differences between the groups.

Next, the MP data were analyzed according to the Paired group performance split. First, an outlier analysis was run using both the box plot analysis and the Outlier Labeling Rule on the Paired Low and Paired High groups. Low responders (n = 7) were subjects that did not show any CRs during EBC training and high responders (n = 18) were subjects that showed at least one CR. No subjects were identified within either analysis (Appendix V).

The same comparisons were done in these analyses as in the WB analyses; therefore, independent samples t-tests were used, but did not revealed any differences between the groups for the following two comparisons: Paired Low (n = 6) versus No Stimulus (n = 22) groups (p = 0.39) and Paired High versus No Stimulus groups (p = 0.97). Overall, these data indicate that there are no differences in Kv1.2 surface expression on BC axon terminals after a shorter training procedure between the groups as measured by MP (Fig. 7C).

Biotinylation and Western Blot Analysis – Surface Kv1.2 at Basket Cell Terminals and Purkinje Cell Dendrites

This measure was used to sample surface Kv1.2 expressed in both PC dendrites and BC axon terminals. In this experiment, we expected Kv1.2 surface expression to be similar between the Paired (n = 22) and Unpaired (n = 23) groups, but different from the No Stimulus group (n = 20). First, a one-way ANOVA was used to determine if there were any differences between the groups on the WB measure. This analysis did not yield any significant differences between the groups (p = 0.15). Independent samples t-tests were used to conduct planned comparisons between all of the groups, with an emphasis on the comparisons between the Paired and Unpaired groups and the Unpaired and No Stimulus groups. There were no differences between the Paired and Unpaired groups (p = 0.66) and no differences between the Paired and No Stimulus groups (p = 0.2). An independent samples t-test revealed a significant difference between the Unpaired and No Stimulus group, $t(41) = 2.01$, $p = 0.05$ (Fig. 8B) The Unpaired group showed increased surface Kv1.2 expression compared to the No Stimulus group (Fig. 8). The hypothesis

that the Paired and Unpaired groups would show similar levels of Kv1.2 surface expression was confirmed, however, only the Unpaired group was significantly different from the No Stimulus group.

In order to better understand the lack of a statistically significant difference between the Paired and No Stimulus groups on this measure, we split the Paired group based on EBC performance (Fig. 6). The split, as mentioned above, was between low and high responders. Low responders (n = 7) were subjects that did not show any CRs during EBC training and high responders (n = 18) were subjects that showed at least one CR. This distinction is important for this experiment since we are interested in what is happening to surface Kv1.2 expression prior to the emergence of CRs. The subjects that did not show any CRs were confirmed to have stable EMG signals; therefore we can reasonably conclude that, if given more time with the learning paradigm, they would have shown CRs (similar to all subjects in the previous experiment).

After the Paired group split analyses, we again ran the outlier analyses on the WB data to treat them the same as in earlier analyses. The boxplot analysis and OLR both identified one of the subjects in the Paired Low group as an outlier (Appendix V). Please refer to Appendix for the paired group split comparison and figure.

Due to the nature of the performance split in the Paired group and the fact that we cannot assign subjects to a non-learning Paired condition, independent samples t-tests were used for these analyses. Two comparisons were made: Paired Low (n = 7) vs. No Stimulus (n = 20) and Paired High (n = 15) vs. No Stimulus. An independent samples t-test revealed a significant difference between the Paired Low group and No Stimulus group, $t(25) = 2.70$, $p = 0.012$ (Fig. 8C). There was no difference between the Paired

High and No Stimulus groups (p = 0.50). These data suggest that the Paired Low group showed the same increase in Kv1.2 surface expression as the Unpaired group (Fig. 8C).

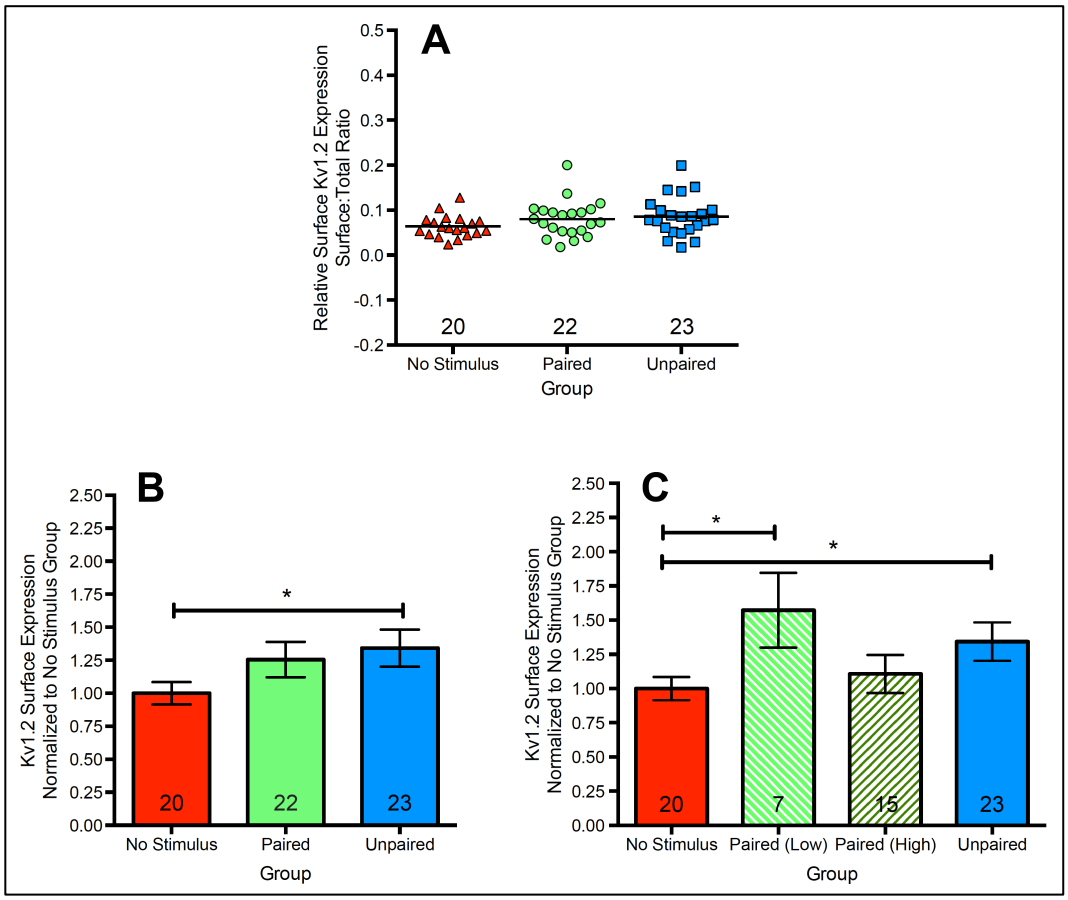

Figure 8. Biotinylation and Western Blot (WB) data showing Kv1.2 surface expression in both BC axon terminals and PC dendrites. Data displayed for the Paired, Unpaired, and No Stimulus groups. A) Raw WB Surface-to-Total ratio for each subject. Numbers under the plots for each group denote the number of subjects in that group. B) WB data normalized to the No Stimulus group (Mean ± SEM). Planned comparisons between each of the groups revealed a significant difference between the Unpaired and No Stimulus groups (p = 0.04), but no other significant effects. C) Paired group is split between subjects that did not show any CRs during the two training blocks (Low; light green stripes) and subjects that showed CRs during the two training blocks (High; dark green stripes). Post hoc comparisons revealed a significant difference between Paired Low and No Stimulus groups (p = 0.012). The significant difference between Unpaired and No Stimulus groups is depicted again. No difference was observed between Paired High and No Stimulus groups. (* denotes p <0.05)

Discussion

The aim of this experiment was to measure surface Kv1.2 expression following a shorter EBC training program (50 trials on Day 1 vs. 100 trials/day for 3 days). We hypothesized that early in training the Paired and Unpaired groups would show similar surface Kv1.2 expression on both the MP and WB measures. Previously, we demonstrated reduced surface Kv1.2 expression on BC axon terminals in the Unpaired group, but not in the Paired group after three days of training. Based on this finding, we theorized that the inhibition of the IO by projections from the IPN in the Paired group as CRs are expressed could contribute to this finding (Sears and Steinmetz, 1991, Hesslow and Ivarsson, 1996, Kim et al., 1998, Medina et al., 2002). With a shorter training procedure and a potential lack of IPN-to-IO inhibition, we hypothesized that the Paired and Unpaired groups would show similar surface Kv1.2 expression to one another, since neither group would exhibit robust CR expression.

In the current experiment, we did not observe any differences between the groups when looking at Kv1.2 surface expression on just BC axon terminals using MP (Fig. 7). In contrast, we observed greater Kv1.2 surface expression in cerebellar cortex in both the Unpaired group and in a subset of the Paired group (Paired Low) that did not exhibit any CRs compared to the No Stimulus group (Fig. 8). Since the WB measure samples Kv1.2 at both BC axon terminals and PC dendrites and no differences were observed at BC axon terminals, by subtraction, the differences observed may be attributed to changes occurring only at PC dendrites. These data lend support to the idea that Kv1.2 surface expression at PC dendrites is regulated prior to CR expression in EBC. Increased surface expression at PC dendrites, which would reduce PC excitability, may be important for

acquisition of the eyeblink CR, while other cerebellar mechanisms may govern the expression or maintenance of the CR. On the other hand, the Paired High group showed a range of CRs during the two training blocks in this experiment (Fig. 6) and as a result, showed similar Kv1.2 surface expression as the No Stimulus group (Fig. 8C), similar to the previous experiment in which all rats in the Paired group exhibited CRs. The observation that there is no difference between the Paired High group and No Stimulus group may suggest that Kv1.2 surface expression on PC dendrites returns to baseline or No Stimulus levels once the eyeblink CR is acquired.

When looking at Kv1.2 on just BC axon terminals using MP, we did not observe a difference between the Paired and Unpaired groups, as hypothesized (Fig. 7B), however these groups did not differ from the No Stimulus group either. Based on the finding in the previous experiment that the Unpaired group showed reduced Kv1.2 surface expression on BC axon terminals, we expected to see a reduction in surface Kv1.2 at BC axon terminals. It is possible that the changes observed in the previous experiment required more US stimulation to produce. In the current experiment, subjects in the Paired and Unpaired groups only experienced 50 US presentations across the two training blocks while the Paired and Unpaired group received 100 US presentations each day for three days before harvest. It may be the case that a reduction in surface Kv1.2 expression at BC axon terminals requires more US stimulation than 50 trials on one day of training, as well as a lack of CR-related US inhibition.

Since the two experiments employed the same methods post-training and the only difference between them was the length of training, then when should we expect to observed a reduction in surface Kv1.2 expression at BC axon terminals? The answer may

lie in the period following the last trials on the first day and the start of training on the next day. In the first experiment, subjects returned to home cages following training until the next morning. Kv1.2 regulation may be taking place in that time in between training sessions, but neither experiment tested this. The key to changes in Kv1.2 surface expression on BC terminals may lie in the consolidation period between training sessions. A follow-up study could sample Kv1.2 surface expression a certain amount of time after training. Perhaps the within session changes are minimal, but Kv1.2 at BC axon terminals aids in the storage of eyeblink CR information.

Overall, these data demonstrate that Kv1.2 surface expression regulation in the cerebellum occurs during mammalian learning and memory. Changes in Kv1.2 surface expression seemed to be dependent upon CR expression. The Unpaired and Paired Low groups, two groups that did not show any CRs during the two training blocks respectively, showed increased Kv1.2 surface expression on PC dendrites, while the Paired High group did not show this same increase. Kv1.2 surface expression in PC dendrites is important for maintenance of membrane excitability (Khavandgar et al., 2005), and since there was increased expression measured in WB and no change between these two groups in Kv1.2 surface expression on BC axon terminals, the changes during early training may be limited to PC dendrites.

When Kv1.2 is present at the cell surface, it acts as a delayed rectifier channel, shunting excitation as it travels down the process (e.g. dendrite or axon) (Brew and Forsythe, 1995, Ebner-Bennatan et al., 2012). Increased Kv1.2 on PC dendrites may be working to limit or reduce PC excitability (Khavandgar et al., 2005). In order for a CR to be generated, the inhibition of the IPN by PCs must be lifted. Therefore, increased Kv1.2

at PC dendrites may facilitate this disinhibition early in training. Since we saw changes in Kv1.2 surface expression in the Paired Low group compared to the No Stimulus group (Fig. 8C) and no difference between the Paired High Group and the No Stimulus group (Fig. 8C), it would suggest that there are other mechanisms that govern the maintenance of the CR, once the learned response is being expressed.

References

Brew HM, Forsythe ID (1995) Two voltage-dependent K+ conductances with complementary functions in postsynaptic integration at a central auditory synapse. J Neurosci 15:8011-8022.

Chung YH, Shin C, Kim MJ, Lee BK, Cha CI (2001) Immunohistochemical study on the distribution of six members of the Kv1 channel subunits in the rat cerebellum. Brain Res 895:173-177.

Ebner-Bennatan S, Patrich E, Peretz A, Kornilov P, Tiran Z, Elson A, Attali B (2012) Multifaceted modulation of K+ channels by protein-tyrosine phosphatase epsilon tunes neuronal excitability. J Biol Chem 287:27614-27628.

Fuchs JR, Robinson GM, Dean AM, Schoenberg HE, Williams MR, Morielli AD, Green JT (2014) Cerebellar secretin modulates eyeblink classical conditioning. Learn Mem 21:668-675.

Hesslow G, Ivarsson M (1996) Inhibition of the inferior olive during conditioned responses in the decerebrate ferret. Exp Brain Res 110:36-46.

Hoaglin DC, Iglewicz B (1987) Fine-Tuning Some Resistant Rules for Outlier Labeling. Journal of the American Statistic Association 82:1147-1149.

Hoaglin DC, Iglewicz B, Tukey JW (1986) Performance of some resistnt rules for outlier labeling. Journal of the American Statistic Association 81:991-999.

Hopkins WF (1998) Toxin and subunit specificity of blocking affinity of three peptide toxins for heteromultimeric, voltage-gated potassium channels expressed in Xenopus oocytes. J Pharmacol Exp Ther 285:1051-1060.

Khavandgar S, Walter JT, Sageser K, Khodakhah K (2005) Kv1 channels selectively prevent dendritic hyperexcitability in rat Purkinje cells. J Physiol 569:545-557.

Kim JJ, Krupa DJ, Thompson RF (1998) Inhibitory cerebello-olivary projections and blocking effect in classical conditioning. Science 279:570-573.

Koch RO, Wanner SG, Koschak A, Hanner M, Schwarzer C, Kaczorowski GJ, Slaughter RS, Garcia ML, Knaus HG (1997) Complex subunit assembly of neuronal voltage-gated K+ channels. Basis for high-affinity toxin interactions and pharmacology. J Biol Chem 272:27577-27581.

Lee SM, Chen L, Chow BK, Yung WH (2005) Endogenous release and multiple actions of secretin in the rat cerebellum. Neuroscience 134:377-386.

Medina JF, Nores WL, Mauk MD (2002) Inhibition of climbing fibres is a signal for the extinction of conditioned eyelid responses. Nature 416:330-333.

Nesti E, Everill B, Morielli AD (2004) Endocytosis as a mechanism for tyrosine kinase-dependent suppression of a voltage-gated potassium channel. Mol Biol Cell 15:4073-4088.

Sears LL, Steinmetz JE (1991) Dorsal accessory inferior olive activity diminishes during acquisition of the rabbit classically conditioned eyelid response. Brain Res 545:114-122.

Steinmetz AB, Freeman JH (2014) Localization of the cerebellar cortical zone mediating acquisition of eyeblink conditioning in rats. Neurobiol Learn Mem 114:148-154.

Williams MR, Fuchs JR, Green JT, Morielli AD (2012) Cellular mechanisms and behavioral consequences of Kv1.2 regulation in the rat cerebellum. J Neurosci 32:9228-9237.

Yung WH, Chan YS, Chow BK, Wang JJ (2006) The role of secretin in the cerebellum. Cerebellum 5:43-48.

Yung WH, Leung PS, Ng SS, Zhang J, Chan SC, Chow BK (2001) Secretin facilitates GABA transmission in the cerebellum. J Neurosci 21:7063-7068.

CHAPTER 4: GENERAL DISCUSSION

The topic of this thesis has been to study the regulation of surface Kv1.2 expression in the cerebellar cortex following cerebellar dependent eyeblink conditioning (EBC). This is a novel endeavor, bridging two research areas. First, EBC serves as a good model for cerebellar behaviors and learning and memory. The neural pathways underlying the acquisition of eyeblink conditioned responses (CRs) are well known, and therefore provide us with known synaptic targets to study cellular mechanisms underlying learning and memory, such as regulation of voltage-sensitive ion channels. The regulation of voltage-gated channels by learning and memory is an understudied area, with most of the literature focusing on regulation of ligand-gated ion channels, such as AMPA. The second research area that was bridged by this project was the pharmacology or biochemical regulation of Kv1.2. By starting from a rich literature on the expression, regulation, and biophysical properties of Kv1.2 (Huang et al., 1993, Wang et al., 1993, Southan and Robertson, 1998a, b, Tsai et al., 1999, Southan and Robertson, 2000, Chung et al., 2001, Hattan et al., 2002, Nesti et al., 2004, Williams et al., 2007, Connors et al., 2008, Williams et al., 2012), changes in expression that resulted from behavioral treatments would extend this knowledge base. What this project has yielded is the finding that Kv1.2 may be regulated by the stimuli that produce EBC and by the expression of the learned response, the eyeblink CR.

When rats were given three days of training, we observed a robust reduction in surface Kv1.2 expression on basket cell (BC) axon terminals in the Unpaired group (Fig. 4), a finding that was in contrast to our original hypothesis. We hypothesized that this effect would be evident in the Paired group, based on infusion studies that lend support

for the idea that blocked or endocytosed surface Kv1.2 expression leads to enhanced EBC (Williams et al., 2012, Fuchs et al., 2014). When we shortened the training period to-one quarter the length of a full session, we found that the regulation Kv1.2 surface expression in Purkinje cell (PC) dendrites seemed to be dependent upon CR expression. This was shown by an increase in surface Kv1.2 expression measured by biotinylation and western blot (WB), which samples Kv1.2 surface expression at both BC axon terminals and PC dendrites (Fig. 8) in the Unpaired (Fig. 8B) and Paired Low groups (Fig. 8C). We did not observe any group differences in the multiphoton microscopy (MP) measure looking at just BC axon terminals (Fig. 7). Therefore we concluded, based on subtraction between these two measures, that the findings in the WB measure (Fig. 8) were due to changes in Kv1.2 surface expression on just PC dendrites. The regulation of Kv1.2 at PC dendrites seemed to be a transient process, setting the stage for other cerebellar mechanisms to govern expression of the learned eyeblink CRs.

It was intriguing to discover that the changes we predicted to be evident in the Paired actually appeared in the Unpaired group. The changes observed in the Unpaired group, however, provided a helpful piece of the story that contributes to our understanding of what is happening to Kv1.2 surface expression early and later in training. Kv1.2 surface expression appeared to be sensitive to US effectiveness in the cerebellar cortex as well as the expression of eyeblink CRs (Fig. 9). The transient effect observed in the second experiment between the Paired Low and Paired High groups when compared to the No Stimulus groups, suggests a transient role for the regulation of Kv1.2 surface expression. Increased Kv1.2 surface expression may lead to acquisition of CRs, but other cerebellar mechanisms appear to govern the expression of the learned response.

The study of voltage-sensitive channels in the cerebellum usually pertains to membrane excitability of specific cell types or how the firing rate of certain neurons changes when these channels are present or absent (Womack et al., 2004, Womack and Khodakhah, 2004, Khavandgar et al., 2005, McKay et al., 2005, Kakizawa et al., 2007). Here, however, the changes we observed may be intrinsic changes on PCs during EBC. Related studies have shown that Kv1 channels regulate PC output and deficiencies in Kv1 channel expression in PCs led to disruptions in deep cerebellar nuclei (DCN) firing patterns (McKay et al., 2005). When Kv1 channels were intact in PCs, they were able to maintain PC excitability and in turn normal firing patterns were observed in the DCN, but when Kv1 channel expression was disrupted, firing patterns in the DCN were disrupted (McKay et al., 2005). Similarly, when Kv1.2 is blocked, an increase in dendritic calcium spikes and in turn somatic sodium spikes are observed in PCs (Khavandgar et al., 2005). This increase in spike frequency prevents the correct integration of inputs to PCs and Kv1.2 is needed to ensure proper encoding of stimuli (Khavandgar et al., 2005). Similar results have been shown on PC excitability for other potassium channels, such as small conductance calcium-active potassium (SK) channels (Hosy et al., 2011, Kaffashian et al., 2011). Furthermore, Kv channels also play a role in limiting membrane excitability in PC axon terminals (Kawaguchi and Sakaba, 2015).

Regulation or disruption of channels here could have a large impact on cerebellar dependent behaviors by exerting more or less control over output from the DCN (Khavandgar et al., 2005, McKay et al., 2005, Kawaguchi and Sakaba, 2015). The data from the current experiments fit well within what has been previously shown. Since proper PC signaling is important for EBC (Steinmetz et al., 1992) and the regulation of

Kv1.2 is important for membrane excitability in PCs (Khavandgar et al., 2005) then changes in Kv1.2 surface expression during EBC may hold the key to understanding how stimuli are integrated during EBC. Increases in surface Kv1.2 expression may allow for faster or more faithful integration of stimuli inputs to the cerebellar cortex. Once the response is expressed in PCs and generated in the IPN, then Kv12 surface expression may return to baseline levels. The changes in Kv1.2 surface expression on PC dendrites in Chapter 3 support the idea that Kv1.2 regulation is linked to learning. We observed an increase in Kv1.2 expression in the Paired Low group, but no such increase in the Paired High group. Both of these groups were treated the same way during training; the only difference was the expression of CRs. Importantly, this group received the same amount of CS and US stimulation, but in an explicitly unpaired fashion. The result again was an increase in Kv1.2 surface expression.

The result in the first experiment (Chapter 2), showing a decrease in surface Kv1.2 in BC axon terminals may be associated with reports on feed-forward inhibition (Mittmann et al., 2005). BCs are targeted by several mechanisms that may be contributing to the reduction in surface Kv1.2 expression. First, we theorized that reductions in Kv1.2 surface expression were exerted through secretin release from PCs during US stimulation (Yung et al., 2001, Lee et al., 2005, Yung et al., 2006). Secretin is linked to Kv1.2 endocytosis in the cerebellar cortex (Williams et al., 2012) and we hypothesize that this mechanism is involved in the results in this experiment. Secretin released from PCs following US stimulation, which in the Unpaired group is uninhibited since no CRs were generated by this group during training, leads to reductions in surface Kv1.2 expression. If US stimulation in the Unpaired group is increasing the release of

secretin from PCs and this increased release is not attenuated due to the lack of CRs expressed by the Unpaired group, then changes in Kv1.2 may be encoding the strength of the US in the cerebellar cortex. Along those same lines, the same reduction in surface Kv1.2 expression was not observed in the Paired group and we hypothesized that this was due to the fact that the subjects in this group showed robust learning. When CRs are generated by the IPN, inhibitory connections from the IPN to the IO are active and US stimulation through the IO is attenuated on subsequent trials (Sears and Steinmetz, 1991, Hesslow and Ivarsson, 1996, Kim et al., 1998, Medina et al., 2002).

Regulation of Kv1.2 in these experiments and as discussed above may be related to both CS and US input to the cerebellum. The data, however, may support a stronger role for Kv1.2 regulation in US integration in the cerebellar cortex. This idea comes from the difference between the Paired Low and Paired High group, when comparing each of them to the No Stimulus group in the second experiment (Chapter 3). No changes in surface Kv1.2 expression were observed in the Paired High group, the subset of Paired group subject expressing eyeblink CRs, but we did see an increase in the Paired Low group. Given the connection between CR generation and US input to the cerebellar cortex, CR expression may hold the key to this relation. These findings may be understood in the context of the Rescorla-Wagner model, a learning based model that helps to account for US strength as the training signal and what can be learned from its relation to the CS (Rescorla and Wagner, 1972). This model would predict that the Unpaired group would not express CRs in either of the experiments because the CS does not provide any useful information about the US, as we observed. Said another way, nothing can be learned about the relationship between the CS and the US, therefore, the

strength of the US would remain high. In the Paired group however, the model would predict that the strength of the US would diminish as training progressed; as the Paired group begins to exhibit eyeblink CRs, the CS-US association is strong and less information is provided by each subsequent presentation of the US. This idea is supported by the finding that the IO is inhibited by neurons in the IPN when CRs are generated (Sears and Steinmetz, 1991, Hesslow and Ivarsson, 1996, Kim et al., 1998, Medina et al., 2002). Even though the Unpaired group did not show any eyeblink CRs during training, the subjects may still have been "learning" information about the stimuli. This learning could take the form of conditioned inhibition (CI), where the CS is associated as a safety signal indicating that the US will not be presented. Data suggest that the IPN is involved in CI (Nicholson and Freeman, 2002), but does not require GABA (Nolan et al., 2002). What is learned by the Unpaired group during training may be represented by changes in Kv1.2 surface expression. If changes in surface Kv1.2 expression during EBC training are setting the stage during acquisition for other cerebellar mechanisms to govern expression of the learned response, then changing the relation between the CS and US in the Unpaired group to where the CS does predict the onset of the US, we might expect CR expression to appear more quickly in the Unpaired group.

This idea of changing the contingencies from a negative association to a positive association has been tested in other learning and memory paradigms (Rescorla and Wagner, 1972, Rizley and Rescorla, 1972, Rescorla, 1973, 1976, Rescorla and Furrow, 1977). The prediction is that previous training with a negative (or unpaired) association slows learning when the contingency is changed (Rescorla, 1976, Claflin and Buffington, 2006), but this has not been shown in EBC in adult rats. In a similar study, CS-US

associations in fear conditioning enhanced acquisition in EBC when using the same CS and an eyeblink eliciting US (Lindquist et al., 2010). If the regulation of Kv1.2 surface expression were encoding the US strength in the cerebellar cortex allowing changes to take place prior to the onset of CRs, we would predict that a change from unpaired CS-alone and US-alone presentations to CS-US presentations would facilitate learning, rather than slow learning, but only after a significant number of US presentations. A future study is designed to test this idea. If the changes in surface Kv1.2 expression observed here are setting the stage for learning to take place, then we would hypothesize that Unpaired training would facilitate rather than impaired learning if the contingencies were changed to the CS did predict the onset of the US.

Another mechanism that may be contributing and that shares similarities to the secretin-induced mechanisms is depolarization-induced suppression of inhibition (DSI) (Duguid and Smart, 2004). Here, the authors report enhanced inhibitory transmission to PCs following calcium influx that is dependent upon presynaptic NMDA receptor activation (Duguid and Smart, 2004). Glutamate, similar to secretin, may be acting as a retrograde messenger to facilitate inhibition of PCs. A recent paper from the same laboratory suggests that these inhibitory mechanisms are exerted through BC-to-PC synapses near the PC soma rather than the stellate cell-to-PC synapse that is distally located on PC dendrites (He et al., 2015). Endogenous cannabinoids (or endocannabinoids) have been implicated in DSI in both the cerebellum (Alger and Pitler, 1995, Kreitzer and Regehr, 2001a, b, 2002, Diana and Marty, 2003) and hippocampus (Pitler and Alger, 1994, Alger and Pitler, 1995, Alger et al., 1996). Endocannabinoids are released from PCs following calcium influx and, like secretin, share presynaptic targets,

such as BCs (Egertova et al., 1998). Although these reports do not directly implicate Kv1.2 as the BC-specific mechanism, research from another lab determined that DSI does involve K+ currents (Diana and Marty, 2003).

Other stimulus inputs to the cerebellum that could be affecting the expression of surface Kv1.2 could include feed-forward mechanisms. BCs are innervated by CS-carrying parallel fibers (PFs) (Mittmann et al., 2005). Feed-forward inhibition through inhibitory interneurons in the cerebellar cortex may facilitate stimulus integration within EBC. This circuitry was shown to help integrate spike timing of PCs (Mittmann et al., 2005, Mittmann and Hausser, 2007), which is important for PC output (Hong and Optican, 2008). Furthermore, this inhibition may be region specific, with inhibition by BCs proximal to the PC soma outweighing inhibition by stellate cells (another cerebellar inhibitory interneuron) distally located from PC cell bodies (He et al., 2015).

Model Revisited

Prior to these experiments, we predicted a simpler role for Kv1.2 surface expression in acquisition of eyeblink CRs. This was based on the finding that blocking Kv1.2 in the cerebellar cortex prior to EBC led to a profound increase in CRs compared to subjects that received vehicle infusions (Williams et al., 2012) and impairing the endocytosis mechanisms of Kv1.2 impaired learning (Fuchs et al., 2014). The data from the current experiments complement and expand this story. Both experiments suggest that Kv1.2 surface expression is involved in processing the CS and US information in the cerebellar cortex. The data from the current experiments lend support for Kv1.2 regulation encoding the effectiveness of the US in the cortex.

To understand the role proposed for surface Kv1.2, we must consider what the current data (Chapters 2 and 3) and previous data (Williams et al., 2012, Fuchs et al., 2014) are demonstrating. Our previous data suggested that blocking Kv1.2 in the cerebellar cortex facilitated EBC (Williams et al., 2012). By infusing TsTX, a selective and potent inhibitor of Kv1.2 (Werkman et al., 1993), our working model predicted that this led to an increase in BC GABAergic input to PCs. This increase in PC inhibition would lead to disinhibition of the IPN and allow the CS-carrying MFs to increase in synaptic strength with the neurons of the IPN, leading to the subjects exhibiting CRs more quickly. A common thread in the EBC literature is that disinhibition of the IPN is important for CR expression. By expediting that process, CS-US associations may form more rapidly and key sites governing expression of the response will undergo necessary changes, leading to faster learning. When those subjects began generating CRs, the IPN would be inhibiting the IO, limiting US strength in the cerebellar cortex. In the first experiment (Chapter 3), this may explain why surface Kv1.2 did not differ between the Paired and No Stimulus groups (Fig. 4).

In the infusion study, however, Kv1.2 would remain blocked during training because infusions were made prior to the first six of seven days of EBC training. In the first experiment (Chapter 2), the Unpaired group showed reduced surface Kv1.2 expression on BC axon terminals following three days of training. Kv1.2 expressed on the surface but blocked by TsTX may be functionally similar to the reduced surface expression exhibited by the Unpaired group in Chapter 2. Prior to CR expression, there was an increased in Kv1.2 surface expression on PC dendrites. Both experiments reported

here (Chapters 2 and 3) suggest that the regulation of Kv1.2 is setting the stage for other mechanisms to govern expression of the CR.

If Kv1.2 is aiding in the encoding of stimuli inputs to PCs Kv1.2 on PC dendrites may help to faithfully encode stimulus inputs. When Kv1.2 is blocked, there is an increase in dendritic spike frequency and somatic burst firing, but no change in baseline firing rates (Khavandgar et al., 2005), suggesting that Kv1.2 plays a role in input sensitivity, but not pace-making for PCs. With this understanding, an increase in Kv1.2 surface expression early in training would facilitate the encoding of stimulus input to PCs by filtering spontaneous activity, which is important for EBC. Once the response is acquired, Kv1.2 returns to baseline expression (Fig. 8). The infusion data, however, suggest that blocking Kv1.2 in the cerebellar cortex facilitates EBC. These infusions presumably block Kv1.2 on BC axon terminals and PC dendrites. Since Khavangdar et al (2005) demonstrated that Kv1.2 does not contribute to the pace-making of PC firing and these experiments (Khavandgar et al., 2005) were conducted in the absence of fast glutamatergic (CNQX) and GABAergic (picrotoxin) presynaptic input, then blocking Kv1.2 on BC axon terminals should have a greater impact on the firing frequency of PCs, limiting this output in the presence of TsTX. Increased surface Kv1.2 would help to faithfully encode stimulus inputs in PCs by reducing dendritic and somatic excitability, based on the observation that blocking Kv1.2 containing channels increased spike frequency (Khavandgar et al., 2005).

Surface Kv1.2 in the cerebellar cortex may be governed by US input to PCs and release of the neuropeptide secretin. The US is relayed through the IO in the brainstem and climbing fiber (CF) projections from the IO synapse with PC dendrites and neurons

of the IPN. Importantly, when a CR is generated by the IPN, inhibitory projections from the IPN to the IO limit US input to the cerebellar cortex on subsequent trials. Although there is no direct evidence supporting the idea that US input causes the release of secretin from PCs, other data examining the mechanisms that lead to secretin release support the idea that US stimulation is connected with secretin release. The other infusion experiment conducted with Williams et al. (2012) infused secretin into the cerebellar cortex prior to acquisition. When this was done, we again observed a facilitation of EBC. Since secretin is endogenously released from PCs and is connected with endocytosis of Kv1.2 from BC axon terminals and PC dendrites, infusions of secretin may have acted to jump-start the system. By exogenously increasing the intercellular concentration of secretin, the regulation of Kv1.2 surface expression was underway. If Kv1.2 were suppressed at the start of training, then as the results from Experiment 2 (Chapter 3) suggest, CRs would emerge more quickly. We hypothesize that the same mechanism is involved in the experiments above.

Figure 9 represents a synthesis of the data from the current experiments, suggesting what is happening to Kv1.2 surface expression in the Unpaired (Fig. 9A) and Paired (Fig. 9B) groups as well as what is going on in the PC dendrites (green circles) and BC axon terminals (maroon squares). In the first experiment, we showed a robust reduction in surface Kv1.2 expression at BC axon terminals in the Unpaired group (Fig. 9A). If we consider this effect in relation to the US strength in the cerebellar cortex, then Kv1.2 is being suppressed because the inhibition of the IO by the IPN is weak, since the Unpaired group did not show any CRs. When the strength of the US is uninhibited, Kv1.2 surface expression at BC axon terminals is reduced. This is not the case when the shorter

training procedure was used. When looking at Kv1.2 on BC axon terminals after a shorter training procedure, we did not observe a reduction in surface Kv1.2. Although the strength of the US through the IO should be the same in the Unpaired groups between the experiments, we did not observe a change if surface Kv1.2 expression in the second experiment. One possibility is that to observe changes at BC axon terminals prolonged US stimulation such that was done in the first experiment is required. Another possibility is that these changes require some post training or consolidation period.

Focusing now on Kv1.2 expressed on PC dendrites, Figure 9 shows higher expression through both experiments in the Unpaired group (Fig. 9A). This effect is inferred from the combined results of WB and MP. There were no differences observed on the WB measure in the first experiment (Chapter 2). We hypothesize that for the Unpaired group this is due to the robust decrease in surface Kv1.2 surface expression on BC axon terminals combined with the lack of CRs. If Kv1.2 surface expression is changing in opposite directions at different sites and both of those sites are measured by the WB technique, then the lack of an effect in the WB measure may be attributed to an offsetting reduction at BC axon terminals. Therefore, we predict that the difference between Kv1.2 expressed on BC axon terminals and PC dendrites, as displayed in Figure 8A, is the reason we did not observe a significant effect in the Unpaired group in the WB measure in the first experiment.

Kv1.2 surface expression seems to be changing differently depending on the location measured and depending on CR expression in the Paired group. Considering first the Kv1.2 expressed on PC dendrites, we showed an increase in surface expression when subjects did not exhibit any CRs (Paired Low group) when compared to the No Stimulus

groups in the second experiment. When subjects in the Paired group did show some CRs (Chapter 3) or robust learning (Chapter 2), there was no difference observed on the WB measures between the Paired groups and No Stimulus groups (Figs. 5 and 8, respectively). Even when splitting the data based on performance in the first experiment, there did not seem to be a gradient for Kv1.2 surface expression in PC dendrites (data no shown). This "all or none" expression pattern for Kv1.2 surface expression suggests further that changes in Kv1.2 surface expression are dependent upon EBC and that these changes lead to acquisition of, but are not involved in the maintenance of eyeblink CRs. Other mechanisms that are governing expression of the CR could be long-term plasticity changes in the connection between the CS-relaying neurons and the neurons of the IPN (Boele et al., 2013), Other PC related mechanisms shown to reduce PC excitability (Garcia and Mauk, 1998, Garcia et al., 1999, Attwell et al., 2001), or other retrograde messenger systems exerting effects on BCs to limit PC output (Kreitzer and Regehr, 2001a, Kreitzer et al., 2002, Kreitzer and Regehr, 2002, Diana and Marty, 2003, Duguid and Smart, 2004, He et al., 2015) likely also plays a role.

The last effect to consider for these experiments is the lack of changes in Kv1.2 surface expression on BC axon terminals in the Paired group across both experiments. In both of the experiments, there was no difference reported between the Paired and No Stimulus groups measured by MP, and this is shown in Figure 9 as no change from baseline levels. This is not to say that Kv1.2 on BC axon terminals is not involved, but these data show that, when we sampled Kv1.2 surface expression at the two time points, there were no changes evident. One idea for why this was observed is that changes in Kv1.2 surface expression take more time than was allotted between the training sessions

and tissue harvest in both experiments. In the two experiments, rats were sacrificed and tissue was harvested immediately following EBC training, a time point that we predicted to be critical. It is possible, however, that changes in surface Kv1.2 expression on BC axon terminals may require longer post-training breaks. If other learning mechanisms such as consolidation are occurring at these sites, one might expect changes in Kv1.2 surface expression to take place 12- or 24-hours after training. Sampling Kv1.2 after one day of training for all groups, but waiting a certain period of time to harvest the tissue may reveal a longer-term role for Kv1.2 expression, a role that goes beyond the short term encoding of US information.

In summary, Kv1.2 surface expression appears to be regulated during EBC. This regulation is dependent upon the specific training procedure used and whether or not CRs are being expressed.

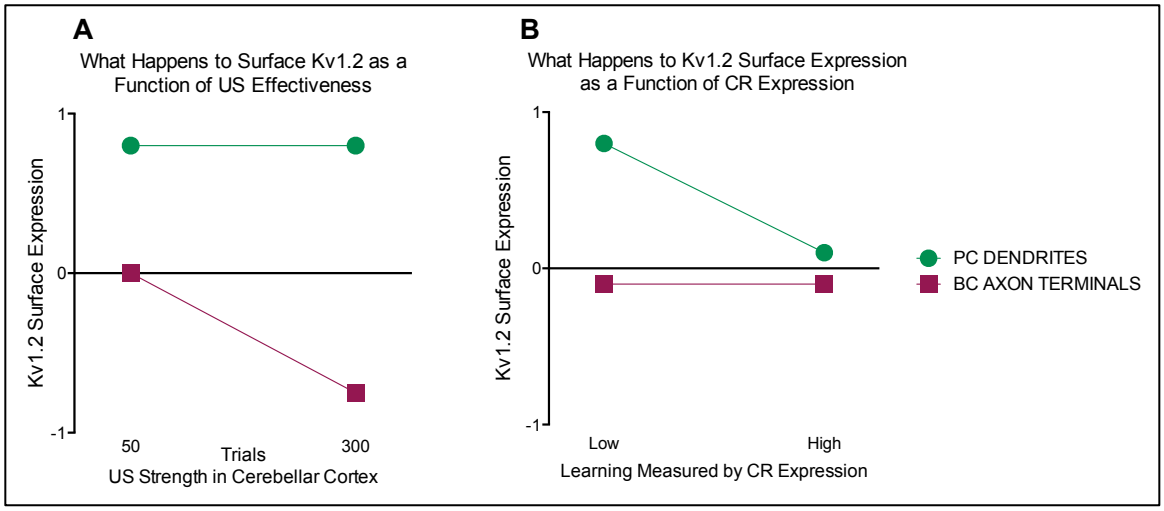

Figure 9. Conceptual depiction of what is happening to Kv1.2 surface expression in the (A) Unpaired groups in both experiments and (B) Paired groups in both experiments. Note that data for PC dendrites (green circles) are an inference from the combined results of WB (which measured PC dendrites and BC axon terminals) and MP (which measured only BC terminals). The Kv1.2 surface expression data are conceptualized as a function of (A) US strength and (B) CR expression.

Significance

First and foremost, this project is one of the first demonstrations of voltage-gated ion channel regulation in mammalian learning and memory. To my knowledge, no studies have looked at changes in voltage-gated ion channels during or after eyeblink conditioning. Many studies demonstrate the regulation of AMPA receptors and how that contributes to learning and memory, but very few focus on the regulation of voltage-sensitive channels. Secondly, these experiments suggest a novel mechanism for detecting US strength in the cerebellar cortex and that this detection is involved in acquisition of eyeblink responses. Finally, the results from these experiments are significant for the two areas of research that were bridged by this project. As mentioned in the introduction, EBC is a useful paradigm for studying the neurobiology of learning and memory. The learned response is easily distinguished from the reflexive response, the neural pathways involved in the acquisition and expression of the learned response are well known, and the stimuli used to produce learning are simple. The finding that voltage-gated potassium channels are regulated in EBC is a novel mechanism for the eyeblink conditioning literature. Furthermore, the current data provide a unique understanding of the types of stimuli that can regulate Kv1.2. Regulation of voltage-gated channels is a fundamental mechanism for maintaining the excitability of neurons. We hypothesized that this regulation would occur during EBC and now we have evidence supporting this idea.

Limitations and Future Directions

While the results showing changes in Kv1.2 surface expression in the cerebellar cortex as a function of eyeblink CR expression may provide insight for a fundamental

mechanism is mammalian learning and memory, there are also some limitations to these experiments. The two techniques that were utilized provided a somewhat comprehensive understanding of what is happening to Kv1.2 surface expression following EBC training by sampling Kv1.2 at the two primary sites of expression: BC axon terminals and PC dendrites (Koch et al., 1997). The MP method provided a measure of localized Kv1.2 surface expression at BC axon terminals within a specific region of the cerebellar cortex (Steinmetz and Freeman, 2014), while the WB method measured Kv1.2 surface expression at both sites, but also across the entire section. Although the WB measure allowed us to sample Kv1.2 surface expression at the two primary sites, one drawback to this method was that, in order to detect Kv1.2 on the blot, a lot of tissue was required. This led to sampling Kv1.2 surface expression in areas within the cortex that may not be involved in EBC. Sampling this extra areas makes detection possible may be introducing noise to the measure as well. Because of this, the changes observed in this measure may not solely be attributed to changes taking place around the base of the primary fissure.

Another consideration for these data pertaining to the region recently identified for EBC within the cerebellar cortex is the number of PCs actually involved to develop an eyeblink CR. The identification of the base of the primary fissure by Freeman and colleagues (2014) was a helpful guide for the sampling for this experiment, but we do not know how many PCs are necessary or how many are just sufficient. Considering the size of the lesion in the aforementioned paper, the number of neurons involved compared to the rest of the section is quite low, but the exact number would be difficult to determine. Depending on the level granularity within the cerebellar cortex for controlling muscle movement and the size and precision of the muscles involved, it is possible that very few

neurons within the network are involved and the reason Freeman and colleagues observed an effect is because those few neurons were included in the lesioned area. It is also possible that more neurons that were affected in that area are necessary, but a critical number of them were lesioned, leading the deficits in learning. The data reported in the current experiments provided little information to this point, but still indicate that the expression of Kv1.2 on certain cell types may still be involved on those critical neurons.

Another important consideration for the WB measure is the treatment of the tissues. This method was previously validated in live tissue (Williams et al., 2012). In order to extract only surface Kv1.2 from paraformaldehyde fixed slices, however, additional steps to create new binding sites on surface proteins and to pull down surface expressed channel were necessary. It is worth considering however, that these treatments can be harsh and may be limiting the amount of surface protein pulled down by the Neutravidin beads. This may not be a major drawback since all of the sections from each of the three groups were treated in the same manner and thus, these methodological drawbacks may be accounted for. We do not suspect that the sections were comprised in such a fashion, but only seek to recognize that is could be a possibility.

A third limitation is that there was only one method sampling Kv1.2 at PC dendrites. Although Kv1.2 expression levels are not as dense as has been observed on BC axon terminals, localized surface expression of Kv1.2 on PC dendrites has been measured by microscopy (Williams et al., 2012). Attempts were made with the multiphoton microscope to sample Kv1.2 surface expression in PC dendrites (data not shown), but it proved difficult. In our previous study, a different microscope system was used and thinner cerebellar sections were imaged (Williams et al., 2012). In the current

experiments, however, we were interested in sampling from a larger region than the aforementioned microscope would allow. We were also interested in obtaining data from the Z-plane. For these reasons, the multiphoton microscope suited our needs, but one drawback was the inability to reliably sample Kv1.2 surface expression on PC dendrites. A follow-up study might use other markers of PC dendrites to more easily identify these structures.

By being able to more precisely sample Kv1.2 on PC dendrites, we may further our understanding of the current data. Since Kv1.2 on BC axon terminals was sampled in both measures, we were able to understand these data by normalizing the results between the measures. For instance, a lack of an effect in the MP and a significant change in the WB could indicate that changed in surface Kv1.2 expression might be limited to PC dendrites. An additional imaging step that allowed us to measure Kv1.2 surface expression on PC dendrites would make for a stronger argument when deducing these data.

Another limitation, that relates more to the physiology of the channel, is what we can be extrapolated from these data. When discussing changes in ion channel expression, we are considering a physiological change. However, since both measures of Kv1.2 surface expression were done on fixed cerebellar sections, inferring a profound physiological change may be overstating the data. The numerous papers that contributed to our hypotheses, in particular the electrophysiology papers, examined the biophysical properties of Kv1.2 in isolation, either through pharmacological blockade of particular channels or currents or by removing a portion of the cellular membrane and studying a few (possibly many) channels at a time. By removing most of the extraneous modulators

of Kv1.2 current, these articles show the refined version of the channels function. This refined function may not be the only one involved in cellular excitability. There are a plethora of other variables to consider. A short list may include changes in Kv-beta subunit expression, changes in the expression of other subunits such as Kv1.1, and importantly, what behaviors like EBC are doing to the channel. Some or all of these could be affecting the Kv1.2 surface expression in the cerebellar cortex during EBC, but by only measuring surface expression without physiology, we only have a smaller portion of the picture depicting the function of Kv1.2. To determine if there are physiological changes that are accompanying the changes in expression observed here, a follow-up study recording from PC dendrites and BC axon terminals may provide useful insight. By recording from PC dendrites using methods employed by Khavangdar et al. (2005) and/or recording from BC axon terminals like Southan and Robertson (1998a,b; 2000), the physiological changes inferred from these data may be observed.

There is the possibility that these changes in Kv1.2 surface expression have nothing to do with the actual physiology of the cells where the expression patterns are changing. Previous reports have suggested that channels containing Kv1 subunits and others or clusters of these channels can remain silent despite synaptic input and changes to membrane excitability (Stocker et al., 1999). If for instance the changes in expression patters that were shown in the current experiments were only on these "silent" channels, then the changes within the cerebellum would not be significant, but only looking at expression. The aforementioned follow-up study could elucidate this idea. We would predict that even changes to these clusters of silent Kv1.2-containing channels is still

having some sort of physiological change, but our current methods are not able to measure what those changes might be.

All together, the parsimonious understanding of these data, based on our previous findings and the findings from other labs, we suggest that changes in Kv1.2 surface expression in the cerebellum is linked to the acquisition, but not the expression of the learned response. Not to be disregarded is the idea that Kv1.2 containing channels do not have a single function, but a dynamic range of functions that depends on the needs of the cell, the input to that cell and surrounding cells, and the intra- and extracellular environment (i.e. messengers, signaling cascade molecules).

References

Aiba A, Kano M, Chen C, Stanton ME, Fox GD, Herrup K, Zwingman TA, Tonegawa S (1994) Deficient cerebellar long-term depression and impaired motor learning in mGluR1 mutant mice. Cell 79:377-388.

Aizenman CD, Linden DJ (2000) Rapid, synaptically driven increases in the intrinsic excitability of cerebellar deep nuclear neurons. Nat Neurosci 3:109-111.

Alger BE, Pitler TA (1995) Retrograde signaling at GABAA-receptor synapses in the mammalian CNS. Trends Neurosci 18:333-340.

Alger BE, Pitler TA, Wagner JJ, Martin LA, Morishita W, Kirov SA, Lenz RA (1996) Retrograde signalling in depolarization-induced suppression of inhibition in rat hippocampal CA1 cells. J Physiol 496 (Pt 1):197-209.

Alkon DL, Collin C, Ito E, Lee CJ, Nelson TJ, Oka K, Sakakibara M, Schreurs BG, Yoshioka T (1993) Molecular and biophysical steps in the storage of associative memory. Ann N Y Acad Sci 707:500-504.

Attwell PJ, Rahman S, Yeo CH (2001) Acquisition of eyeblink conditioning is critically dependent on normal function in cerebellar cortical lobule HVI. J Neurosci 21:5715-5722.

Baumann A, Grupe A, Ackermann A, Pongs O (1988) Structure of the voltage-dependent potassium channel is highly conserved from Drosophila to vertebrate central nervous systems. EMBO J 7:2457-2463.

Bayliss WM, Starling EH (1902) The mechanism of pancreatic secretion. J Physiol 28:325-353.

Bekele-Arcuri Z, Matos MF, Manganas L, Strassle BW, Monaghan MM, Rhodes KJ, Trimmer JS (1996) Generation and characterization of subtype-specific monoclonal antibodies to K+ channel alpha- and beta-subunit polypeptides. Neuropharmacology 35:851-865.

Berthier NE, Moore JW (1986) Cerebellar Purkinje cell activity related to the classically conditioned nictitating membrane response. Exp Brain Res 63:341-350.

Berthier NE, Moore JW (1990) Activity of deep cerebellar nuclear cells during classical conditioning of nictitating membrane extension in rabbits. Exp Brain Res 83:44-54.

Boele HJ, Koekkoek SK, De Zeeuw CI, Ruigrok TJ (2013) Axonal sprouting and formation of terminals in the adult cerebellum during associative motor learning. J Neurosci 33:17897-17907.

Brew HM, Forsythe ID (1995) Two voltage-dependent K+ conductances with complementary functions in postsynaptic integration at a central auditory synapse. J Neurosci 15:8011-8022.

Brodal P, Brodal A (1981) The olivocerebellar projection in the monkey. Experimental studies with the method of retrograde tracing of horseradish peroxidase. J Comp Neurol 201:375-393.

Burnashev N, Khodorova A, Jonas P, Helm PJ, Wisden W, Monyer H, Seeburg PH, Sakmann B (1992) Calcium-permeable AMPA-kainate receptors in fusiform cerebellar glial cells. Science 256:1566-1570.

Cachero TG, Morielli AD, Peralta EG (1998) The small GTP-binding protein RhoA regulates a delayed rectifier potassium channel. Cell 93:1077-1085.

Cerda O, Trimmer JS (2010) Analysis and functional implications of phosphorylation of neuronal voltage-gated potassium channels. Neurosci Lett 486:60-67.

Chapman PF, Steinmetz JE, Sears LL, Thompson RF (1990) Effects of lidocaine injection in the interpositus nucleus and red nucleus on conditioned behavioral and neuronal responses. Brain Res 537:149-156.

Chapman PF, Steinmetz JE, Thompson RF (1988) Classical conditioning does not occur when direct stimulation of the red nucleus or cerebellar nuclei is the unconditioned stimulus. Brain Res 442:97-104.

Chen C, Thompson RF (1995) Temporal specificity of long-term depression in parallel fiber--Purkinje synapses in rat cerebellar slice. Learn Mem 2:185-198.

Chey WY, Chang TM (2003) Secretin, 100 years later. Journal of gastroenterology 38:1025-1035.

Chow BK (1995) Molecular cloning and functional characterization of a human secretin receptor. Biochem Biophys Res Commun 212:204-211.

Christian KM, Thompson RF (2003) Neural substrates of eyeblink conditioning: acquisition and retention. Learn Mem 10:427-455.

Chung YH, Shin C, Kim MJ, Lee BK, Cha CI (2001) Immunohistochemical study on the distribution of six members of the Kv1 channel subunits in the rat cerebellum. Brain Res 895:173-177.

Claflin DI, Buffington ML (2006) CS-US preexposure effects on trace eyeblink conditioning in young rats: potential implications for functional brain development. Behav Neurosci 120:257-266.

Clark RE, Zhang AA, Lavond DG (1992) Reversible lesions of the cerebellar interpositus nucleus during acquisition and retention of a classically conditioned behavior. Behav Neurosci 106:879-888.

Coesmans M, Weber JT, De Zeeuw CI, Hansel C (2004) Bidirectional parallel fiber plasticity in the cerebellum under climbing fiber control. Neuron 44:691-700.

Connors EC, Ballif BA, Morielli AD (2008) Homeostatic regulation of Kv1.2 potassium channel trafficking by cyclic AMP. J Biol Chem 283:3445-3453.

Crepel F, Krupa M (1988) Activation of protein kinase C induces a long-term depression of glutamate sensitivity of cerebellar Purkinje cells. An in vitro study. Brain Res 458:397-401.

De Zeeuw CI, Hoebeek FE, Bosman LW, Schonewille M, Witter L, Koekkoek SK (2011) Spatiotemporal firing patterns in the cerebellum. Nat Rev Neurosci 12:327-344.

Diana MA, Marty A (2003) Characterization of depolarization-induced suppression of inhibition using paired interneuron--Purkinje cell recordings. J Neurosci 23:5906-5918.

Doi T, Kuroda S, Michikawa T, Kawato M (2005) Inositol 1,4,5-trisphosphate-dependent Ca2+ threshold dynamics detect spike timing in cerebellar Purkinje cells. J Neurosci 25:950-961.

Duguid IC, Smart TG (2004) Retrograde activation of presynaptic NMDA receptors enhances GABA release at cerebellar interneuron-Purkinje cell synapses. Nat Neurosci 7:525-533.

Ebner-Bennatan S, Patrich E, Peretz A, Kornilov P, Tiran Z, Elson A, Attali B (2012) Multifaceted modulation of K+ channels by protein-tyrosine phosphatase epsilon tunes neuronal excitability. J Biol Chem 287:27614-27628.

Eccles JC, Llinas R, Sasaki K, Voorhoeve PE (1966) Interaction experiments on the responses evoked in Purkinje cells by climbing fibres. J Physiol 182:297-315.

Egertova M, Giang DK, Cravatt BF, Elphick MR (1998) A new perspective on cannabinoid signalling: complementary localization of fatty acid amide hydrolase and the CB1 receptor in rat brain. Proc Biol Sci 265:2081-2085.

Ekerot CF, Kano M (1989) Stimulation parameters influencing climbing fibre induced long-term depression of parallel fibre synapses. Neuroscience research 6:264-268.

Feil R, Hartmann J, Luo C, Wolfsgruber W, Schilling K, Feil S, Barski JJ, Meyer M, Konnerth A, De Zeeuw CI, Hofmann F (2003) Impairment of LTD and cerebellar learning by Purkinje cell-specific ablation of cGMP-dependent protein kinase I. J Cell Biol 163:295-302.

Finch EA, Augustine GJ (1998) Local calcium signalling by inositol-1,4,5-trisphosphate in Purkinje cell dendrites. Nature 396:753-756.

Finch EA, Tanaka K, Augustine GJ (2012) Calcium as a trigger for cerebellar long-term synaptic depression. Cerebellum 11:706-717.

Freeman JH, Jr., Carter CS, Stanton ME (1995) Early cerebellar lesions impair eyeblink conditioning in developing rats: differential effects of unilateral lesions on postnatal day 10 or 20. Behav Neurosci 109:893-902.

Freeman JH, Jr., Nicholson DA (1999) Neuronal activity in the cerebellar interpositus and lateral pontine nuclei during inhibitory classical conditioning of the eyeblink response. Brain Res 833:225-233.

Freeman JH, Jr., Rabinak CA, Campolattaro MM (2005) Pontine stimulation overcomes developmental limitations in the neural mechanisms of eyeblink conditioning. Learn Mem 12:255-259.

Fuchs JR, Robinson GM, Dean AM, Schoenberg HE, Williams MR, Morielli AD, Green JT (2014) Cerebellar secretin modulates eyeblink classical conditioning. Learn Mem 21:668-675.

Gao Z, van Beugen BJ, De Zeeuw CI (2012) Distributed synergistic plasticity and cerebellar learning. Nat Rev Neurosci 13:619-635.

Garcia KS, Mauk MD (1998) Pharmacological analysis of cerebellar contributions to the timing and expression of conditioned eyelid responses. Neuropharmacology 37:471-480.

Garcia KS, Steele PM, Mauk MD (1999) Cerebellar cortex lesions prevent acquisition of conditioned eyelid responses. J Neurosci 19:10940-10947.

Glickstein M, Cohen JL, Dixon B, Gibson A, Hollins M, Labossiere E, Robinson F (1980) Corticopontine visual projections in macaque monkeys. J Comp Neurol 190:209-229.

Glickstein M, Sultan F, Voogd J (2011) Functional localization in the cerebellum. Cortex; a journal devoted to the study of the nervous system and behavior 47:59-80.

Glitsch M, Marty A (1999) Presynaptic effects of NMDA in cerebellar Purkinje cells and interneurons. J Neurosci 19:511-519.

Gould TJ, Steinmetz JE (1996) Changes in rabbit cerebellar cortical and interpositus nucleus activity during acquisition, extinction, and backward classical eyelid conditioning. Neurobiol Learn Mem 65:17-34.

Green JT, Steinmetz JE (2005) Purkinje cell activity in the cerebellar anterior lobe after rabbit eyeblink conditioning. Learn Mem 12:260-269.

Gruart A, Yeo CH (1995) Cerebellar cortex and eyeblink conditioning: bilateral regulation of conditioned responses. Exp Brain Res 104:431-448.

Hansel C, Linden DJ (2000) Long-term depression of the cerebellar climbing fiber--Purkinje neuron synapse. Neuron 26:473-482.

Hartmann J, Konnerth A (2005) Determinants of postsynaptic Ca2+ signaling in Purkinje neurons. Cell calcium 37:459-466.

Harvey RJ, Napper RM (1991) Quantitative studies on the mammalian cerebellum. Progress in neurobiology 36:437-463.

Hashimoto K, Miyata M, Watanabe M, Kano M (2001) Roles of phospholipase Cbeta4 in synapse elimination and plasticity in developing and mature cerebellum. Mol Neurobiol 23:69-82.

Hattan D, Nesti E, Cachero TG, Morielli AD (2002) Tyrosine phosphorylation of Kv1.2 modulates its interaction with the actin-binding protein cortactin. J Biol Chem 277:38596-38606.

He Q, Duguid I, Clark B, Panzanelli P, Patel B, Thomas P, Fritschy JM, Smart TG (2015) Interneuron- and GABAA receptor-specific inhibitory synaptic plasticity in cerebellar Purkinje cells. Nat Commun 6:7364.

Hesslow G, Ivarsson M (1996) Inhibition of the inferior olive during conditioned responses in the decerebrate ferret. Exp Brain Res 110:36-46.

Hesslow G, Jirenhed DA, Rasmussen A, Johansson F (2013) Classical conditioning of motor responses: what is the learning mechanism? Neural networks : the official journal of the International Neural Network Society 47:81-87.

Hoaglin DC, Iglewicz B (1987) Fine-Tuning Some Resistant Rules for Outlier Labeling. Journal of the American Statistic Association 82:1147-1149.

Hoaglin DC, Iglewicz B, Tukey JW (1986) Performance of some resistnt rules for outlier labeling. Journal of the American Statistic Association 81:991-999.

Hong S, Optican LM (2008) Interaction between Purkinje cells and inhibitory interneurons may create adjustable output waveforms to generate timed cerebellar output. PLoS One 3:e2770.

Hopkins WF (1998) Toxin and subunit specificity of blocking affinity of three peptide toxins for heteromultimeric, voltage-gated potassium channels expressed in Xenopus oocytes. J Pharmacol Exp Ther 285:1051-1060.

Hosy E, Piochon C, Teuling E, Rinaldo L, Hansel C (2011) SK2 channel expression and function in cerebellar Purkinje cells. J Physiol 589:3433-3440.

Huang XY, Morielli AD, Peralta EG (1993) Tyrosine kinase-dependent suppression of a potassium channel by the G protein-coupled m1 muscarinic acetylcholine receptor. Cell 75:1145-1156.

Ishihara T, Nakamura S, Kaziro Y, Takahashi T, Takahashi K, Nagata S (1991) Molecular cloning and expression of a cDNA encoding the secretin receptor. EMBO J 10:1635-1641.

Ito M (2002) The molecular organization of cerebellar long-term depression. Nat Rev Neurosci 3:896-902.

Ito M, Kano M (1982) Long-lasting depression of parallel fiber-Purkinje cell transmission induced by conjunctive stimulation of parallel fibers and climbing fibers in the cerebellar cortex. Neurosci Lett 33:253-258.

Ito M, Sakurai M, Tongroach P (1982) Climbing fibre induced depression of both mossy fibre responsiveness and glutamate sensitivity of cerebellar Purkinje cells. J Physiol 324:113-134.

Kaffashian M, Shabani M, Goudarzi I, Behzadi G, Zali A, Janahmadi M (2011) Profound alterations in the intrinsic excitability of cerebellar Purkinje neurons following neurotoxin 3-acetylpyridine (3-AP)-induced ataxia in rat: new insights into the role of small conductance K+ channels. Physiol Res 60:355-365.

Kakizawa S, Kishimoto Y, Hashimoto K, Miyazaki T, Furutani K, Shimizu H, Fukaya M, Nishi M, Sakagami H, Ikeda A, Kondo H, Kano M, Watanabe M, Iino M, Takeshima H (2007) Junctophilin-mediated channel crosstalk essential for cerebellar synaptic plasticity. EMBO J 26:1924-1933.

Kano K, Kato M (1988) Mode of induction of long-term depression at parallel fibre--Purkinje cell synapses in rabbit cerebellar cortex. Neuroscience research 5:544-556.

Kawaguchi SY, Nagasaki N, Hirano T (2011) Dynamic impact of temporal context of Ca(2)(+) signals on inhibitory synaptic plasticity. Scientific reports 1:143.

Kawaguchi SY, Sakaba T (2015) Control of inhibitory synaptic outputs by low excitability of axon terminals revealed by direct recording. Neuron 85:1273-1288.

Khavandgar S, Walter JT, Sageser K, Khodakhah K (2005) Kv1 channels selectively prevent dendritic hyperexcitability in rat Purkinje cells. J Physiol 569:545-557.

Kim JJ, Krupa DJ, Thompson RF (1998) Inhibitory cerebello-olivary projections and blocking effect in classical conditioning. Science 279:570-573.

Kishimoto Y, Fujimichi R, Araishi K, Kawahara S, Kano M, Aiba A, Kirino Y (2002) mGluR1 in cerebellar Purkinje cells is required for normal association of temporally contiguous stimuli in classical conditioning. Eur J Neurosci 16:2416-2424.

Kitamura K, Hausser M (2011) Dendritic calcium signaling triggered by spontaneous and sensory-evoked climbing fiber input to cerebellar Purkinje cells in vivo. J Neurosci 31:10847-10858.

Kleim JA, Freeman JH, Jr., Bruneau R, Nolan BC, Cooper NR, Zook A, Walters D (2002) Synapse formation is associated with memory storage in the cerebellum. Proc Natl Acad Sci U S A 99:13228-13231.

Knowlton BJ, Thompson RF (1988) Microinjections of local anesthetic into the pontine nuclei reduce the amplitude of the classically conditioned eyelid response. Physiol Behav 43:855-857.

Koch RO, Wanner SG, Koschak A, Hanner M, Schwarzer C, Kaczorowski GJ, Slaughter RS, Garcia ML, Knaus HG (1997) Complex subunit assembly of neuronal voltage-gated K+ channels. Basis for high-affinity toxin interactions and pharmacology. J Biol Chem 272:27577-27581.

Koves K, Kausz M, Reser D, Horvath K (2002) What may be the anatomical basis that secretin can improve the mental functions in autism? Regul Pept 109:167-172.

Koves K, Kausz M, Reser D, Illyes G, Takacs J, Heinzlmann A, Gyenge E, Horvath K (2004) Secretin and autism: a basic morphological study about the distribution of secretin in the nervous system. Regul Pept 123:209-216.

Kreider JC, Mauk MD (2010) Eyelid conditioning to a target amplitude: adding how much to whether and when. J Neurosci 30:14145-14152.

Kreitzer AC, Carter AG, Regehr WG (2002) Inhibition of interneuron firing extends the spread of endocannabinoid signaling in the cerebellum. Neuron 34:787-796.

Kreitzer AC, Regehr WG (2001a) Cerebellar depolarization-induced suppression of inhibition is mediated by endogenous cannabinoids. J Neurosci 21:RC174.

Kreitzer AC, Regehr WG (2001b) Retrograde inhibition of presynaptic calcium influx by endogenous cannabinoids at excitatory synapses onto Purkinje cells. Neuron 29:717-727.

Kreitzer AC, Regehr WG (2002) Retrograde signaling by endocannabinoids. Curr Opin Neurobiol 12:324-330.

Krupa DJ, Thompson JK, Thompson RF (1993) Localization of a memory trace in the mammalian brain. Science 260:989-991.

Larsell O (1952) The morphogenesis and adult pattern of the lobules and fissures of the cerebellum of the white rat. J Comp Neurol 97:281-356.

Laube G, Roper J, Pitt JC, Sewing S, Kistner U, Garner CC, Pongs O, Veh RW (1996) Ultrastructural localization of Shaker-related potassium channel subunits and synapse-associated protein 90 to septate-like junctions in rat cerebellar Pinceaux. Brain Res Mol Brain Res 42:51-61.

Lavond DG, Steinmetz JE (1989) Acquisition of classical conditioning without cerebellar cortex. Behav Brain Res 33:113-164.

Lee SM, Chen L, Chow BK, Yung WH (2005) Endogenous release and multiple actions of secretin in the rat cerebellum. Neuroscience 134:377-386.

Liljelund P, Netzeband JG, Gruol DL (2000) L-Type calcium channels mediate calcium oscillations in early postnatal Purkinje neurons. J Neurosci 20:7394-7403.

Linden DJ, Connor JA (1991) Participation of postsynaptic PKC in cerebellar long-term depression in culture. Science 254:1656-1659.

Linden DJ, Dickinson MH, Smeyne M, Connor JA (1991) A long-term depression of AMPA currents in cultured cerebellar Purkinje neurons. Neuron 7:81-89.

Lindquist DH, Mahoney LP, Steinmetz JE (2010) Conditioned fear in adult rats is facilitated by the prior acquisition of a classically conditioned motor response. Neurobiol Learn Mem 94:167-175.

Maiz J, Karakossian MH, Pakaprot N, Robleto K, Thompson RF, Otis TS (2012) Prolonging the postcomplex spike pause speeds eyeblink conditioning. Proc Natl Acad Sci U S A 109:16726-16730.

Mauk MD, Donegan NH (1997) A model of Pavlovian eyelid conditioning based on the synaptic organization of the cerebellum. Learn Mem 4:130-158.

Mauk MD, Steinmetz JE, Thompson RF (1986) Classical conditioning using stimulation of the inferior olive as the unconditioned stimulus. Proc Natl Acad Sci U S A 83:5349-5353.

McCormick DA, Clark GA, Lavond DG, Thompson RF (1982a) Initial localization of the memory trace for a basic form of learning. Proc Natl Acad Sci U S A 79:2731-2735.

McCormick DA, Guyer PE, Thompson RF (1982b) Superior cerebellar peduncle lesions selectively abolish the ipsilateral classically conditioned nictitating membrane/eyelid response of the rabbit. Brain Res 244:347-350.

McCormick DA, Lavond DG, Thompson RF (1983) Neuronal responses of the rabbit brainstem during performance of the classically conditioned nictitating membrane (NM)/eyelid response. Brain Res 271:73-88.

McCormick DA, Steinmetz JE, Thompson RF (1985) Lesions of the inferior olivary complex cause extinction of the classically conditioned eyeblink response. Brain Res 359:120-130.

McCormick DA, Thompson RF (1984a) Cerebellum: essential involvement in the classically conditioned eyelid response. Science 223:296-299.

McCormick DA, Thompson RF (1984b) Neuronal responses of the rabbit cerebellum during acquisition and performance of a classically conditioned nictitating membrane-eyelid response. J Neurosci 4:2811-2822.

McKay BE, Molineux ML, Mehaffey WH, Turner RW (2005) Kv1 K+ channels control Purkinje cell output to facilitate postsynaptic rebound discharge in deep cerebellar neurons. J Neurosci 25:1481-1492.

McNamara NM, Averill S, Wilkin GP, Dolly JO, Priestley JV (1996) Ultrastructural localization of a voltage-gated K+ channel alpha subunit (KV 1.2) in the rat cerebellum. Eur J Neurosci 8:688-699.

McNamara NM, Muniz ZM, Wilkin GP, Dolly JO (1993) Prominent location of a K+ channel containing the alpha subunit Kv 1.2 in the basket cell nerve terminals of rat cerebellum. Neuroscience 57:1039-1045.

Medina JF, Garcia KS, Nores WL, Taylor NM, Mauk MD (2000) Timing mechanisms in the cerebellum: testing predictions of a large-scale computer simulation. J Neurosci 20:5516-5525.

Medina JF, Mauk MD (1999) Simulations of cerebellar motor learning: computational analysis of plasticity at the mossy fiber to deep nucleus synapse. J Neurosci 19:7140-7151.

Medina JF, Nores WL, Mauk MD (2002) Inhibition of climbing fibres is a signal for the extinction of conditioned eyelid responses. Nature 416:330-333.

Miller C (2000) An overview of the potassium channel family. Genome Biol 1:REVIEWS0004.

Miller LJ, Dong M, Harikumar KG (2012) Ligand binding and activation of the secretin receptor, a prototypic family B G protein-coupled receptor. Br J Pharmacol 166:18-26.

Mittmann W, Hausser M (2007) Linking synaptic plasticity and spike output at excitatory and inhibitory synapses onto cerebellar Purkinje cells. J Neurosci 27:5559-5570.

Mittmann W, Koch U, Hausser M (2005) Feed-forward inhibition shapes the spike output of cerebellar Purkinje cells. J Physiol 563:369-378.

Miyata M, Kim HT, Hashimoto K, Lee TK, Cho SY, Jiang H, Wu Y, Jun K, Wu D, Kano M, Shin HS (2001) Deficient long-term synaptic depression in the rostral cerebellum correlated with impaired motor learning in phospholipase C beta4 mutant mice. Eur J Neurosci 13:1945-1954.

Napper RM, Harvey RJ (1988) Number of parallel fiber synapses on an individual Purkinje cell in the cerebellum of the rat. J Comp Neurol 274:168-177.

Nesti E, Everill B, Morielli AD (2004) Endocytosis as a mechanism for tyrosine kinase-dependent suppression of a voltage-gated potassium channel. Mol Biol Cell 15:4073-4088.

Ng SS, Yung WH, Chow BK (2002) Secretin as a neuropeptide. Mol Neurobiol 26:97-107.

Nicholson DA, Freeman JH, Jr. (2002) Neuronal correlates of conditioned inhibition of the eyeblink response in the anterior interpositus nucleus. Behav Neurosci 116:22-36.

Nieto-Bona MP, Garcia-Segura LM, Torres-Aleman I (1997) Transynaptic modulation by insulin-like growth factor I of dendritic spines in Purkinje cells. Int J Dev Neurosci 15:749-754.

Nolan BC, Nicholson DA, Freeman JH, Jr. (2002) Blockade of GABAA receptors in the interpositus nucleus modulates expression of conditioned excitation but not

conditioned inhibition of the eyeblink response. Integr Physiol Behav Sci 37:293-310.

Nozaki S, Nakata R, Mizuma H, Nishimura N, Watanabe Y, Kohashi R, Watanabe Y (2002) In vitro autoradiographic localization of (125)i-secretin receptor binding sites in rat brain. Biochem Biophys Res Commun 292:133-137.

Ohtani Y, Miyata M, Hashimoto K, Tabata T, Kishimoto Y, Fukaya M, Kase D, Kassai H, Nakao K, Hirata T, Watanabe M, Kano M, Aiba A (2014) The synaptic targeting of mGluR1 by its carboxyl-terminal domain is crucial for cerebellar function. J Neurosci 34:2702-2712.

Ohtsuki G, Piochon C, Hansel C (2009) Climbing fiber signaling and cerebellar gain control. Frontiers in cellular neuroscience 3:4.

Ohyama T, Nores WL, Medina JF, Riusech FA, Mauk MD (2006) Learning-induced plasticity in deep cerebellar nucleus. J Neurosci 26:12656-12663.

Pekhletski R, Gerlai R, Overstreet LS, Huang XP, Agopyan N, Slater NT, Abramow-Newerly W, Roder JC, Hampson DR (1996) Impaired cerebellar synaptic plasticity and motor performance in mice lacking the mGluR4 subtype of metabotropic glutamate receptor. J Neurosci 16:6364-6373.

Piochon C, Levenes C, Ohtsuki G, Hansel C (2010) Purkinje cell NMDA receptors assume a key role in synaptic gain control in the mature cerebellum. J Neurosci 30:15330-15335.

Pitler TA, Alger BE (1994) Depolarization-induced suppression of GABAergic inhibition in rat hippocampal pyramidal cells: G protein involvement in a presynaptic mechanism. Neuron 13:1447-1455.

Pongs O, Kecskemethy N, Muller R, Krah-Jentgens I, Baumann A, Kiltz HH, Canal I, Llamazares S, Ferrus A (1988) Shaker encodes a family of putative potassium channel proteins in the nervous system of Drosophila. EMBO J 7:1087-1096.

Ramnani N (2006) The primate cortico-cerebellar system: anatomy and function. Nat Rev Neurosci 7:511-522.

Rescorla RA (1973) Effect of US habituation following conditioning. Journal of comparative and physiological psychology 82:137-143.

Rescorla RA (1976) Stimulus generalization: some predictions from a model of Pavlovian conditioning. J Exp Psychol Anim Behav Process 2:88-96.

Rescorla RA, Furrow DR (1977) Stimulus similarity as a determinant of Pavlovian conditioning. J Exp Psychol Anim Behav Process 3:203-215.

Rescorla RA, Wagner AR (1972) A theory of pavlovian conditioning: Variations in the effectiveness of reinforcement and nonreinforcement. In: Classical Conditioning (Black, A. H. and Prokasy, W. F., eds), pp 64-99: Appleton-Century-Crofts.

Rizley RC, Rescorla RA (1972) Associations in second-order conditioning and sensory preconditioning. Journal of comparative and physiological psychology 81:1-11.

Ross WN, Nakamura T, Watanabe S, Larkum M, Lasser-Ross N (2005) Synaptically activated ca2+ release from internal stores in CNS neurons. Cell Mol Neurobiol 25:283-295.

Sarkisov DV, Wang SS (2008) Order-dependent coincidence detection in cerebellar Purkinje neurons at the inositol trisphosphate receptor. J Neurosci 28:133-142.

Satake S, Saitow F, Yamada J, Konishi S (2000) Synaptic activation of AMPA receptors inhibits GABA release from cerebellar interneurons. Nat Neurosci 3:551-558.

Satake S, Song SY, Cao Q, Satoh H, Rusakov DA, Yanagawa Y, Ling EA, Imoto K, Konishi S (2006) Characterization of AMPA receptors targeted by the climbing fiber transmitter mediating presynaptic inhibition of GABAergic transmission at cerebellar interneuron-Purkinje cell synapses. J Neurosci 26:2278-2289.

Schonewille M, Gao Z, Boele HJ, Veloz MF, Amerika WE, Simek AA, De Jeu MT, Steinberg JP, Takamiya K, Hoebeek FE, Linden DJ, Huganir RL, De Zeeuw CI (2011) Reevaluating the role of LTD in cerebellar motor learning. Neuron 70:43-50.

Schreurs BG, Alkon DL (1993) Rabbit cerebellar slice analysis of long-term depression and its role in classical conditioning. Brain Res 631:235-240.

Sears LL, Steinmetz JE (1991) Dorsal accessory inferior olive activity diminishes during acquisition of the rabbit classically conditioned eyelid response. Brain Res 545:114-122.

Siu FK, Lam IP, Chu JY, Chow BK (2006) Signaling mechanisms of secretin receptor. Regul Pept 137:95-104.

Southan AP, Robertson B (1998a) Modulation of inhibitory post-synaptic currents (IPSCs) in mouse cerebellar Purkinje and basket cells by snake and scorpion toxin K+ channel blockers. Br J Pharmacol 125:1375-1381.

Southan AP, Robertson B (1998b) Patch-clamp recordings from cerebellar basket cell bodies and their presynaptic terminals reveal an asymmetric distribution of voltage-gated potassium channels. J Neurosci 18:948-955.

Southan AP, Robertson B (2000) Electrophysiological characterization of voltage-gated K(+) currents in cerebellar basket and purkinje cells: Kv1 and Kv3 channel subfamilies are present in basket cell nerve terminals. J Neurosci 20:114-122.

Steinmetz AB, Freeman JH (2010) Central cannabinoid receptors modulate acquisition of eyeblink conditioning. Learn Mem 17:571-576.

Steinmetz AB, Freeman JH (2011) Retention and extinction of delay eyeblink conditioning are modulated by central cannabinoids. Learn Mem 18:634-638.

Steinmetz AB, Freeman JH (2014) Localization of the cerebellar cortical zone mediating acquisition of eyeblink conditioning in rats. Neurobiol Learn Mem 114:148-154.

Steinmetz JE, Lavond DG, Ivkovich D, Logan CG, Thompson RF (1992) Disruption of classical eyelid conditioning after cerebellar lesions: damage to a memory trace system or a simple performance deficit? J Neurosci 12:4403-4426.

Steinmetz JE, Lavond DG, Thompson RF (1989) Classical conditioning in rabbits using pontine nucleus stimulation as a conditioned stimulus and inferior olive stimulation as an unconditioned stimulus. Synapse 3:225-233.

Steinmetz JE, Logan CG, Rosen DJ, Thompson JK, Lavond DG, Thompson RF (1987) Initial localization of the acoustic conditioned stimulus projection system to the

cerebellum essential for classical eyelid conditioning. Proc Natl Acad Sci U S A 84:3531-3535.

Steinmetz JE, Rosen DJ, Chapman PF, Lavond DG, Thompson RF (1986) Classical conditioning of the rabbit eyelid response with a mossy-fiber stimulation CS: I. Pontine nuclei and middle cerebellar peduncle stimulation. Behav Neurosci 100:878-887.

Stocker M, Hellwig M, Kerschensteiner D (1999) Subunit assembly and domain analysis of electrically silent K+ channel alpha-subunits of the rat Kv9 subfamily. J Neurochem 72:1725-1734.

Stuhmer W, Stocker M, Sakmann B, Seeburg P, Baumann A, Grupe A, Pongs O (1988) Potassium channels expressed from rat brain cDNA have delayed rectifier properties. FEBS Lett 242:199-206.

Sugiyama T, Hirono M, Suzuki K, Nakamura Y, Aiba A, Nakamura K, Nakao K, Katsuki M, Yoshioka T (1999) Localization of phospholipase Cbeta isozymes in the mouse cerebellum. Biochem Biophys Res Commun 265:473-478.

Sultan F, Glickstein M (2007) The cerebellum: Comparative and animal studies. Cerebellum 6:168-176.

Svensson P, Jirenhed DA, Bengtsson F, Hesslow G (2010) Effect of conditioned stimulus parameters on timing of conditioned Purkinje cell responses. J Neurophysiol 103:1329-1336.

Takechi H, Eilers J, Konnerth A (1998) A new class of synaptic response involving calcium release in dendritic spines. Nature 396:757-760.

Tanaka J, Nakagawa S, Kushiya E, Yamasaki M, Fukaya M, Iwanaga T, Simon MI, Sakimura K, Kano M, Watanabe M (2000) Gq protein alpha subunits Galphaq and Galpha11 are localized at postsynaptic extra-junctional membrane of cerebellar Purkinje cells and hippocampal pyramidal cells. Eur J Neurosci 12:781-792.

Tay J, Goulet M, Rusche J, Boismenu R (2004) Age-related and regional differences in secretin and secretin receptor mRNA levels in the rat brain. Neurosci Lett 366:176-181.

Teune TM, van der Burg J, de Zeeuw CI, Voogd J, Ruigrok TJ (1998) Single Purkinje cell can innervate multiple classes of projection neurons in the cerebellar nuclei of the rat: a light microscopic and ultrastructural triple-tracer study in the rat. J Comp Neurol 392:164-178.

Thompson RF, Krupa DJ (1994) Organization of memory traces in the mammalian brain. Annual review of neuroscience 17:519-549.

Thompson RF, Steinmetz JE (2009) The role of the cerebellum in classical conditioning of discrete behavioral responses. Neuroscience 162:732-755.

Tsai W, Morielli AD, Cachero TG, Peralta EG (1999) Receptor protein tyrosine phosphatase alpha participates in the m1 muscarinic acetylcholine receptor-dependent regulation of Kv1.2 channel activity. EMBO J 18:109-118.

Veh RW, Lichtinghagen R, Sewing S, Wunder F, Grumbach IM, Pongs O (1995) Immunohistochemical localization of five members of the Kv1 channel subunits: contrasting subcellular locations and neuron-specific co-localizations in rat brain. Eur J Neurosci 7:2189-2205.

Voogd J, Glickstein M (1998) The anatomy of the cerebellum. Trends Neurosci 21:370-375.

Wang H, Kunkel DD, Martin TM, Schwartzkroin PA, Tempel BL (1993) Heteromultimeric K+ channels in terminal and juxtaparanodal regions of neurons. Nature 365:75-79.

Wang H, Kunkel DD, Schwartzkroin PA, Tempel BL (1994) Localization of Kv1.1 and Kv1.2, two K channel proteins, to synaptic terminals, somata, and dendrites in the mouse brain. J Neurosci 14:4588-4599.

Wang YT, Linden DJ (2000) Expression of cerebellar long-term depression requires postsynaptic clathrin-mediated endocytosis. Neuron 25:635-647.

Weber JT, De Zeeuw CI, Linden DJ, Hansel C (2003) Long-term depression of climbing fiber-evoked calcium transients in Purkinje cell dendrites. Proc Natl Acad Sci U S A 100:2878-2883.

Werkman TR, Gustafson TA, Rogowski RS, Blaustein MP, Rogawski MA (1993) Tityustoxin-K alpha, a structurally novel and highly potent K+ channel peptide toxin, interacts with the alpha-dendrotoxin binding site on the cloned Kv1.2 K+ channel. Mol Pharmacol 44:430-436.

Williams MR, Fuchs JR, Green JT, Morielli AD (2012) Cellular mechanisms and behavioral consequences of Kv1.2 regulation in the rat cerebellum. J Neurosci 32:9228-9237.

Williams MR, Markey JC, Doczi MA, Morielli AD (2007) An essential role for cortactin in the modulation of the potassium channel Kv1.2. Proc Natl Acad Sci U S A 104:17412-17417.

Womack MD, Chevez C, Khodakhah K (2004) Calcium-activated potassium channels are selectively coupled to P/Q-type calcium channels in cerebellar Purkinje neurons. J Neurosci 24:8818-8822.

Womack MD, Khodakhah K (2004) Dendritic control of spontaneous bursting in cerebellar Purkinje cells. J Neurosci 24:3511-3521.

Woodruff-Pak DS, Steinmetz JE, Thompson RF (1988) Classical conditioning of rabbits 2-1/2 to 4 years old using mossy fiber stimulation as a CS. Neurobiol Aging 9:187-193.

Xia J, Chung HJ, Wihler C, Huganir RL, Linden DJ (2000) Cerebellar long-term depression requires PKC-regulated interactions between GluR2/3 and PDZ domain-containing proteins. Neuron 28:499-510.

Yeo CH, Hardiman MJ (1992) Cerebellar cortex and eyeblink conditioning: a reexamination. Exp Brain Res 88:623-638.

Yuan Y, Lee LT, Ng SS, Chow BK (2011) Extragastrointestinal functions and transcriptional regulation of secretin and secretin receptors. Ann N Y Acad Sci 1220:23-33.

Yung WH, Chan YS, Chow BK, Wang JJ (2006) The role of secretin in the cerebellum. Cerebellum 5:43-48.

Yung WH, Leung PS, Ng SS, Zhang J, Chan SC, Chow BK (2001) Secretin facilitates GABA transmission in the cerebellum. J Neurosci 21:7063-7068.

Zhang L, Chow BK (2014) The central mechanisms of secretin in regulating multiple behaviors. Frontiers in endocrinology 5:77.

Zhang L, Chung SK, Chow BK (2014) The knockout of secretin in cerebellar Purkinje cells impairs mouse motor coordination and motor learning. Neuropsychopharmacology 39:1460-1468.

Appendix I: VALIDATION OF EXPERIMENTAL METHODS

Section 1: Biotinylation of Kv1.2 in Fixed Versus Non-Fixed Tissue

Introduction

The goal of these experiments was to measure surface Kv1.2 expression immediately following EBC. In order to do so and for best results, we decided that a perfusion with paraformaldehyde to halt all cellular activity would "freeze" the cerebellum in the state that is was in after the last training session. This, however, created a problem with the biotinylation technique used in Williams et al. (2012) because the Biotin used in those experiments utilizes the same binding site as paraformaldehyde. Thus, we need to determine if we could detect surface Kv1.2 using the same procedure but with a different Biotin that binds to different extracellular sites. We selected alkoxyamine-biotin-PEG4 (Biotin), which requires a new binding site to be created before it can bind to surface proteins. To create a new binding site, sections are incubated in sodium meta-periodate, which will create a new binding site that compliments the one necessary for Biotin. The experiment discussed below was designed to test these new methods with fixed versus non-fixed tissue to determine if we could use this new Biotin to quantify changes in Kv1.2 surface expression following EBC.

Materials and Methods

Tissue Harvest and Biotinylation

In this experiment, paraformaldehyde-fixed and non-fixed tissue was probed for surface expression of Kv1.2. For the live cerebellar sections, rats were anesthetized with isoflurane and perfused with ~100ml ice cold artificial cerebral spinal fluid (aCSF). The cerebellum was extracted, bisected down the vermis, and mounted with crazy glue to a

pre-chilled cutting plate. During the adhesion to the cutting plate, the cerebellum was dabbed with aCSF to keep the tissue from drying. Once adhered, the chamber was filled with ice-cold aCSF. Prior to cutting, meninges were carefully removed from the tissue so as not to interfere with sectioning. The whole mounting apparatus was moved to the vibratome and 12-400µm sections were obtained and allowed to recover in a recovery buffer for 1 hour before biotinylation treatments. After recovery, half of the sections were post-fixed with 2% paraformaldehyde for 15 minutes at room temperature. After the post fixation step, the well plate was returned to the ice bath and all sections were carefully rinsed three times for five minutes each with ice-cold Hanks Balanced Salt Solution (HBSS). After rinses, 1ml of 20mM sodium meta-periodate (SMP) replaced the HBSS, the sections were protected from light with foil, and placed on a rocker at 4°C for one hour for oxidation. All sections were rinsed again with HBSS three times for five minutes each. HBSS was replaced with 800µl of PBS and 200µl of 50mM alkoyamine-biotin-PEG4 (Biotin) and sections were protected from light and rocked for two hours at room temperature. After two hours, Biotin was quenched with 50mM TRIS in HBSS. Sections were rinsed four times for five minutes each. Slices were then transferred gently with a fine tipped paintbrush to 1.5ml centrifuge tubes containing a lysis buffer (1ml RIPA + 10µl HALT). Each tube and section was sonicated twice at 25% power for 2-4 seconds. The sonication tip was rinsed with water and dried in between each sonication. Sections and tubes were then spun down at high speed for 20 minutes at 4°C. After centrifuging the tubes, 200µl of the supernatant was transferred to different tubes marked as the "Total" input. The remaining ~800µl was transferred to tubes containing rinsed Neutravidin beads (Sigma) and marked as the "Surface" input. The Surface tubes were

rocked at 4°C for one hour. After, the tubes were centrifuged at 2,000RPM at 4°C for two minutes. The supernatant was transferred to different tubes marked as the "Post" fraction. The beads were then rinsed three times with HBSS. With each rinse, 1ml of HBSS was added to the tubes, the tubes were rocked at 4°C for approximately five minutes and centrifuged at 2,000RPM at 4°C for two minutes. After the last rinse, the supernatant was removed and the beads were dried using a 27G needle.

For the Total and Post fractions, 50µl of each were transferred into new centrifuge tubes. These were used at the loading fractions for the gel. To each tube, 50µl of 5X Sample buffer with 200mM DTT were added bringing the final concentration to 2.5X Sample Buffer with 100mM DTT. The same sample buffer was diluted to that final concentration and 50µl of the diluted buffer was added to the Beads samples. All tubes were flicked to mix the solutions. The tubes were then incubated at 55°C for 10 minutes. After the incubation, the tubes were centrifuged at high speed for 15 seconds, flicked to mix, and centrifuged at high speed again. The tubes were kept at room temperature until the gels were ready to be loaded.

Gel Preparation and Imaging

Gels were cast and prepped according to the methods detailed in the General Method section. The specific methods for this experiment are detailed below, starting once the gels had polymerized and samples were prepped.

Once the gels were ready, 15µl of each sample was loaded into individual lanes using a fine tipped 200µl pipette tip. Gels were run at 100V for 90 minutes and checked periodically to make sure they were running straight. Gels were transferred to nitrocellulose membrane at 100V for 60 minutes at 4°C. Once the transfer was complete,

samples were blocked for one hour in 3% bovine serum albumin (BSA) at room temperature. The samples were rinsed three times for five minutes with 1X TRIS buffered saline with Tween (TBST) followed by an overnight incubation with 1:5000 anti-Kv1.2 mouse mono-clonal antibody (K14/16; Neuromab) and 1:2000 rabbit polyclonal anti-glyceraldehyde-3-phosphate dehydrogenase (GAPDH) (ab9485; Abcam). Samples were rinsed again and incubated for one hour at room temperature with 1:5000 Goat anti-mouse 700 antibody (GAM700) and 1:5000 Goat anti-rabbit 800 (GAR800). Samples were rinsed again and imaged.

Western blot analysis was done according to the methods detailed in the General Method section.

Results and Discussion

In this experiment, live cerebellar sections were generated from a male rat, sectioned, and half were post-fixed with 2% paraformaldehyde. Following post-fix or not, slices were oxidized with 20mM SMP and surface Kv1.2 was probed with Biotin. The purpose of this experiment was to determine if we could in fact pull down surface Kv1.2 onto Neutravidin beads in a fixed-tissue preparation. We have previously done similar studies with live cerebellar tissue (Williams et al., 2012). Figure 2 shows the qualitative results from the experiment. In the three lanes marked “Biotin + Fixed” we observed strong Kv1.2 signal, indicating that the new biotinylation method worked with fixed tissue. There was also strong signal in the non-fixed tissue that was probed with biotin in two of the three lanes used. In the third lane, highlighted in purple, we saw fainter signal. In the majority of the lanes that were not treated with biotin, we did not observe any surface Kv1.2 signal. In one of the lanes, marked in green, we saw strong signal. It is

possible that sample from one of the adjacent lanes spilled over into this lane. Other reasons for this unusual result could include contamination of this sample in one of the many previous steps.

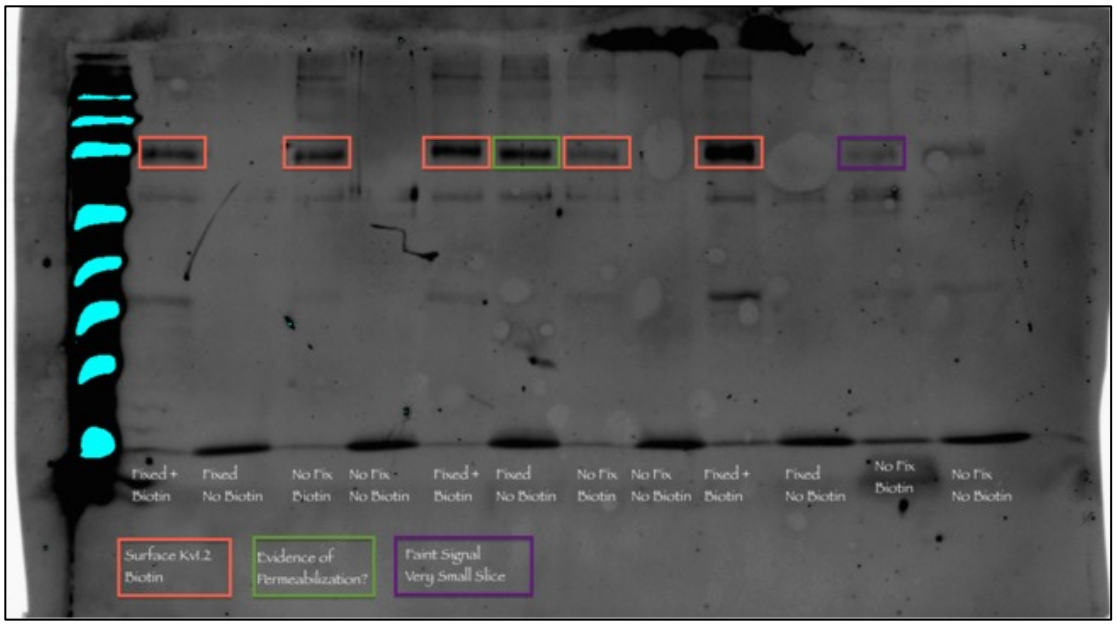

Figure 10. Western blot showing surface Kv1.2 expression following surface probe with alkoxyamine-biotin-PEG4. Conditions marked in white text at bottom of the blot. Orange boxes denotes Surface Kv1.2 Expression in the +Biotin conditions. Green boxes denote evidence of permeabilization. Purple boxes denote slight signal when using a smaller than normal section for analysis. Strong Kv1.2 signal observed in 5 of 6 lanes probed with biotin.

The results from this experiment indicate that it is feasible to extract surface Kv1.2 from live and fixed sections using the biotin marker described above. We observed strong signal in all three samples that were fixed and probed with biotin. A similar result was observed for the samples that were not fixed, but probed with biotin. Overall, it appears feasible to use this biotinylation method with fixed cerebellar sections, which was necessary for later experiments.

Section 2: Testing the Concentration of Sodium Meta-Periodate

Introduction

After the initial experiment, we started observing problems with being able to pull down surface Kv1.2 in our samples. The signal on the western blots was very faint, an effect that can be seen in several of the lanes in **Figure 1.** While the signal here may appear strong, the ratios of Kv1.2 to the loading control are lower than we would expect. Upon further examination of the protocol developed for these experiments, we noticed the concentration of sodium meta-periodate (SMP) was higher than it should have been. Thus, this experiment was used to test varying concentrations of SMP in an attempt to find the appropriate concentration. Previously, samples were oxidized using 20mM SMP. In the current experiment, we tested four different concentrations: 0mM SMP, 1mM SMP, 10mM SMP, and 20mM SMP to not only test if the higher concentration was interfering with our samples, but find an ideal concentration to use for the rest of the experiments.

The second goal of this experiment was to determine whether or not we were observing permeabilization in the sections as a result of a step in this method. Several of the sections harvested for this experiment were assigned to a permeabilization condition. Besides this step, these sections were treated the same as the non-permeabilized sections. There are several potential problems if the sections in these experiments were being permeabilized: (1) If we do observe changes in Kv1.2 expression with permeabilization, then we would not be able to say that changes are just to Kv1.2 surface expression; (2) permeabilization may increase the noise and thus occlude us from observing changes in

Kv1.2 surface expression following EBC. Thus, the second goal of this experiment was to determine if permeabilization is problem that we may encounter with these methods.

Materials and Methods

Subjects, Perfusion, and Sectioning

One male Wistar rat was anesthetized with isoflurane. The transcardial perfusion began when the rat was no longer responsive to painful stimuli and its heart rate dropped to low levels. Approximately 100ml of PBS was perfused through the rat followed by ~40ml of 4% paraformaldehyde. The cerebellar hemispheres were transported separately in PBS containing 4% paraformaldehyde. Eight 400μm parasagittal sections were kept, and four were assigned to the permeabilized condition and the other four were treated without being permeabilized.

Biotinylation, Gel Preparation, and Imaging

Prior to oxidation, the permeabilized sections were treated with 10% triton mixed in PBS at room temperature for ~35 minutes. The non-permeabilized sections were kept in PBS at room temperature for the same time. After permeabilizing the sections, the well plate was put back on ice and all sections were rinsed with PBS two times for five minutes each. During the oxidation step, the 0mM SMP condition remained in PBS. For the other conditions, the PBS was replaced with 1ml of the assigned concentration of SMP, and all sections were protected from light, rocked, and incubated for 30 minutes at 4°C. Prior to biotinylation, all sections were rinsed again with PBS for five minutes on ice. All sections were incubated with 50mM Biotin for two hours at room temperature.

After the Biotin step, all methods were the same as in the previous experiment and are detailed in the General Method section.

Results and Discussion

In this experiment, we tested varying concentrations of SMP, including 0mM SMP, to see if the high concentration we were using in previous experiments was interfering with our ability to detect Kv1.2 surface expression in the western blot experiments. Half of the samples were permeabilized using a rinse with 10% Triton. In the non-permeabilized samples, the results showed that with increasing concentrations of SMP there was a reduction in the surface expression of Kv1.2 when looking at the ratio of Kv1.2 to Glyceraldehyde 3-phosphate dehydrogenase (GAPDH; Table 1). GAPDH was used as the loading control; it is an enzyme associated with later steps in glucose metabolism and is only expressed internally in the neurons. Using GAPDH as a loading control allowed us to determine if we were observing permeabilization in our samples. Interestingly, the highest expression of surface Kv1.2 was observed in the 0mM SMP condition. This is contrary to what would be expected because the SMP should be necessary to create a new binding site for this particular Biotin to bind to Kv1.2, since the normal binding site is already occupied by paraformaldehyde. Despite this, our hypothesis that higher concentrations of SMP were interfering with the expression of surface Kv1.2 was confirmed.

A similar trend was observed for the permeabilized samples. The findings in these samples are not limited to just surface Kv1.2 because those sections were permeabilized by a rinse with Triton. However, the fact that there was still a similar trend in these

samples confirms the hypothesis that higher concentrations of SMP were interfering with our ability to observe changes in surface Kv1.2 expression (Table 1).

One problem with these results was that the ratios for the Surface-to-Total comparisons for the non-permeabilized samples were contrary to what we would have expected. Here, it appeared that the 0mM SMP, 1mM SMP, and 20mM SMP were about equal while the 10mM SMP showed the greatest expression. One explanation for this could be contamination of the samples when being loaded into the gel, thus changing the amount of Kv1.2 present. Another explanation could be that, since this ratio relies on the Total expression of Kv1.2 in the samples, if those numbers were off or those samples were contaminated, then the ratios with the surface expression would be altered as well.

Permeabilized Samples		0 SMP	1mM SMP	10mM SMP	20mM SMP
Kv1.2:GAPDH	Beads	6.919	2.724	0.516	0.344
	Total	9.852	6.200	0.617	0.637
	Post	19.900	5.238	0.919	0.747
Surface:Total	Beads	0.760	0.130	0.085	0.074
Post:Total	Post	0.666	1.465	0.606	0.772
Non-Permeabilized Samples		0 SMP	1mM SMP	10mM SMP	20mM SMP
Kv1.2:GAPDH	Beads	5.424	2.032	1.751	1.800
	Total	8.760	8.025	1.056	0.749
	Post	6.541	8.269	0.963	0.738
Surface:Total	Beads	0.270	0.239	0.521	0.235
Post:Total	Post	1.152	0.864	1.152	0.720

Table 1. Kv1.2 Expression ratios (to GAPDH) for sodium meta-periodate (SMP) experiment. Beads represent the surface expression of Kv1.2 for the non-permeabilized samples. In the permeabilized conditions, Beads represent all Kv1.2 that was tagged with Biotin and pulled onto the Neutravidin beads, not limited to just surface. Total represents all proteins and Post represents the samples taken after incubation with the Beads. Results show greater surface Kv1.2 expression with lower SMP concentrations. Overall, increasing SMP concentration limits Kv1.2 expression on blots, especially in permeabilized samples.

Altogether, based on these findings, we selected the 1mM concentration as the concentration for subsequent experiments. SMP is an oxidative compound that is used in this preparation to create a new binding site on surface Kv1.2 for the Biotin to bind to. Despite the greater surface expression of Kv1.2 in the 0mM SMP conditions, other experiments have shown that SMP is necessary for measuring surface expression of Kv1.2 (data not shown).

Section 3: Testing the Laser Scanning Microscope (LSM) 7 Multiphoton Microscope System to Detect Changes in Kv1.2 Surface Expression

Introduction

The third preliminary experiment for this project was to determine if the Zeiss Laser Scanning Microscope 7 (LSM 7; Zeiss, Oberkochen, Germany) system was sensitive enough to detect changes in Kv1.2 surface expression in cerebellar sections following EBC. Multiphoton microscopy (MP) offers some strong advantages over other microscopy techniques, such as reduced background fluorescence through illumination limited to the focal plane, the ability to image thicker sectioned tissue, and the ability to optically dissect the tissue and measure Kv1.2 surface expression in reference to the Z-plane.

To induce changes in surface Kv1.2 expression, we used treatment with forskolin. Forskolin activates adenylyl cyclase (AC) and was previously shown to reduce surface Kv1.2 expression in cerebellar sections (Williams et al., 2012). In order to measure changes in Kv1.2 surface expression, we incubated sections with a fluorescent conjugate of TsTX, TsTX-ATTO-594. This compound, prepared by Alomone Lab (Jerusalem,

Israel) features a biologically active version of TsTX with the ATTO-594 dye attached. The TsTX-ATTO-594 still displays the same high affinity for the binding site on Kv1.2 channels and is therefore an excellent marker for this channel's expression. Following the incubation with TsTX-ATTO-594, sections were rinsed, post-fixed with paraformaldehyde, and imaged. The efficacy of TsTX-ATTO-594 for binding to Kv1.2 in cerebellar sections was shown in Williams et al. (2012) to measure Kv1.2 surface expression on BC axon terminals in the cerebellar cortex. The data shown below indicate that the LSM7 multiphoton microscope system is sensitive enough to detect changes in surface Kv1.2 expression, we are able measure Kv1.2 surface expression in thicker tissue, and that the TsTX-ATTO-594 is an effective marker of Kv1.2 on BC axon terminals.

Materials and Methods

Subject, Perfusion, and Sectioning

The subject for this experiment was one male Sprague-Dawley rat ~28 days old. For tissue harvest, the rat was anesthetized using isoflurane. The perfusion began once the rat was no longer responsive to painful stimuli. Ice-cold aCSF was perfused through the rat at a constant pressure of 100mmHg. The brain was then rapidly extracted and placed into a dish containing oxygenated aCSF. Here the cerebellum was bisected from the rest of the brain and the cerebellar hemispheres were bisected through the vermis. The two hemispheres were then mounted to a pre-chilled cutting stage with crazy glue. The hemispheres were dabbed with aCSF while the glue dried. The chamber was then filled with oxygenated aCSF and the entire cutting apparatus was transported to the vibratome. The tissue was sectioned parasagittally at 400μm. Of the sections obtained, four were used for this experiment.

Drug Treatment and Tissue Preparation

The sections were allowed to recover for one hour in a recovery buffer. They were then transferred to 35mm dishes. Vehicle (PBS) and forksolin (100μM; Calbiochem) treated sections were incubated for 15 minutes at room temperature. Forskolin was previously shown to significantly reduce surface Kv1.2 expression in cerebellar sections, as measured by biotinylation and western blot (Williams et al., 2012). The sections were then transferred to individual wells in a 12 well plate, placed on ice, and rinsed with ice-cold HBSS. Sections were fixed with 2% paraformaldehyde for 30 minutes at room temperature. The sections were placed back on ice and rinsed prior to staining with TsTX-ATTO-594. The sections were incubated with TsTX-ATTO-594 (4nM; Alomone, Jerusalem, Israel) over night at 4°C. Sections were left in TsTX-ATTO-594 for ~18 hours, rinsed, post-fixed with 2% paraformaldehyde, and imaged.

Imaging

All imaging was done on the LSM7 system. Microscope settings remained the same throughout imaging all sections across experiments in order to make comparisons between sections, conditions, and experiments. The microscope settings were as follows: 3% laser power set to 820nm, NDDR4 Gain: 1000 (Range 300-1100), Bit Depth: 16 bit, Resolution: 256x256, and Digital zoom: 1.5X. A more detailed explanation of imaging methods can be found in the General Methods section.

Image Processing and Analysis

Image processing was done in ImageJ (NIH). Images were converted to 32-bit images before analysis started. In order to isolate individual PCX from the images in three dimensions, images were converted so that ImageJ could isolate specific regions of

interest (ROIs). To do so, a Z-projection using the maximum pixel intensity was taken, collapsing the intensity information across all of the z-sections. For this image, the bit depth was set back down to 8-bit and the threshold was adjusted so that individual PCXs could be identified without altering their structure. A mask was created by covering up all parts of the image that were not a part of the PCX layer. From the original, 32-bit image, another Z-projection was created using the sum of the pixel intensities. This image was used to extract the actual PCX data. Using an object analysis tool, measurements were redirected to the masked image of the maximum projection and, referencing this mask, data were taken from objects that ranged from 50-500 pixels. Any objects fitting this dimensional range in the mask were measured in the sum projection. Data from each object were placed in a separate text file and copied to Microsoft Excel®. The data taken from each image included the object number, the area in pixels, the mean intensity value, the standard deviation of the intensity values, the minimum and the maximum pixel value, the perimeter of the object, the integrated density and the raw integrated density. The primary dependent measure for the imaging data was the mean intensity value for each PCX.

Results and Discussion

This experiment was designed to determine if we could observe changes in surface Kv1.2 expression using multiphoton microscopy. Using forskolin, which was previously shown to reduce surface Kv1.2 expression (Williams et al., 2012), we tested the LSM7 to determine if it was sensitive enough to detect and measure changes in Kv1.2 expression. Sections were treated with either forskolin or vehicle for 15 minutes, post fixed with paraformaldehyde, stained with TsTX-ATTO-594 overnight, and post fixed

again prior to imaging. Of the four sections stained with TsTX-ATTO-594, one vehicle and one forskolin treated section provided usable data. Images were taken in the x-, TsTX-, and z-planes.

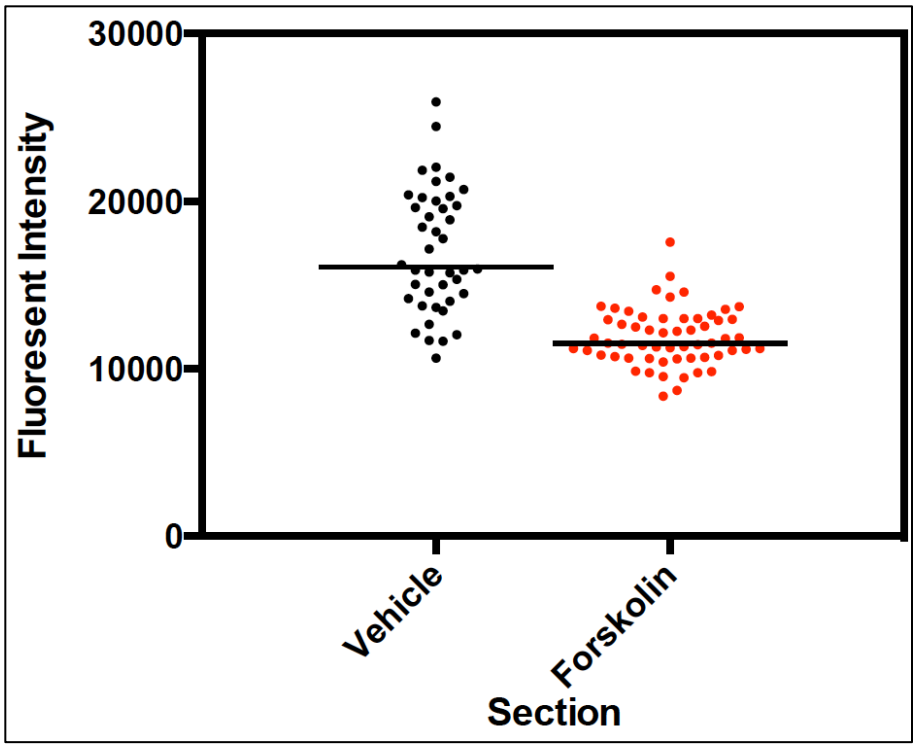

Figure 11. Live cerebellar sections were treated with forskolin (100µm) or vehicle prior to fixation and TsTX-ATTO-594 incubation. Data points represent pinceaus extracted from Z-stack images for vehicle (black) and forskolin (red) treated sections. Reduced surface Kv1.2 expression in section treated with Forskolin, detected by multiphoton microscopy.

We predicted that forskolin, an activator of adenylyl cyclase in cerebellar cortex, would reduce surface Kv1.2, similar to findings reported in Williams et al. (2012) using biotinylation and western blot. We also wanted to determine if the multiphoton microscopy technique would be sensitive enough to detect changes in Kv1.2 surface expression in the PCX layer of the cerebellar cortex. Figure 10 shows reduced fluorescent intensity in the forskolin treated sections compared to the vehicle treated section. The data points in Figure 10 display the fluorescent intensity of individual PCX, but statistical

analyses were not done on these data because of the low number of subjects (n = 1) per group. Based on the exploratory nature of this experiment, it appeared that forskolin did reduce surface Kv1.2 expression and the multiphoton microscope is sensitive enough to detect these changes.

One problem with this experiment was the sample size. Without more sections and more data we could not determine the threshold for detecting changes in surface Kv1.2 expression. Given that this experiment was exploratory in nature and the main goal of the experiment was to determine if we could observe changes in TsTX-ATTO-594 fluorescent intensity in cerebellar sections in response to forskolin, we were successful. Overall, the data confirmed our expectation that this microscopy system is viable for detecting changes in surface Kv1.2 expression. Furthermore, using the analysis procedure discussed above, we established a method for extracting data from 3-dimensional images without too much difficulty.

APPENDIX II: OUTLIER ANALYSIS FOR EXPERIMENT 1 (CHAPTER 2)

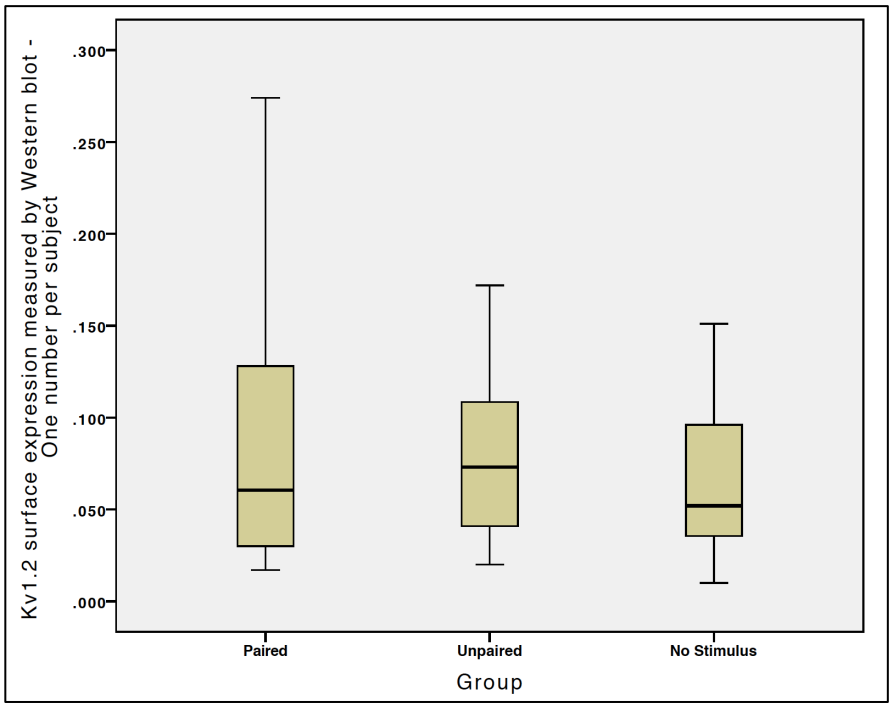

Figure 12. Boxplot outlier analysis for western blot (WB) data for Experiment 1. No outliers identified within The Paired (green), Unpaired (blue), and No Stimulus (Red) groups.

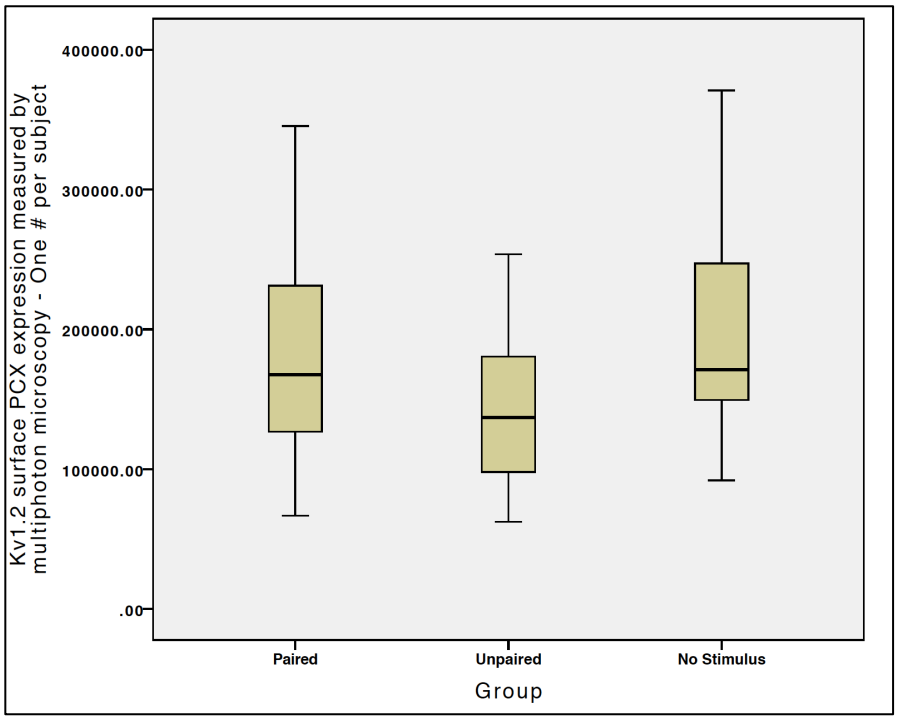

Figure 13. Boxplot outlier analysis for multiphoton microscopy (MP) data for Experiment 1. No outliers identified within the Paired (green), Unpaired (blue), or No Stimulus (red) groups.

Table 2. Outlier Labeling Rule (OLR) Analysis for Western Blot data in Experiment 1. The Lower and Upper limits for outlier threshold are based on the first (Q1) and third (Q3) quartile percentages based on the distribution of the data in each group. Subjects whose score fall outside of the lower or upper range were considered outliers. No outlier identified in any of the groups in the WB measure in experiment 1.

Experiment 1			Western Blot		
Paired					
Q1	Median	Q3	g	Lower	Upper
0.03		0.131	2.2	-0.1922	0.3532
	Q3-Q1=	0.101			
	g'=	0.2222			
Unpaired					
Q1	Median	Q3	g	Lower	Upper
0.04		0.12	2.2	-0.136	0.296
	Q3-Q1=	0.08			
	g'=	0.176			
No Stimulus					
Q1	Median	Q3	g	Lower	Upper
0.035		0.099	2.2	-0.1058	0.2398
	Q3-Q1=	0.064			
	g'=	0.1408			

Table 3. Outlier Labeling Rule (OLR) Analysis for Multiphoton Microscopy data in Experiment 1. The Lower and Upper limits for outlier threshold are based on the first (Q1) and third (Q3) quartile percentages based on the distribution of the data in each group. Subjects whose score fall outside of the lower or upper range were considered outliers.

Experiment 1			Multiphoton Microscopy		
Paired					
Q1	Median	Q3	g	Lower	Upper
124382.15		235037.83	2.2	-119060.346	478480.326
	Q3-Q1=	110655.68			
	g'=	243442.496			
Unpaired					
Q1	Median	Q3	g	Lower	Upper
92618.6		184723.84	2.2	-110012.928	387355.368
	Q3-Q1=	92105.24			
	g'=	202631.528			
No Stimulus					
Q1	Median	Q3	g	Lower	Upper
148929.73		249108.39	2.2	-71463.322	469501.442
	Q3-Q1=	100178.66			
	g'=	220393.052			

APPENDIX III: CR ONSET LATENCY AND ONSET LATENCY STANDARD DEVIATION FROM EXPERIMENT 1 (CHAPTER 2)

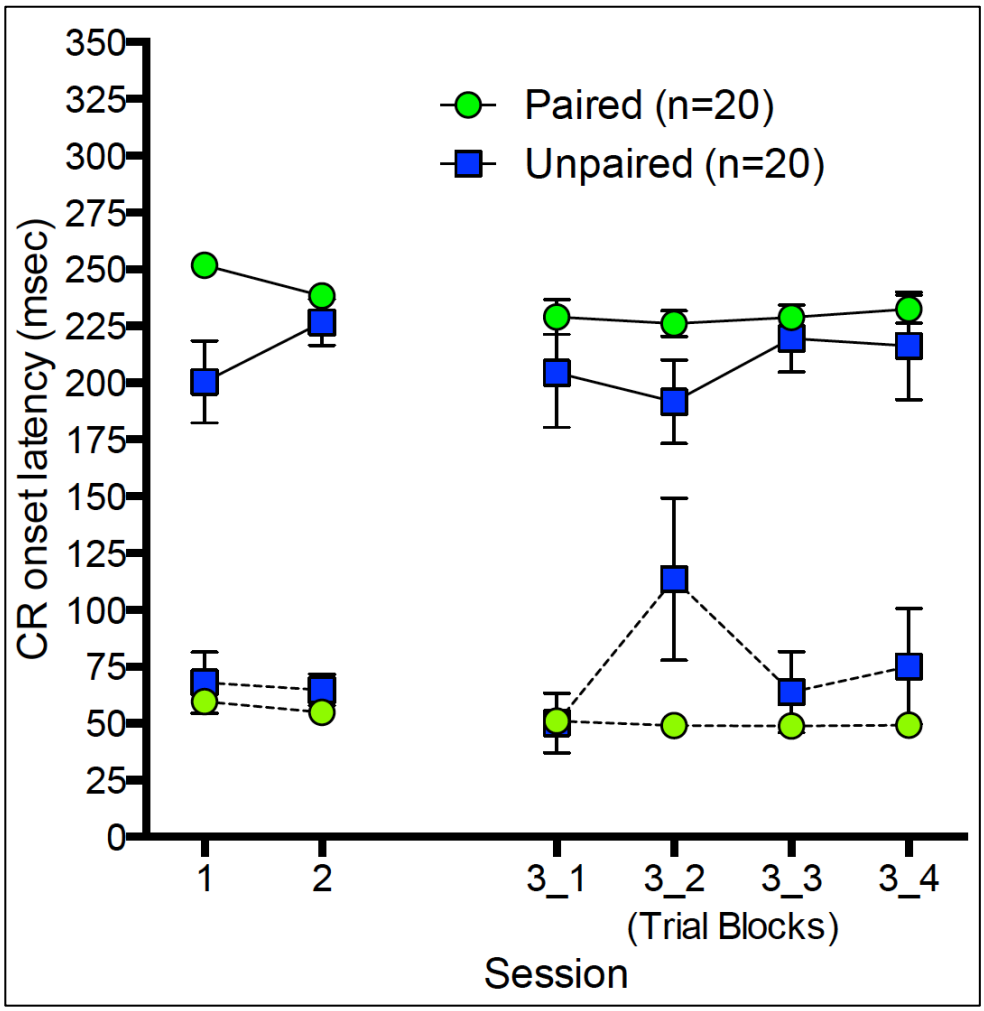

Figure 14. Conditioned response (CR) onset latency for Paired (green circles) and Unpaired (blue squares) subjects (solid lines). The dotted lines represent the standard deviation of the CR onset latencies for each of the groups within each of the sessions. Responses scored as CRs for the Paired group remained consistent across the training sessions, while the timing of the "responses" score for the Unpaired group fluctuate within and across sessions. The dotted lines show the variability within each session. The variability within each session for the Paired group remains consistently low and the Unpaired group shows some variability.

APPENDIX IV: OUTLIER ANALYSIS FOR EXPERIMENT 2 (CHAPTER 3)

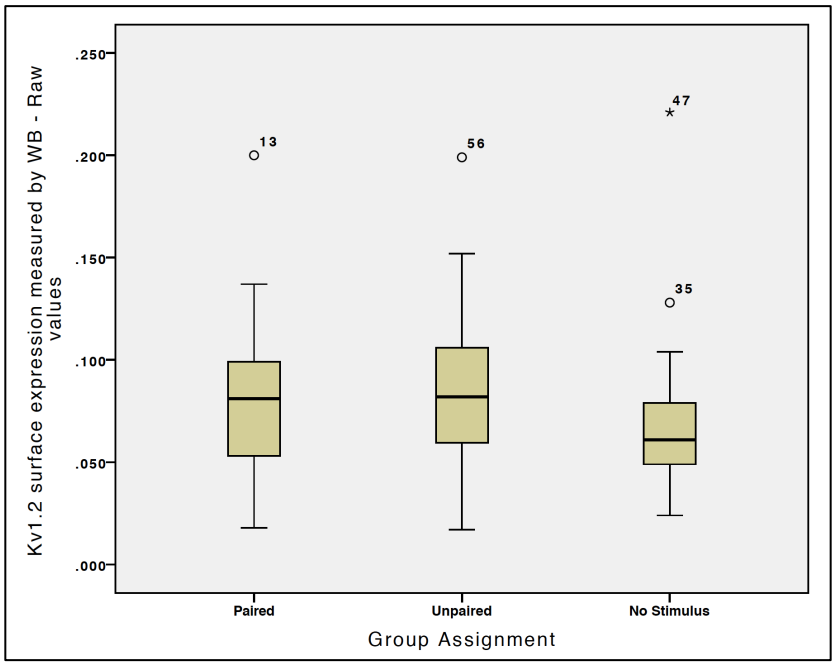

Figure 15. Boxplot outlier analysis for Experiment 2 Western Blot (WB) Data. One outlier (*47) identified in this analysis as an outlier in the No Stimulus group. Three other subjects (1/group; circles) fell outside of error bars but not considered statistical outliers.

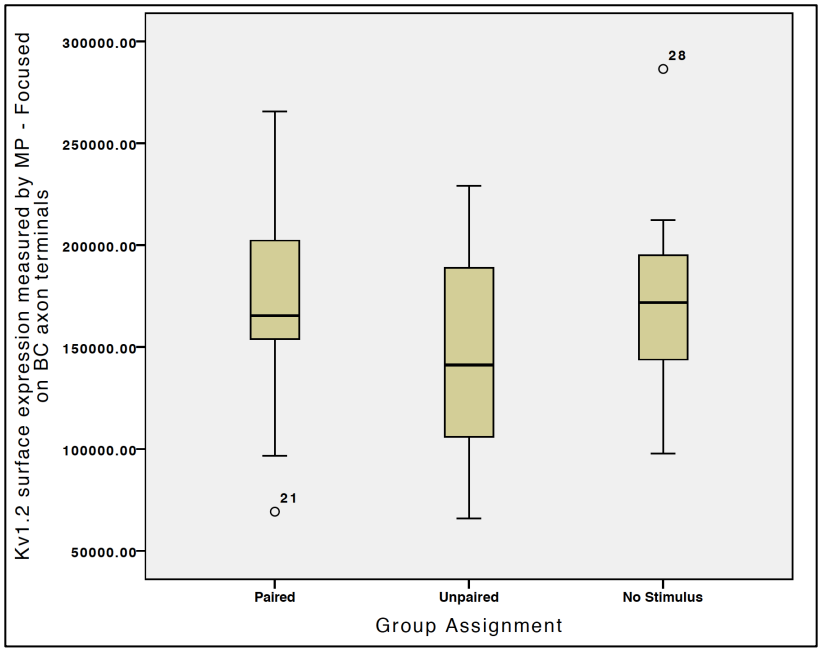

Figure 16. Boxplot Analysis for Multiphoton Microscopy (MP) data for Experiment 2. No outliers were identified in this analysis. Two subjects show Kv1.2 surface expression on BC axon terminals that falls outside of error bars for Paired (n=1) and No Stimulus (n=1) groups. These subjects were not considered statistical outliers.

Table 4. Outlier Labeling Rule (OLR) Analysis for Western Blot data for Experiment 2. The Lower and Upper limits for outlier threshold are based on the first (Q1) and third (Q3) quartile percentages based on the distribution of the data in each group. Subjects whose score fall outside of the lower or upper range were considered outliers. Subject 15-188 was identified as an outlier in this analysis in the No stimulus group. This subject was the same as was identified in the boxplot analysis (Fig. 14) and was subsequently removed from analyses.

Experiment 2 – 50 Trials			Western Blot		
Paired					
Q1	Median	Q3	g	Lower	Upper
0.051		0.101	2.2	-0.059	0.211
	Q3-Q1=	0.05			
	g'=	0.11			
Unpaired					
Q1	Median	Q3	g	Lower	Upper
0.059		0.11	2.2	-0.0532	0.22
	Q3-Q1=	0.051			
	g'=	0.1122			
No Stimulus					
Q1	Median	Q3	g	Lower	Upper
0.048		0.078	2.2	-0.018	0.14
	Q3-Q1=	0.03			
	g'=	0.066	15-188 = 0.221		

Table 5. Outlier Labeling Rule (OLR) Analysis for Multiphoton Microscopy data in Experiment 2. The Lower and Upper limits for outlier threshold are based on the first (Q1) and third (Q3) quartile percentages based on the distribution of the data in each group. Subjects whose score fall outside of the lower or upper range were considered outliers. No subjects were identified as outliers.

Experiment 2 – 50 Trials			Multiphoton Microscopy		
Paired					
Q1	Median	Q3	g	Lower	Upper
142375.86		204021.55	2.2	6755.342	339642.07
	Q3-Q1=	61645.69			
	g'=	135620.518			
Unpaired					
Q1	Median	Q3	g	Lower	Upper
105036		188955.3	2.2	-79586.46	373577.76
	Q3-Q1=	83919.3			
	g'=	184622.46			
No Stimulus					
Q1	Median	Q3	g	Lower	Upper
102741.65		198134.38	2.2	-107122.356	407998.386
	Q3-Q1=	95392.73			
	g'=	209864.006			

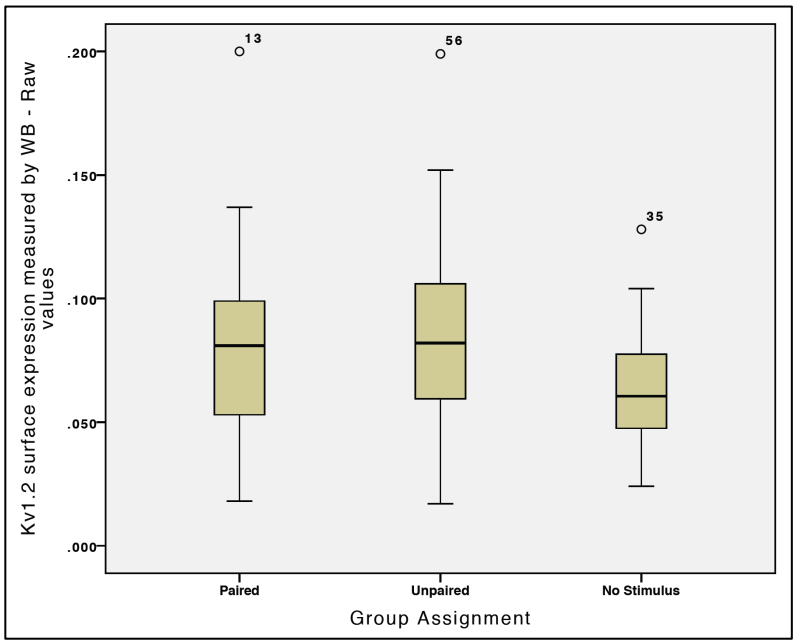

Figure 17. Boxplot outlier analysis for the Western Blot data from Experiment 2. Follow up analysis to determine if there were any other outliers after the subject in the No Stimulus group was removed. No other subjects identified as a statistical outlier.

APPENDIX V: CHAPTER 3 (EXPERIMENT 2) PAIRED GROUP PERFORMANCE SPLIT OUTLIER ANALYSIS

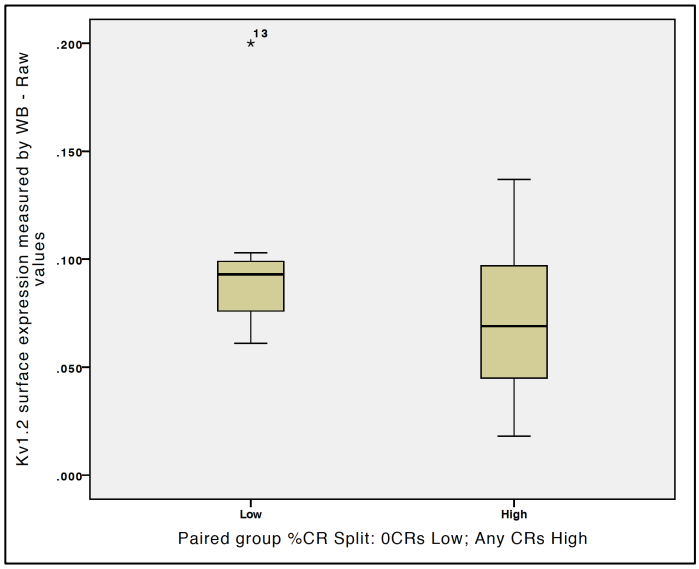

Figure 18. Boxplot outlier analysis for Paired split data from Experiment 2. Subjects that did not show any CRs during the training blocks were split into the Paired Low group and subjects that showed any CRs during the two training blocks split into the Paired High group. One outlier (*13) identified in the Paired Low group

Table 6. Outlier Labeling Rule (OLR) for Western Blot data from Experiment 2 for the Paired High and Paired Low groups. The Lower and Upper limits for outlier threshold are based on the first (Q1) and third (Q3) quartile percentages based on the distribution of the data in each group. Subjects whose score fall outside of the lower or upper range were considered outliers. Subject 15-103 in the Paired Low group identified as an outlier, the same subject identified in the boxplot analysis (Fig. 17).

Experiment 2 – 50 Trials			Western Blot		
Paired Low Group (0% CRs)					
Q1	Median	Q3	g	Lower	Upper
0.071		0.103	2.2	0.0006	0.1734
	Q3-Q1=	0.032			
	g'=	0.0704	Outlier: 15103 = 0.200		
Experiment 2 – 50 Trials			Western Blot		
Paired High Group (any CRs)					
Q1	Median	Q3	g	Lower	Upper
0.04		0.099	2.2	-0.0898	0.2288
	Q3-Q1=	0.059			
	g'=	0.1298			

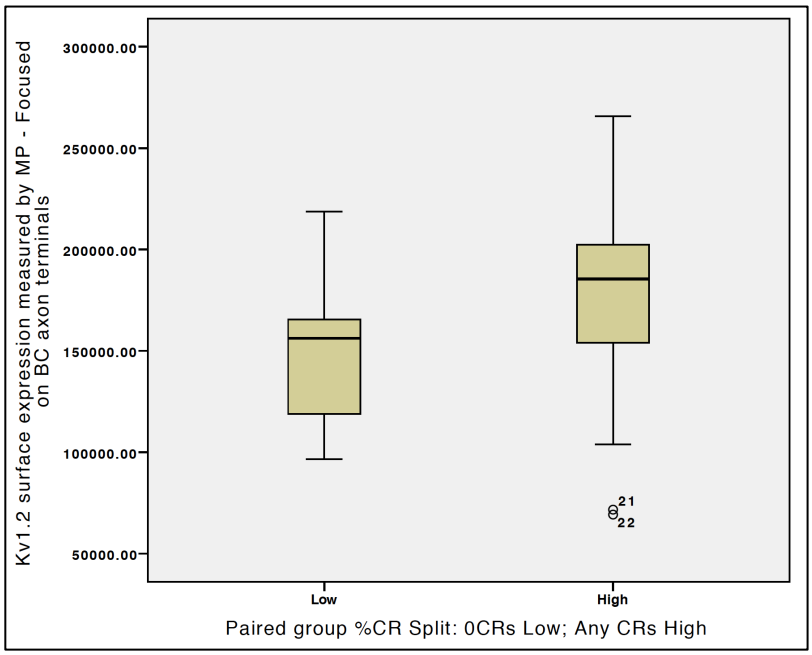

Figure 19. Boxplot outlier analysis for Paired Split groups for Multiphoton Microscopy data from Experiment 2. No subjects were identified as statistical outliers. Two subject in the Paired High group fall outside of the error bars but were not considered outliers.

Table 7. Outlier Labeling Rule (OLR) for Multiphoton Microscopy data between the Paired split. The Lower and Upper limits for outlier threshold are based on the first (Q1) and third (Q3) quartile percentages based on the distribution of the data in each group. Subjects whose score fall outside of the lower or upper range were considered outliers. No Subjects were identified at an outlier.

Experiment 2 – 50 Trials			Multiphoton Microscopy		
Paired Low Group (0% CRs)					
Q1	Median	Q3	g	Lower	Upper
113274.103		178750.178	2.2	-30773.262	322797.543
	Q3-Q1=	65476.075			
	g'=	144047.365			
Experiment 2 – 50 Trials			Multiphoton Microscopy		
Paired High Group (any CRs)					
Q1	Median	Q3	g	Lower	Upper
148141.99		203150.033	2.2	27124.2954	324167.7276
	Q3-Q1=	55008.043			
	g'=	121017.6946			

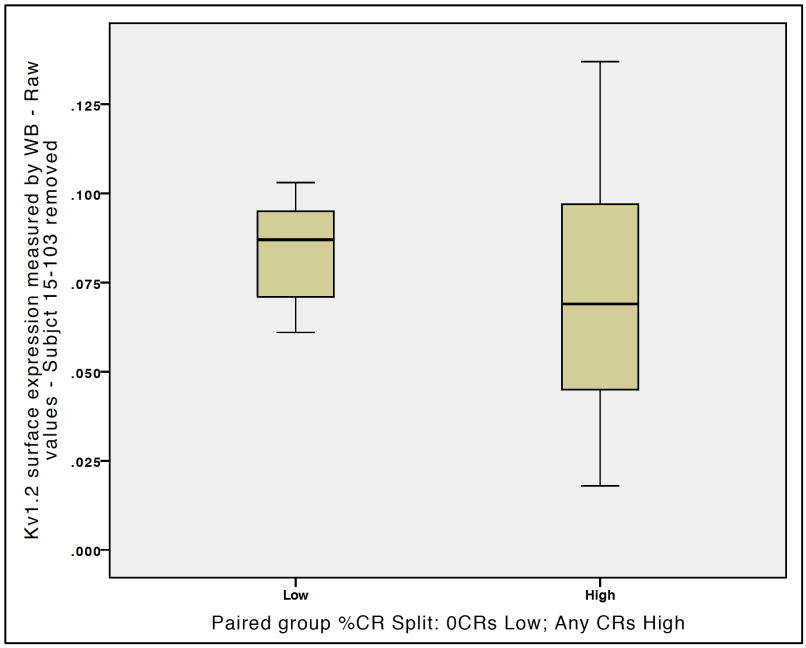

Figure 20. Boxplot outlier re-analysis for Paired High and Paired Low groups on Western Blot data following removal of one outlier. No other subjects identified as outliers.

APPENDIX VI: CHAPTER 3: BIOTINYLATION AND WESTERN BLOT DATA FOLLOWING OUTLIER ANALYSIS ON PAIRED HIGH AND PAIRED LOW GROUPS

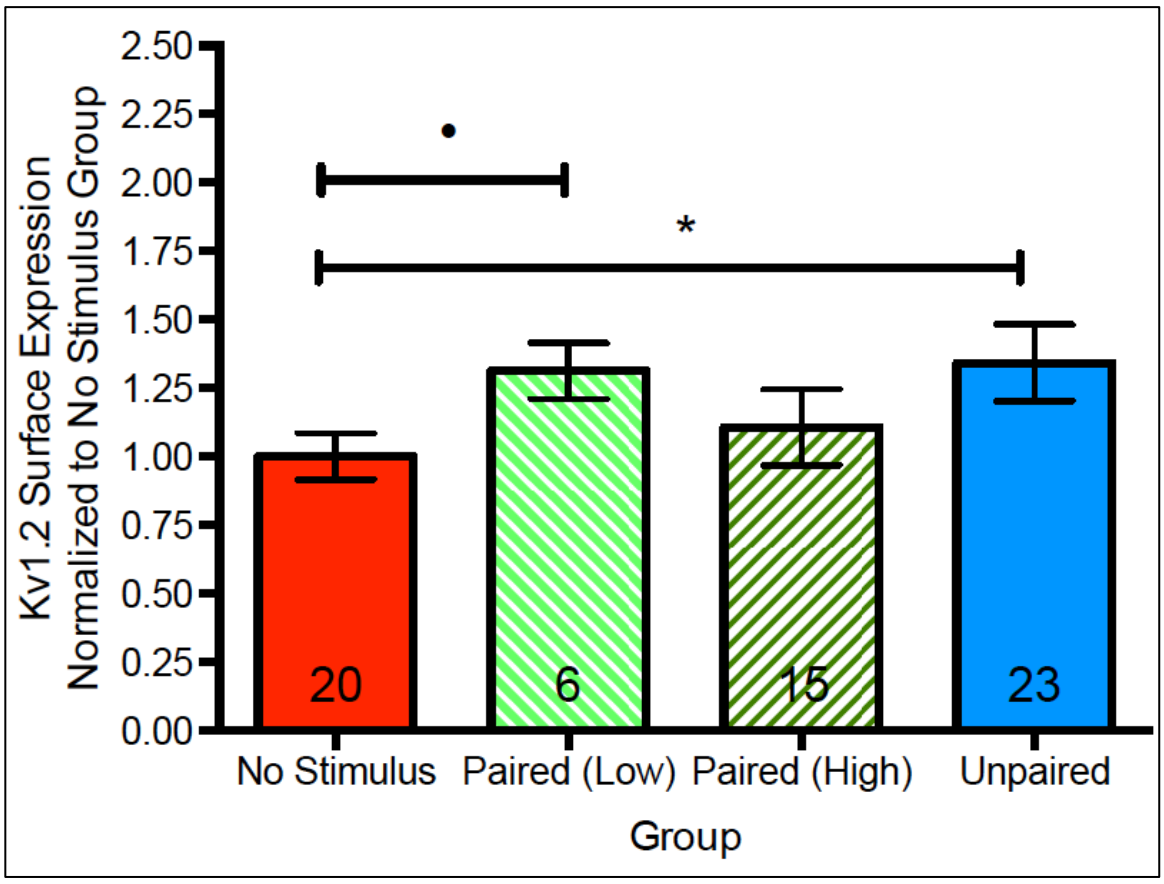

Figure 21. Biotinylation and Western Blot (WB) data showing Kv1.2 surface expression in both BC axon terminals and PC dendrites. Data displayed as mean ± SEM for the Paired Low (No CRs during training blocks; light green stripes), Paired High (Any CRs during training blocks; dark green stripes), Unpaired (blue), and No Stimulus groups (red). Data normalized to the No Stimulus group. These data exclude one subject from Paired Low group that was identified as an outlier. Planned comparisons between each of the groups revealed a significant difference between the Unpaired and No Stimulus groups (p = 0.04), but no other significant effects. Post hoc comparisons between the four groups in Fig. 21 revealed a marginally significant difference between Paired Low and No Stimulus groups (p = 0.07). No Differences observed between Paired High and Paired Low, and Paired High and No Stimulus. (* denotes p <0.05; • denotes p = 0.07).

APPENDIX VII: MAPPING THE SPREAD OF TITYUSTOXIN INFUSIONS IN THE CEREBELLAR CORTEX

An important experiment when drawing conclusions from infusion studies is to determine how far each infusion is spreading within the targeted tissue. Here, we tested to how far infusions of tityustoxin-Kα (TsTX) were spreading within the cerebellar cortex. To do this, we infused 0.50 µl of a fluorescently conjugated version of TsTX (TsTX-ATTO-594). Data from the laboratory that developed the peptide suggest that the fluorescently labeled TsTX is still an active peptide able to block Kv1.2 (Alomone; data not shown), but just has an ATTO-594 molecule attached.

Two male Wistar rats (Aged: 59-63 days) were implanted with a stainless steel guide cannula targeting the lobulus simplex in the cerebellar cortex (AP: 11.0mm, ML: 3.0mm, DV: -3.2mm). The rats were allowed to recover for five days post surgery. For the infusion, a 30-gauge infusion cannula was paced through the guide cannula and extended 1mm past the end of the guide (Final infusion depth of DV: -3.3mm). 0.50µl of TsTX-ATTO-594 was infused (0.25µl/min) into the cerebellar cortex. Once the infusion finished, the infusate was allowed to spread away from the infusion cannula for two minutes prior to the infusion cannula being removed. Rats were returned to the colony room for 20 minutes prior to the perfusion. Subjects were deeply anesthetized with isoflurane and a cardiac perfusion was performed. First 100ml of PBS was circulated through followed by 100 ml of 4% paraformaldehyde.

The whole cerebellum from each of the subjects was harvested. One of the cerebella was sectioned taking 400µm parasagittal sections of the left hemisphere and the other was sectioned taking 400µm coronal sections. For both cerebella, sections from the

entire cerebellum we kept to determine the outer limits of the spread of the infusion. Sections were kept in individual wells on a 12-well plate.

Imaging was done on a LSM 7 multiphoton microscope (see Chapter 2 for specifics). Detection of the TsTX-ATTO-594 signal was the same as in the previous experiments (Chapters 2 and 3). For this experiment, transmitted images were collected simultaneously with multiphoton excitation and through DIC optics using a transmitted-path PMT detector. Large tile scans were used to capture large portions of the cerebellar cortex, including the anterior lobe, lobulus simples, other lobules, and the deep cerebellar nuclei (Fig. 21). The different channels were merged in ImageJ (NIH) to create RGB images within both channels.

The infusion data suggest that infusions of TsTX, as mapped by a fluorescent version of the same compound, are limited to regions associated with eyeblink conditioning (EBC). Two areas implicated in EBC are the anterior lobe and lobulus simplex (Green and Steinmetz, 2005, Steinmetz and Freeman, 2014). The area sampled in the experiments above (base of the primary fissure; Chapters 2 and 3) is proximal to both of those regions. As can be seen in Figure 21, the infusion of TsTX-ATTO-594 does not spread far from the infusion site. Individual basket cell axon terminals can be seen in red in the cerebellar cortex. The infusion does not spread far from the two regions mentioned above and remains distant from the deep cerebellar nuclei region. Overall, the spread of the infusion suggests that infusions of TsTX are not spreading to off target sites.

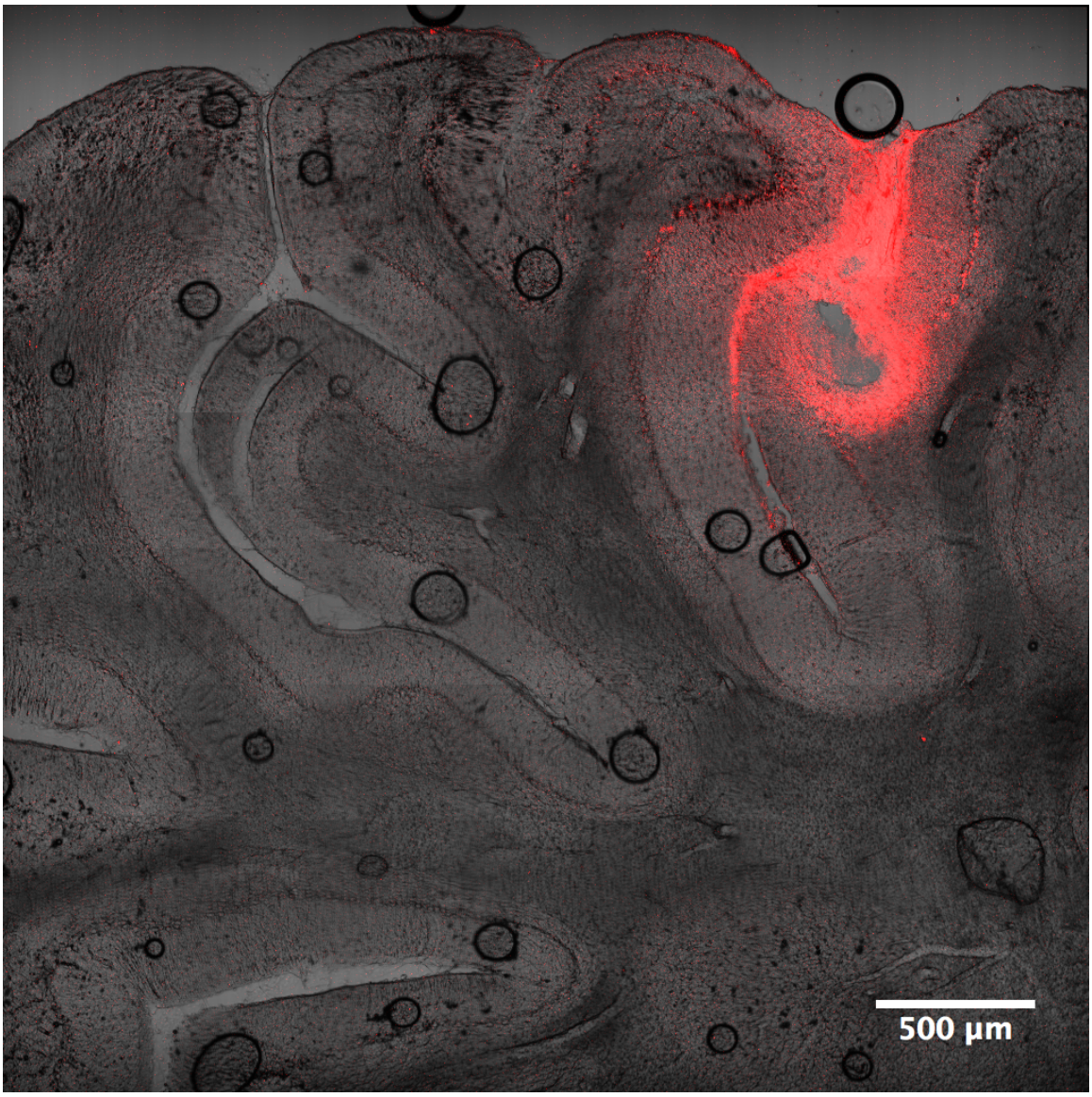

Figure 22. Parasagittal section of cerebellum following an infusion of ATTO-TsTX-594 into the lobulus simplex of the cerebellar cortex above the base of the primary fissure. The infusions (red) is limited to regions of the anterior lobe, lobulus simples, and remains above the deep cerebellar nuclei region.